eman ta zabal zazu

Universidad del País Vasco

Euskal Herriko Unibertsitatea

Development of a stem cells-based gene therapy approach mediated by non-viral vectors with potential clinical applications in regenerative medicine

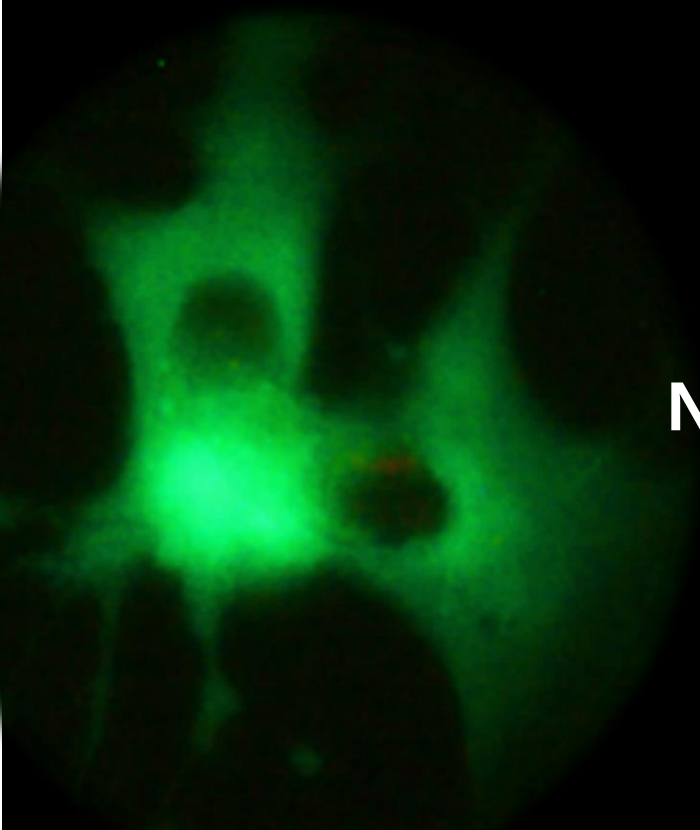

Noha Elsayed Attia Hussien

Vitoria-Gasteiz, 2020

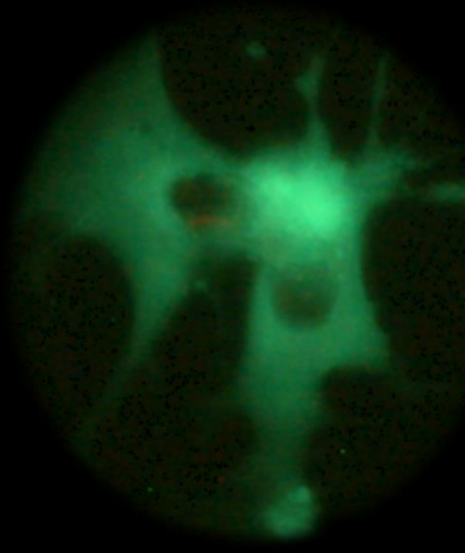

eman ta zabal zazu

Universidad del País Vasco

Euskal Herriko Unibertsitatea

Development of a stem cells-based gene therapy approach mediated by non-viral vectors with potential clinical applications in regenerative medicine

Noha Elsayed Attia Hussien

NanoBiocel Group, Laboratory of Pharmaceutics

University of the Basque Country (UPV/EHU)

Faculty of Pharmacy

Vitoria-Gasteiz

2020

eman ta zabal zazu

Universidad del País Vasco

Euskal Herriko Unibertsitatea

Development of a stem cells-based gene therapy approach mediated by non-viral vectors with potential clinical applications in regenerative medicine

Noha Elsayed Attia Hussien

NanoBiocel Group, Laboratory of Pharmaceutics

University of the Basque Country (UPV/EHU)

Faculty of Pharmacy

Vitoria-Gasteiz

2020

ACKNOWLEDGMENTS

"الْحَمْدُ لِلَّهِ رَبِّ الْعَالَمِين"

This thesis would not have been accomplished without the love, support, guidance and encouragement of multitude of individuals.

I would like to begin by expressing my deepest gratitude to my dearest supervisor Prof. Dr. Jose Luis Pedraz for giving me the opportunity to work on this thesis in his laboratory. He taught me the preciseness in science and the good practice in the lab. I feel myself privileged for being able to work under his experienced supervision towards accomplishing this research successfully. Dr. Pedraz, no words can express my gratitude to you!

It is with great pleasure that I am expressing my thanks and appreciations to my dearest supervisor, Prof. Dr. Gustavo Puras, to whom I am immensely indebted. I truly thank him for being so enthusiastic about the work, for his great scientific guidance, reviewing the thesis manuscript and for his decent constructive comments.

I would like to greatly acknowledge my soul mate, husband and co-worker, Dr. Mohamed Mashal, for what no words can describe. Mohamed, without your creativity, clear vision, and persistence (*not patience*), obtaining my second Ph.D. would have been totally impossible.

Research is an exciting journey of discovery. Thus, I extend my gratitude to all co-authors for their sincere invaluable support. Colleagues in the lab are thanked for their skillful technical advice as well as the good and friendly atmosphere for doing research.

Lastly, I own my warmest thanks to my dear ones, my family members.

Thanks a ton!

ACKNOWLEDGMENT FOR THE FINANCIAL SUPPORT

This project was supported by the Basque Country Government (CGIC10/172), Spanish Ministry of Education (Grant CTQ2017-84415-R, MAT2015-69967-C3-1R), the Generalitat de Catalunya (2014/SGR/624), and the Instituto de Salud Carlos III (CB06_01_0019, CB06_01_1028). The authors also wish to thank the intellectual and technical assistance from the ICTS “NANBIOSIS”, more specifically by the Drug Formulation Unit (U10) of the CIBER in Bioengineering, Biomaterials, and Nanomedicine (CIBER-BBN) at the University of Basque Country (UPV/EHU). Technical and human support provided by SGIker (UPV/EHU) is gratefully acknowledged. Noha Attia gratefully acknowledges the support provided by the science and technology development fund (STDF), Egypt.

ACKNOWLEDGMENT TO THE EDITORIALS

Authors would like to thank the editorials for granting permission to reuse their previously published articles in this thesis.

Attia N, et al. "Stem cell-based gene delivery mediated by cationic niosomes for bone regeneration." Nanomedicine: Nanotechnology, Biology and Medicine 14.2 (2018): 521-531.

Attia N, et al. "Gene transfer to rat cerebral cortex mediated by polysorbate 80 and poloxamer 188 nonionic surfactant vesicles." Drug design, development and therapy 12 (2018): 3937.

Attia N, et al. "Cationic niosome-based hBMP7 gene transfection of neuronal precursor NT2 cells to reduce the migration of glioma cells in vitro." Journal of Drug Delivery Science and Technology 53 (2019): 101219.

وَقُلْ رَبِّ زِدْنِي عِلْمًا

And say, "My **Lord**, increase me in knowledge."
The Holly Quran (20:114)

Table of Contents

Chapter 1

Introduction

1.1. Background

1.1.1. Cell therapy

The concept of regenerative medicine using the body's own stem cells and/or growth factors to repair tissues might become a reality as initial clinical research endeavors have "teamed-up" aspiring to develop alternative therapeutic strategies to treat various disorders. Stem cells are known as a population of undifferentiated tissue precursor cells capable of self-renewal and provision of cells for many tissues. In addition, stem cells could be isolated from a variety of sources including embryonic, fetal, and adult tissues.[1] Embryonic stem cells were obtained from the inner cell mass of the embryonal blastocyst. It has been already shown that human embryonic stem cells can differentiate into derivatives of all three embryonic germ layers. However, due to the ethical considerations associated, these cells may be restricted to experimental *in vitro* studies and their therapeutic potential remains arguable.[2] In contrast, adult stem cells have been isolated from several tissue sources, including the bone marrow (BM), central nervous system, retina and skeletal muscle. The plasticity of adult stem cells can probably generate various lineages of cells, different from their original one.[3] Thereafter, these cells can be used for organ regeneration and cellular repair in several species, as well as in humans. Thus far, there are no ethical issues for adult autologous stem cells. Nonetheless, much experimental work remains to be done before their clinical relevance and therapeutic benefits are considered.[4]

In 1867, the German pathologist Cohnheim was the first to identify mesenchymal stem cells (MSCs) in BM as non-hematopoietic stem cells.[5] Dr. Cohnheim's work raised the possibility that BM may differentiate to fibroblasts that synthesize collagen fibers normally and during repair of wounds. Evidence is now available that BM contains cells that can differentiate into other types of mesenchymal cells, thanks to the pioneer studies by Friedenstein and

colleagues.[6] They placed whole BM in tissue culture dishes and removed the non-adherent cells after 4 hours, thus discarding most of the hematopoietic cells. They have also reported that the adherent cells had a heterogeneous in appearance. Yet, the most tightly adherent cells were spindle shaped and formed foci of few cells that began to multiply rapidly after a lag phase (2– 4 days). However, after several passages, the adherent cells acquired a more homogeneously fibroblastic appearance. These cells were also able to differentiate into colonies that resembled small deposits of bone or cartilage. Friedenstein's research observations were further extended by many other scientists coming to a conclusion that the cells isolated by Friedenstein's method were multipotent and could differentiate into osteoblasts, chondrocytes, adipocytes, and myoblasts.[7] Currently, they are referred to as either "MSCs", because of their ability to differentiate into mesenchymal-type cells, or as "marrow stromal cells" because they arise from the complex array of supporting niche found in the bone marrow.

The ability to culture expand MSCs easily, differentiate them into different cell types *in vitro*, in addition to their appealing immunologic characteristics, clearly render MSCs a promising source of stem cells, for both tissue repair/regeneration and gene therapy.[8] Although local transplantation/injection of MSCs represents a potential approach that may be useful in certain settings, the potential for minimally invasive delivery of MSCs via systemic infusion is of particular interest. However, a significant barrier to the effective implementation of MSC therapy is the lack of full understanding of MSC trafficking. The targeted delivery of MSCs has shown their engraftment in several tissues, particularly after injury. Their homing is defined as the arrest/retention of MSCs within the vasculature of a specific tissue followed by transmigration across the endothelial cells. Interestingly, there is much evidence to support the theory of MSC homing to tissues, particularly when injured or inflamed, involves migration across endothelial

cell layers. The mechanism of MSC homing to tissues and migration across endothelium is not fully understood yet. However, it is likely that injured tissues expresses specific ligands/receptors to facilitate trafficking, adhesion, and infiltration of MSCs to the site of injury, similar to the recruitment of leukocytes to sites of inflammation.[9] It is known that chemokine receptors and their ligands are key components implicated in the attraction and migration of leukocytes to sites of inflammation. Similarly, it has been shown that MSCs express some of these molecules in addition to several adhesion molecules, known to be involved in leukocytic migration across endothelium cells, are also expressed on MSCs. Such lack of data describing the exact positioning of the MSCs following infusion makes it difficult to determine if the cells remain arrested within blood vessels (localization) or have undergone trans-endothelial migration (homing). Interestingly, several research endeavors demonstrated that cultured MSCs are able to engraft into healthy, as well as injured tissues, then differentiate into several cell types *in vivo*. Herein, we mention a few research studies that highlighted this fact later on. Amongst many research teams, Hofstetter and colleagues injected MSCs into the spinal cords of paraplegic rats 1 week after injury.[10] Surprisingly, they found that MSCs have guided regeneration through the spinal cord lesion, thus promoting recovery. Their work demonstrated that the beneficial effect of MSCs in sites of injury may not be necessarily based on their differentiation into the injured cell types, but rather on the physical attributes, such as forming guiding strands in the injured spinal cord.

In another study, MSCs injected into the cavity of heart ventricles where rats with induced myocardial infarction depicted a significantly higher cell uptake compared to rats with healthy myocardium. Nevertheless, 4 hours later, only less than 1% of the injected cells were retained in the infarcted heart. Early infusion also resulted in significantly higher uptake in the heart. Therefore, a conclusion was made that MSCs are preferentially attracted to, and retained in, the

ischemic tissue.[7] Their conclusion suggests that the injured tissue might express specific receptors/ligands to facilitate homing, adhesion, and infiltration of MSCs to the site of injury. Nonetheless, such expressed molecules may be down regulated a short time after injury takes place. When MSCs were injected via the intravenous (IV) route in rats with myocardial infarction, most of the cells were trapped in lungs while a few numbers engraft the heart, liver, and spleen. While MSCs can home to the injured heart tissue, they are way less than after direct injection into the ventricle.[11]

Despite the entrapment of MSCs in the lungs, evidence has accumulated that MSCs are capable of homing to injured tissues after IV injection. Another example for that is the ability of cultured MSCs to migrate into sites of brain injury after being transplanted intravenously in rats with cerebral ischemia.[12] Similarly, MSCs delivered by the IV route to treat heart allograft rejection in rats migrated to sites of allograft rejection.[13]

Another example, cultured MSCs have been injected systemically to treat osteogenesis imperfecta (OI), a disease in which osteoblasts produce defective type I collagen. Horwitz and co-workers [14] used BM transplants, after ablative chemotherapy, to treat children with OI. Three months later, evidence of new dense bone formation, increase in total bone mineral content, increase in growth rate, and reduced frequency of bone fracture in all treated patients. In this study, mesenchymal progenitor cells in transplanted BM migrated to the bone tissue and then differentiated to osteoblasts whose presence correlated with an improvement in bone structure and function.

Over the past decades, the advances of gene delivery into stem cells have raised hopes towards the feasibility of using such stem cell-based gene therapy approaches to provide long-term therapeutic impacts.[15] Various studies have deepened our understanding of the behavior of

individual stem cells in different tissue microenvironments. In parallel, the implementation of more accurate assays for stem cells and enhancement in gene vehicles have increased the gene transfer efficiency into MSCs. It is envisaged that a thorough evaluation of human gene therapy protocols will lead to a better understanding of the potential of stem cells as a gene therapy strategy directed towards both inherent and acquired diseases. Several approaches were introduced to deliver transgenes into MSCs. Although viral vectors permit efficient transgene delivery, their safety concerns have prompted the search for a non-viral gene delivery alternative.[16] Interestingly, the genetically-engineered MSCs may have direct applications on several diseases in different types of cells, in various microenvironments, and in different tissues *in situ*. The ability to genetically-engineer MSCs provides a means for long-term expression of therapeutic genes for the lifetime of the patient for various disorders. MSCs can be engineered to secrete a variety of different proteins, *in vitro* and *in vivo,* that could potentially treat a variety of genetic or acquired diseases, including bone, cartilage and BM disorders, or even cancer.[15]

Several research groups have investigated the use of MSCs for gene therapy, including transplantation of MSCs transfected with genes coding for vascular endothelial growth factor (VEGF) to improve heart function in a rat model of myocardial infarction, MSCs as vehicles to deliver interferon-beta protein into tumors in mice, and gene therapy with bone morphogenic protein-expressing MSCs to boost bone formation.[17] Various reports have made use gene transfection of stem cell in tracking them *in vivo* by the help of reporter genes. In another study, *ex vivo*-expanded MSCs, transduced with a retroviral construct encoding green fluorescent protein (GFP), were infused into adult baboons. Data suggested that MSCs were initially widely distribute following systemic infusion. Later on, they participated in the ongoing cellular turnover and replacement in a various tissues.[18]

The culture of neural stem cells (NSCs) or neural progenitor cells (NPCs) is an essential tool for assessing the molecular mechanisms controlling differentiation in the nervous system. Human NPCs can be obtained from brain biopsy or can be differentiated from pluripotent stem cells.[19] Regardless of their source, one of the main challenges in this field is to mimic *in vitro* neural development as similar as possible to the *in vivo* situation. Much has been done in order to confirm similarities between cells growing in dishes and cells *in vivo* context in the brain. Indeed, *in vitro* models have evolved as reliable tools for studying cellular and molecular aspects of neural differentiation.

The NT2 lineage is derived from human testicular embryonic teratocarcinoma and differentiates into functional post-mitotic neurons. They resemble stem cells with the potentials of self-renewal and neuronal differentiation.[20] The obtained NT2-derived-neurons express many neuronal markers, such as cytoskeletal proteins, secretory markers and surface markers. Also, NT2 cells express nestin and vimentin (neuroepithelial precursor cell markers), while NT2-derived-neurons express MAP2, NF-L and α-internexin, among other neuronal specific proteins, and produce a variety of neurotransmitters, namely GABA and glutamine. Moreover, NT2-derived neurons can form functional synapses and have also been used in several transplantation studies in experimental animals and in human patients. [21]

Neuronal differentiation is a complicated process that involves many steps. First, proliferation of the precursor cells, then migration of the neurons to their target regions, neurite outgrowth, and finally maturation within synaptic circuits.[22] There are three sources for human neurons: embryonic stem cells (ESCs), embryonic germ cells (EGC) and embryonal carcinoma cells (ECC). ESCs are derived from inner cell mass of the pre-implanted human embryo. While EGC are derived from primordial germ cells obtained from embryonic gonads, ECC could be

derived from testicular tumors in adult humans. Human NT2 neurons are obtained from ECC via the free-floating aggregate method. Such procedure is based on the proliferation of the precursor NT2 cells *in vitro* in normal medium, differentiation upon addition of retinoic acid (RA) to the culture media, expansion of adherent cells, purification using mitotic inhibitors, and finally selective trypsinization to obtain pure, post-mitotic neuron.[23] Such "classical" protocol comprises 6 weeks of treatment with RA, followed by 2 successive seedings, exposure to mitotic inhibitors (7-10 days) and 1-2 selective trypsinization steps to obtain purified fractions of neuronal cells. Therefore, the whole process of cell culture takes about 2 months, which is the major disadvantage of this "classical" differentiation method. Another attempt to differentiate NT2 cells was a cell aggregation procedure that cuts the culturing time in half, [24] resulting in a low percentage of neuronal cells in the aggregates, which were hard to purify.

Cell-based therapy is an alternative approach, for the central nervous system (CNS) disorders, in which neurological defects are caused by loss of a defined population of the neurons. The major source for cells, used in the transplantation studies, is the fetal embryonic tissue. Nevertheless, widespread application of such tissue is hampered by logistic as well as ethical concerns. Thereafter, cell lines obtained from human tissues, that could multiply and differentiate *in vitro* into neurons, are a promising source of cells to be used for transplantation. NT2-derived neurons (NT2-N) may be considered as a potential source of transplantable neurons.[25] Till now, many studies were successful to transplant NT2 neurons into the brains of rodent [25], showing that neurons could survive, integrate and differentiate in the intact environment of the host CNS. Transplanted neurons could extend neurites, express neuronal markers, survive for up to 15 months and show no signs of phenotype reversion. In addition, local environment of host CNS seems to play a paramount role in the specification of neurotransmitter phenotypes in NT2 cells. Moreover,

and most interestingly, the transplanted undifferentiated NT2 precursor cells did not show any tumor formation. [26] Human NT2N cells express markers of cholinergic phenotype, therefore it was logical to proceed with the pre-clinical studies to engraft NT2N cells to restore motor function in neurological disorders as amyotrophic lateral sclerosis (ALS) and stroke.[27] The transplants of NT2-N into the CNS aim to work in concert to afford the neuroprotection and neuroregeneration. Several studies have shown a positive effect of engrafted cells that was based mainly on the secretion of trophic factors.[28] The promising findings obtained from animal transplantation experiments have generated great expectations for using NT2 neurons in clinical trials. Nevertheless, issues such as long-term monitoring of cell survival and progression after transplantation still needs to be resolved.

1.1.2. Gene therapy

According to the Food and Drug Administration (FDA), gene therapy is defined as "the administration of genetic material to modify or manipulate the expression of a gene product or to alter the biological properties of living cells for therapeutic use." Such transfer of genetic materials could be done for cells *in vitro*, *in vivo* and *ex vivo*. An essential aspect of gene therapy depends on designing a suitable delivery system to carry the correct gene to the affected target cells. Safe and effective gene delivery for long-term remains a big challenge for gene therapy. More than 5 decades after the concept was first introduced, gene therapy is now considered as a promising treatment option for various human disorders.[29] Serious adverse effects were encountered in early clinical trials. Yet, such hurdles have fueled basic research that led to safer and more efficient gene carriers. Gene therapy, in different forms, depicted marked clinical benefits in patients with

various clinical conditions, such as blindness, neuromuscular disease, hemophilia, immunodeficiencies, and cancer (Fig. 1).

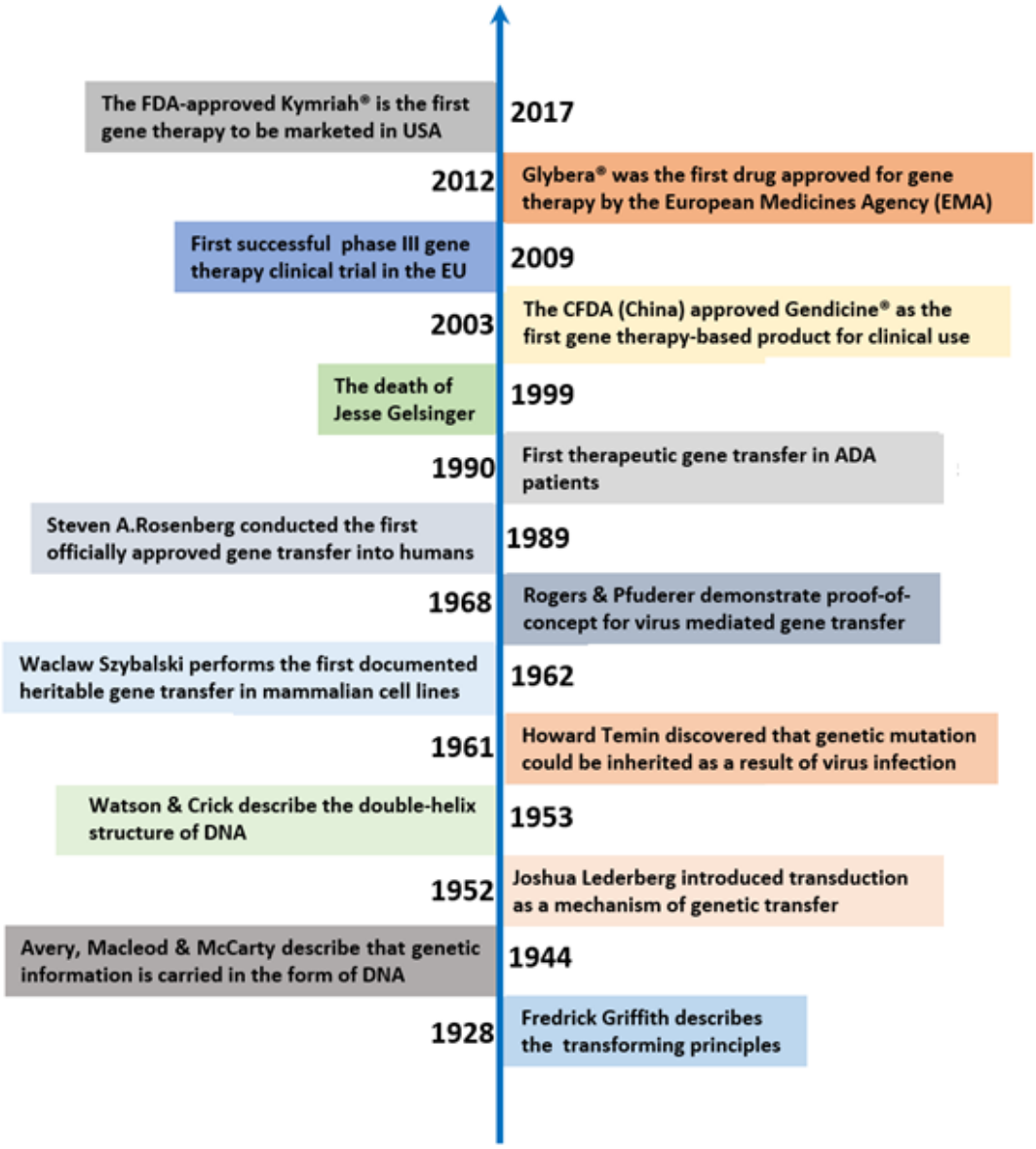

Figure 1. Timeline of salient events of gene therapy, adapted from [30]

The double-helix structure of deoxyribonucleic acid (DNA) was first described by Watson and Crick (1953). Later (in 1961), Howard M Temin's DNA provirus hypothesis was enunciated. In 1972, Theodore Friedmann and Richard Roblin proposed that “good DNA” could be used to

replace “defective DNA” in people with genetic disorders. This was considered the first suggestion to treat genetic disease by gene therapy. In September 1990, DeSilva at the age of 4 had been the first subject with severe combined immune deficiency (SCID) to undergo gene therapy in the United States. This clinical trial was authorized by the NIH Recombinant DNA Advisory Committee (RAC) and the Food and Drug Administration (FDA). The gene coding for functional adenosine deaminase (ADA) was transferred by retroviral vectors into T lymphocytes. The transfected cells were reinfused back into the girl.[31] Additionally, in 1991, Cynthia at age of nine underwent another trial at the national institute of health (NIH) Clinical Center. Unfortunately, in September 1999, the 18-year-old boy, Jesse Gelsinger, with an inherited enzyme deficiency passed away after 4 days of being treated by injection of genetically altered viruses into his liver. This was a direct reason for strict regulations in the research field of this technology. In the year 2002, a marked shock to the scientific community happened again when a 3-year-old child with SCID who was treated in a clinical trial developed leukemia. Therefore, gene therapy trials were frozen again till China’s Food and Drug Administration (CFDA) approved Gendicine® (recombinant human p53 adenovirus) in 2003 as the first gene therapy product to treat cancer of head and neck. Subsequently, in 2007, British doctors carried out the world’s first clinical trial to provide gene therapy for Leber Congenital Amaurosis (LCA), a rare inherited eye disease, where RPE65 mutations were targeted by ocular injection of adeno-associated virus (AAV). In 2012, Alipogene tiparvovec (marketed under the trade name Glybera®) was the first gene therapy drug approved by the European Medicines Agency (EMA) for the treatment of lipoprotein lipase deficiency in muscles. Recently, in 2017, is considered distinguished start for gene therapy in United States. in August 20, 2017 Kymriah® was approved by the FDA as the first gene therapy for acute lymphoblastic leukemia to be marketed in the United States. During the same year,

Yescarta®, was approved by FDA for treatment of large B-cell lymphoma. By the end of 2017, Luxturana® was approved by FDA as the first gene therapy for the treatment for LCA.

1.1.3. BMP7 applications

Bone morphogenetic proteins (BMPs), as extracellular matrix-associated proteins, are known to govern a plethora of biological processes. BMPs comprise a variety of members of the transforming growth factor-β protein superfamily that actively participate in kidney development, digit and limb formation, angiogenesis, tissue fibrosis, and tumor development. Once discovered, BMPs have attracted the attention of the scientific community for their fascinating perspectives in tissue engineering and regenerative medicine. Therefore, the importance of BMP signals in pathophysiology cannot be overstated because of the multitude of dysregulated BMP signaling in numerous pathological processes. Clinically, BMP family members have been associated with various pathologies, including obesity, diabetes, various vascular diseases as well as cancer and its related comorbidities.[32] During years of research, BMP7 has gained the podium for their use in the treatment of various disorders. For example, BMP7 alone emerges as a potential therapeutic agent that can decrease vascular calcification, for which there is no adequate therapy at present. Additionally, the recent discovery of BMP7 in promoting brown adipocyte differentiation and thermogenesis offers a new clinical potential. BMP7 triggers commitment of MSCs to a brown adipocyte lineage, and subcutaneous injection of these cells into athymic mice results in development of adipose tissue containing mostly of the brown subtype. Tail vein injection of

adenovirus expressing BMP7 increased brown fat leading to increased energy expenditure, higher basal body temperature, suppressing obesity.[33]

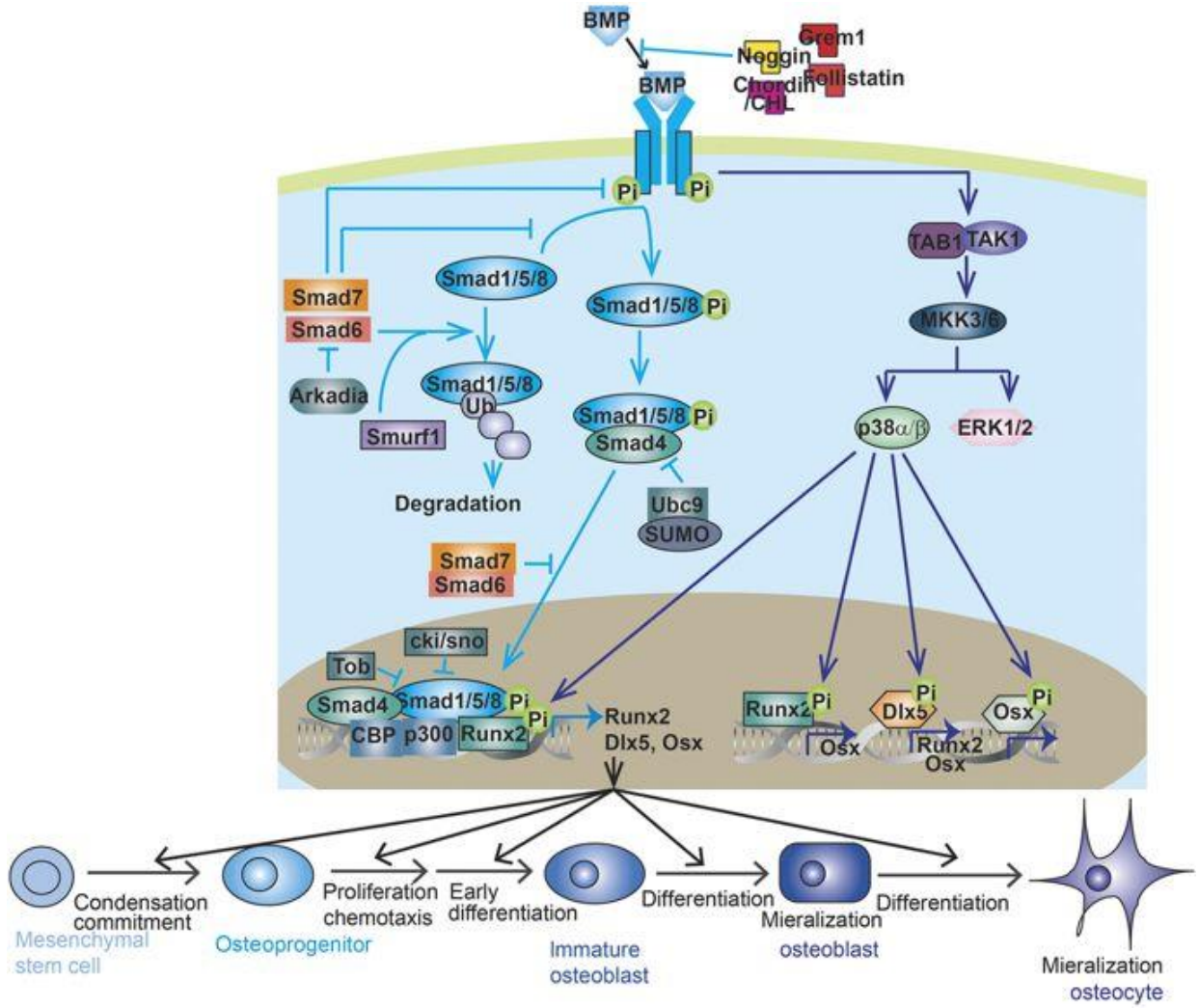

Figure 2: Signaling of BMP in bone cells. [34]

BMP–Smad signaling boosts almost every step during the differentiation and maturation of osteoblasts (Fig. 2). In addition to their roles in bone development, TGF-βs and BMPs are known to regulate the maintenance of postnatal bone and cartilage. Moreover, TGF-βs are key in coupling bone synthesis by osteoblasts and bone resorption by osteoclasts through osteoclast-mediated *Atp6i*-specific extracellular acidification and *Cathepsin K*-specific extracellular matrix proteins. Several BMPs are potent osteogenic agents that were found to possess significant clinical

implication to accelerate healing in bone fracture. BMP7 induces the expression of osteoblast-specific differentiation markers, such as alkaline phosphatase (ALP). In addition, it accelerates matrix mineralization. Therefore, recombinant human BMP7 is currently used for spinal fusion, fracture healing and dental tissue engineering. More recently, transplantation of the recombinant human BMPs (rhBMPs) with autologous stem-cells has also emerged as a promising technique in tissue engineering for the regeneration of various body parts.

On the other side, many studies to date report that BMP7, as well as other BMPs, are over-expressed in various cancer types. However, changes in gene expression, epigenetic alterations and mutations in genes related to BMPs appear to be mostly a characteristic of a certain type of cell or tissue, not necessarily any direct nor indirect cause of carcinogenesis. At the time being, no reports are available for the adverse carcinogenic events in patients who underwent operations using BMP7. However, the lack of reported cases may be due to the relatively recent introduction of BMPs to clinical use and extra precautions must be made in determining appropriate dosage and length of retention time in the body.[35]

1.2. Non-viral gene delivery vectors

As mentioned before, gene transfection is defined by introducing exogenous nucleic acids such as, DNA, mRNA, small interfering RNA (siRNA), microRNA (miRNA) or antisense oligonucleotides. Some of these macromolecules depict a large size and a strong negative charge. Therefore, their delivery is typically dependent on vectors or carriers. Recently, non-viral delivery of genome editing systems could facilitate precise and permanent correction of perturbed genes. Zinc-finger nucleases (ZFNs), transcription activator-like effector nucleases (TALENs), and clustered regularly interspaced short palindromic repeat (CRISPR/Cas) are programmable nucleases that can be designed to target -in theory- any gene in a precise manner. All three gene-

editing systems result in sequence-specific DNA cleavage, at which point the DNA repair machinery of the host cell can be harnessed to achieve gene modification. The development of advanced gene delivery carriers should increase the potential of gene therapy to treat various disorders and to silence, correct or introduce specific genes with trivial side effects. Interestingly, recent advances in nanotechnology, material sciences, and nucleic acid chemistry have provided promising non-viral delivery systems, some of which are currently under clinical trials as summarized in table 1.

Table 1: Non-viral DNA vectors used in clinical trials. [36]

Delivery system	Gene therapy drug	Indications	Phase	Status	Clinical Trials. gov identifier
DOTAP–cholesterol	DOTAP–Chol-fus1	Non-small-cell lung cancer	I I/II	Completed Active	NCT00059605 NCT01455389
GAP-DMORIE–DPyPE	Tetravalent dengue vaccine	Dengue disease vaccine	I	Active	NCT01502358
GL67A–DOPE–DMPE–PEG	pGM169/GL67A	Cystic fibrosis	II	Active	NCT01621867
PEI	BC-819/PEI	Bladder cancer	II	Active	NCT00595088
	BC-819	Ovarian cancer	I/II	Completed	NCT00826150
	DTA-H19	Pancreatic cancer	I/II	Completed	NCT00711997
	SNS01-T	Multiple myeloma and B cell lymphoma	I/II	Recruiting	NCT01435720
	CYL-02	Pancreatic ductal adenocarcinoma	I	Completed	NCT01274455
PEG–PEI–cholesterol	EGEN-001	Ovarian, tubal and peritoneal cancers	I II	Recruiting Active	NCT01489371 NCT01118052
	EGEN-001-301	Colorectal peritoneal cancer	I/II	Recruiting	NCT01300858
PEI-mannose–dextrose	DermaVir/LC002	HIV vaccine	II	Active	NCT00711230
Poloxamer CRL1005–benzalkonium chloride	ASP0113	CMV vaccine	III II	Recruiting Recruiting	NCT01877655 NCT01903928
	VCL-CB01	CMV vaccine	II	Completed	NCT00285259

Although being simple in theory, non-viral vectors are complex in practice. In addition to the intra/extra cellular barriers, they face quite a big number of other challenges that needs to be circumvented in order to increase their gene transfer effectiveness. Moreover, other obstacles categorized as production, formulation and storage.

1.2.1. Cationic lipids

Lipid-based gene carriers are among the most widely used non-viral vectors. A big list of lipid library has been developed for gene transfer. A positively charged hydrophilic head and hydrophobic tail with linker structure that connects both has been a common structural feature in all of them. The positively charged head groups binds with negatively charged phosphate groups in nucleic acids and form a compacted structure, the lipoplexes. Their transfection efficiency depends, in a way or another, on their overall geometric shape, number of charged groups per molecules, nature of lipid anchor, and linker bondage. Lipoplexes, thanks to their net positive charge, can electrostatically interact with negatively charged glycoproteins and proteoglycans of cell membrane that may facilitate their cellular uptake. The positively charged lipids, complexed with the genetic material, provide protection against intracellular and extracellular digestive enzymes, nucleases. Nevertheless, the main problem with such positive surface charge is that it reduces the half-life of lipoplexes circulation in blood limiting its efficiency beyond vascular endothelial cells.[37] Therefore, a neutral polymer as polyethylene glycol (PEG) is used as surface shielding to circumvent the excessive charge, thus extend the half-life.[38] Though being well-tolerated by cells, lipoplexes could be cytotoxic beyond 3/1 ratio of lipid:/DNA. In 1987, Felgner and colleagues synthesized the first cationic lipid for DNA delivery, DOTMA (the chloride salt of 1,2-di-O-octadecenyl-3-trimethylammonium propane). Since that date, cationic lipids become one

of the most important tools for the delivery of DNA, RNA and many other therapeutic molecules.[39] They are easily designed, synthesized and characterized. Presently used lipids possess a positively charged hydrophilic head linked to hydrophobic tail (s) by means of a linker structure (Fig. 3).

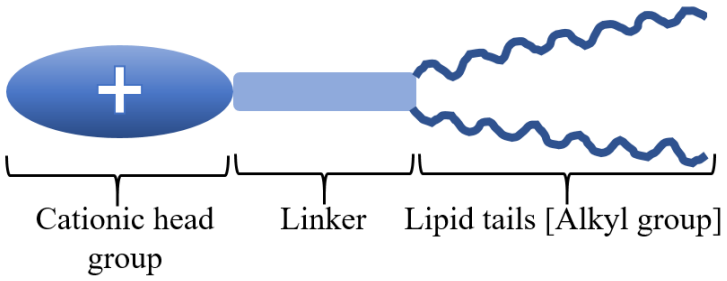

Figure 3: Schematic structure of cationic lipids.

The hydrophilic head consists of cationic (positively charged) groups such as quaternary ammonium salts, primary, secondary, tertiary amines, phosphorus, imidazole, pyridinium, guanidine, arsenic, etc. As said earlier, this positive charge is key for binding with the anionic (negatively charged) phosphate groups of nucleic acids. The linker bond is an important determinant of the chemical stability and biodegradability of cationic lipid, and further governs its transfection efficiency and cytotoxicity. Based on the structures of linker bonds, they can be grouped into many types, such as ether, ester, amide, carbamate, disulfide, urea, acylhydrazone, phosphate, and other unusual types (carnitine, vinyl ether, ketal, glutamic acid, aspartic acid, malonic acid diamide and dihydroxybenzene).

The cationic lipid plays many roles in the process of transfection. The head groups (positively charged) bind electrostatically to the phosphate group in nucleic acids (negatively charged) to form a complex. As well, they facilitate cellular uptake of nucleic acid by direct interaction with cell membrane glycoproteins and proteoglycans (negatively charged). In addition, the positively charged lipid protects genetic material against intracellular and extracellular

nucleases. Moreover, it triggers their endosomal escape thanks to the proton sponge effect. The hydrophobic domain determines phase transition temperature, bilayer fluidity, stability of nano formulation, DNA protection from nucleases, endosomal escape, DNA release from complex, and eventually nuclear trafficking.[40]

1.2.2. Liposomes

Liposomes are spherical vesicles having an aqueous core enclosed by one or more phospholipid bilayers or lamellae. Lipids comprise fatty acid derivatives with numerous head group moieties. Liposomes are composed of one or more simple or functional concentric lipid bilayer membranes that enclose hydrophilic spaces (Fig. 4).

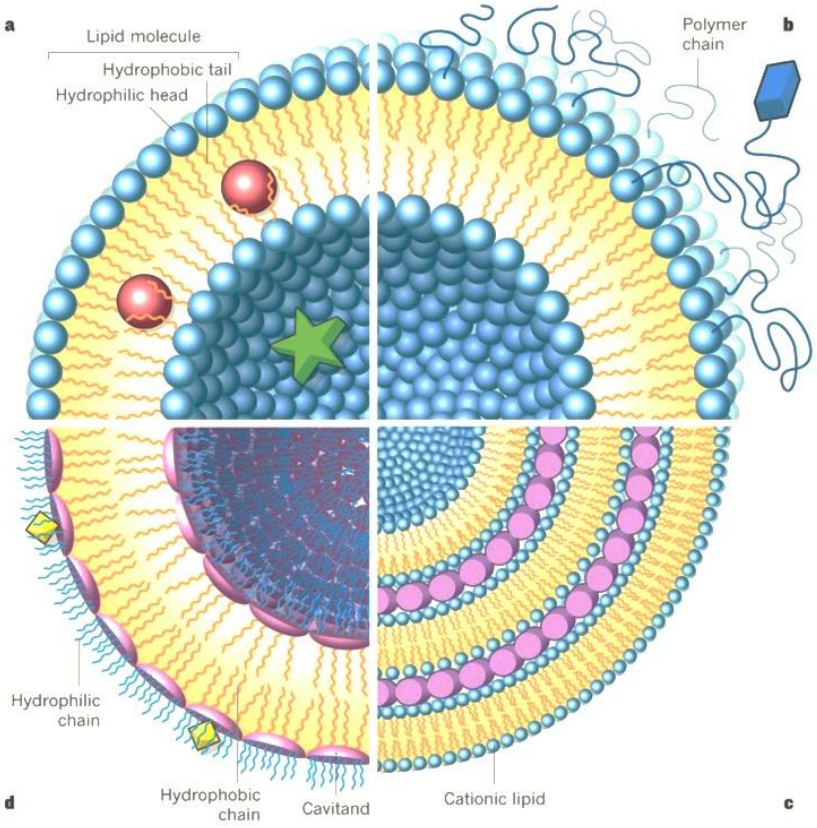

Figure 4: Schematic structure of liposomes showing different compositions. [41]

Over the years, different methodologies for large scale liposome preparation have been developed and optimized. The techniques for liposome preparation can be divided into (1) bulk

methods, in which liposomes are obtained by transfer of phospholipids from an organic phase into an aqueous phase, and (2) film methods, where lipid films are initially deposited on a substrate, and subsequently hydrated to give liposomes. Recently, various synthetic modifications to phospholipids were made to avoid liposome detection and clearance by the immune system, as well as to target the afflicted sites.[42]

Liposomes belong to the lipid-based category of non-viral gene carriers that are widely used in gene delivery. Successful examples of liposomes include Lipofectamine® 2000, Lipofectin® and LipofectACE®, have been successfully used to deliver genes delivery to cultured cells, animals and patients enrolled to clinical trials, phase I and II.[43] Liposomes are mainly composed of lipid and/or phospholipid molecules. The success of liposomes to deliver genetic material depends on their properties, administration route and the barriers that they face to reach their target inside the cells. These hindrances include, but not limited to, stability in the site of administration, permeation of particles through epithelial barriers, stability in the bloodstream, low target cell specificity, especially when applied through routes that are far from the target, escape from the reticuloendothelial system (RES), uptake by the cells and access to the appropriate site within the cytosol or nucleus.[44]

1.2.3. Niosomes

Niosomes are membranous vesicles that are composed of non-ionic surfactants, amphipathic compounds with a net neutral charge. The non-ionic surfactant component of niosomes tend to be oriented in a way that hydrophilic ends face the aqueous phase (outward), whereas the hydrophobic ends face inward to form a closed bilayer structure that could enclose solutes in the aqueous solution. As a consequence, the closed bilayer structure of niosomes has hydrophilic inner and outer surfaces, with a sandwiched lipophilic area in between. The non-ionic

surfactants are safe and affordable for the use in biomedicine, *e.g.* as niosome as gene and drug carriers for both hydrophilic and hydrophobic drugs. There are several methods for the preparation of niosomes. Ether injection, hand shaking, sonication, and microfluidics methods are just to mention a few examples.[45]

Niosomes were first applied by the cosmetic industry in the seventies. They were also proposed as potential vehicles for transporting all sorts of drug molecules thanks to their structural similarities with liposomes and other colloidal systems. Therefore, niosomes are potential tools for targeted drug delivery by promoting sustained release of potential small drugs in specific cells and tissues. Additionally, niosomes were found to be stable particles that have ensured enhanced stabilities to a good number of encapsulated drugs. As vehicles for various drugs, many routes were used to administer drug-loaded niosomes, such as oral (e.g., Methotrexatetopical and Flurbiprofen); ocular (e.g., Acetazolamide, Chloramphenicol, Fluconazole) or topical administrations (e.g., Erythromycin, Rofecoxib, Minoxidil, and others).[45] Moreover, efficacy and safety of these routes have been proven in numerous pre-clinical and clinical studies which that have emphasized the biocompatibility, biodegradability and low immunogenicity of niosomal components (non-ionic surfactants, cholesterol, fatty acids, in addition to charged molecules). Cytotoxicity is a major factor that should not be overlooked when niosomes are used as a therapeutic tool. Cationic lipids are well known to have serious cytotoxicity in transfection due to their positively charged molecules. Therefore, the incorporation of non-ionic molecules to formulate niosomes could reduce such undesirable toxicity. That is why niosomes are way more tolerated by transfected cells compared to their anionic or cationic counterparts.[46] All the aforementioned properties, in addition to the low cost and ease of preparation, have paved the way

for niosomes to stand out versus liposomes and other conventional systems for drug/gene delivery (summarized in table 2).

Recently, several pharmaceutical companies have invested in niosome adaptability by utilizing them in various applications (e.g., nutraceuticals, anti-bacterial, antioxidant and anti-cancer, among others).

Table 2: Niosomes versus liposomes. [47]

	Niosomes	**Liposomes**
Components	Surfactant	Phospholipids
Component availability	High	Low
Component purity	Good	Variable
Preparation and storage	No special conditions required	Inert atmosphere and low temperature
Stability	Very good	Low
Cost	Low	High

1.3. Strategies to improve regenerative medicine by cell therapy

Idealistically, the aim of cell therapy is to replace damaged/aged cells with healthy functioning cells in various conditions, including, yet not limited to, congenital defects, tissue injuries, autoimmune disorders, and degenerative diseases. Below, we review a number of emerging strategies to improve cell-based regenerative medicine.

1.3.1. Cell microencapsulation

Cell microencapsulation is simply defined as the immobilization of cells from an outside environment within a semi-permeable membrane barrier protecting cells from both mechanical stress and components of the host immune system (such as immunoglobulins, complement and immune cells).[48] Meanwhile, the membrane allows the inward diffusion of nutrients and oxygen

as well as the outward delivery of waste products and therapeutic agents. Additionally, it permits cell transplantation without the use of long-term immunosuppressive therapies, which have potentially severe side effects. In comparison with other immobilization systems, the high surface/volume ratio of the microcapsules increases membrane permeability, ensuring an optimal product exchange to ensure adequate cell viability. Cell encapsulation technology displays important advantages over other delivery systems because it permits a sustained and controlled release of de novo-produced therapeutic molecules. Additional advantages include the enhancement of biosafety, because the toxicity caused by a rapid delivery of high concentrations of the drug does not occur. Moreover, the genetically modified cells can express any protein desired for *in vivo* therapy without the modification of the host genome. It is possible to create small capsules (100-500 μm) and implant them in close contact with the blood stream, improving oxygen transfer into the cells, which may be beneficial in certain applications. Eventually, microcapsules could be directly injected/transplanted into implantation sites, such as intra peritoneally or subcutaneously, reducing the frequency of administration and thus improving patient comfort.[49]

The most widely employed cell microencapsulation method was originally developed by Lim and Sun. In recent decades, the initial technique has undergone modifications, leading to several methods to produce microcapsules, including extrusion methods, emulsion (thermal gelation), microfluidics, and microlithography. Microencapsulation, originally, was based on the polyelectrolyte complexation of alginate with a polycation, normally poly-L-lysine (PLL) or poly-L-ornithine (PLO). These types of microcapsules are commonly referred to as alginate-PLL-alginate (APA) or alginate PLO-alginate (APO) microcapsules, respectively. Apart from microcapsules formed with these polycations, other polymers [such as chitosan, lactose-modified

chitosan, oligochitosan, poly(methylene-co-guanidine), sodium silicate, and multilayers] have been implemented to coat alginate. The drawback of these materials is that they are associated with cytotoxicity and cell necrosis, which has generated much controversy among research groups. Unfortunately, it is still unclear which of these strategies is the best for cell encapsulation.[49] Using an appropriate encapsulation biomaterial is one of the most important requirements in the development of encapsulated cells. These biomaterials play important roles, providing three-dimensional synthetic extracellular matrix (ECM) that mimics certain beneficial properties of the normal ECM and improving protection against immune reaction by isolating encapsulated cells from the host immune cells. These materials should have the ability to form a gel in mild and physiological conditions (in terms of temperature, pH, and ionic strength). In addition, they must be biocompatible and should not interfere with cellular function. Although many types of natural and synthetic polymers have been explored, including collagen, hyaluronic acid, or alginate in combination with chitosan, agarose, gelatin, and tyramine, the majority of the studies in the field of cell encapsulation have employed sodium alginate.[50]

Alginate polymer is produced by some seaweeds and by some bacterial species, such as Pseudomonas aeruginosa. Alginate, extracted from brown algae, has been implemented in a variety of biomedical applications. Nowadays, alginates are used primarily as a thickening agent, for example in paint and food industry. In addition, they have been used in the production of many chemicals such as ammonia, ethanol, and interferons.

Over the past decades, alginates' biocompatibility in relation to their composition has been controversial.[48] Structurally, alginates are composed of unbranched, linear binary copolymers of β-D-mannuronic acid (M) and α-L-guluronic acid (G) residues linked by 1–4 glycosidic bonds. It has been reported that alginates with a high M content provoke an inflammatory response by

stimulating macrophages to produce cytokines such as IL-1, IL-6 and tumor necrosis factor (TNF). In contrast, some research groups found that guluronic acids is associated with more severe inflammatory cell overgrowth and adhesions. Meanwhile, others suggested that the presence of contaminants had a greater impact on the immune response than the alginate composition (i.e. M/G ratio). The extent of contamination, however, appeared to be related to the alginate composition; it was observed that the high M alginate presented a higher content in polyphenol, endotoxins and proteins compared to the other alginates tested. This controversy might be caused in part by the lack of a standard definition for high-G alginate and high-M alginates.

To evade the negative charge of alginate droplets, they are coated with a polycation to stabilize and control the molecular weight cut-off of the microcapsule membrane. PLL is the most widely studied polycation for alginate bead coating. In fact, it has been reported that more than 85% of the articles dealing with cell encapsulation technology published since the original manuscript of Lim and Sun, have introduces significant modifications to the alginate–PLL system. Since charged PLL is known to be immunogenic, the PLL coated alginate beads undergo a final incubation in alginate to form the alginate—PLL–alginate (APA) system.

Recently, the modification of alginates with various peptides and proteins, to provide control over the cell fate, is gaining significant attention. These functional groups ignite the intracellular signaling pathways through the focal adhesions that provide tight control over the cell-to-matrix interactions. The Arg-Gly-Asp (RGD) peptide sequence derived from fibronectin is a natural peptide sequence present in the ECM. Alginate itself does not support cell attachment, but it is easily modified by the simple coupling of cell adhesion domains such as the RGD. As a result of such a coupling, the interaction between the alginate and the integrin receptors of the enclosed cells is improved, enhancing cell survival and functionality. Alginate gels have also been

functionalized with the Asp-Gly- Glu-Ala (DGEA) and Tyr-Ile-Gly-Ser-Arg (YIGSR) sequences derived from other ECM proteins to enhance the gels' adhesive interactions with various cell types. Combination of alginate and the ECM has been applied recently in microcapsules, the matter that resulted in a synergistic activity of both materials.[51] The microcapsules offer the mechanical and material properties of the alginates, which can be controlled with the consideration of some issues; at the same time, the ECM increases the bioactivity of the microcapsules to modulate and improve the viability and function of the encapsulated cells. Biomimetic microcapsules using RGD-alginate have also been employed. These capsules performed the cell adhesion for the encapsulated cells and prolonged their long-term functionality and drug release for more than 10 months, suggesting that these capsules promote the *in vivo* long-term functionality of the enclosed cells and that the mechanical stability of the capsules is improved.[50]

Another attractive modification is focused on the control of the biodegradation rate of the alginates under physiological conditions. An example of such a modification is the partial oxidation of the alginate chains so that they become sensitive to hydrolysis. The degree of this oxidation as well as the pH and temperature of the media influences the degradation rate of the gels. Additionally, MSCs were entrapped in oxidized alginate-fibrin microbeads to achieve a rapid degradation profile and the release of the cells in an effort to promote bone engineering. Moreover, alginate may also be covalently crosslinked via the addition of bi-functional molecules such as poly (ethylene glycol) [PEG] or methacrylate moieties to the alginate chains. The selective modification of the alginate resulted in an enhanced covalent stabilization and an increased mechanical strength of the alginate beads.[49]

Collagen is the main component of the ECM of the mammalian connective tissues. Some of the advantages it offers include its biocompatibility, abundance in nature, natural ability to

anchor cells and degradability mediated by metalloproteases. Its gelation can be induced by changes in pH, allowing cells to be encapsulated under mild conditions. However, the challenges of using collagen as a material for cell immobilization include the high cost of its purification, the natural variability of the isolated collagen, its immunogenicity, and the variation in its enzymatic degradation depending on the implant site.[52] A novel drug delivery system based on collagen-alginate composite structures has been developed to prevent the cell leakage, maintain the cell growth, and control the protein secretion. Collagen has been experimentally used to engineer a variety of tissues, including skin, bone, heart valves, and ligaments.[53]

Chitosan is chitin isolated from the exoskeleton of shellfish, and it has a structure similar to natural glycosaminoglycans (GAGs). It can be formed into hydrogels by ionic interaction and chemical crosslinking with glutaraldehyde. Scaffolds made of this material can be degraded by lysozymes, in addition to their ability to support the release of growth factors synthetized by the immobilized cells. Thermosensitive chitosan has also been investigated as a material to create an aligned cell sheet and to encapsulate MSCs. A crosslinked chitosan hydrogel was used to distribute the cells and enable cell growth. The chondrocytes within scaffolds were able to proliferate, exhibit an increased metabolic activity, and secrete ECM over 14-days culture period.[54]

Agarose is another algae-derived polysaccharide; but unlike alginate, the formation of its gel microbeads is thermally reversible. Its most appealing qualities include the ease of its processing and a wide range of mechanical (e.g. matrix stiffness) and structural (e.g. pore size) possibilities, which are influenced by its concentration in the gel and the cooling rate. In addition, agarose can be modified to include cell-adhesion moieties. There have been many studies involving the enclosure of various cell types in agarose micro particles. In previous research, porcine islets were encapsulated in agarose macro beads and transplanted into spontaneously

diabetic rats. All the rats that received encapsulated porcine islets did not require exogenous insulin therapy for the entire study.[55]

Poly N-isopropylacrylamide [pNIPAM] is a thermo-responsive and biocompatible polymer with a quick phase transition and a low critical solution temperature (approximately 32 ºC). RGD-conjugated pNIPAM hydrogel micro carriers have been employed as cell culture substrates. In addition to cell adhesion applications, cell encapsulation using pNIPAM particles has also been reported. In this case, pancreatic cells were encapsulated into pNIPAM-based microcapsules that exhibited a reversible sol-to-gel transition at 0 ºC. In another approach, pNIPAM thermo-responsive hydrogels have been used to immobilize a chondrogenic cell line, revealing that the biomaterial did not affect the cell viability or proliferation. The results also demonstrated an increase in the synthesis of GAGs during the culture period. This study supported the hypothesis that thermally reversible pNIPAM hydrogel may be suitable as an injectable cell carrier and has great potential for cartilage repair.[56]

Gelatin could be obtained by the partial hydrolysis of collagen fibers derived from skin dermis, white connective tissue, cartilage, and bone tissue. As a natural macromolecule, its major limitation is the variability caused by its derivation from animal tissue, making batch-to-batch reproducibility difficult. This problem could be solved by the use of recombinant gelatins with defined molecular weights. The formation of gelatin cell micro particles is based on crosslinking reactions. Examples of gelatin micro carriers include Spheramine® and Cultispher®. Cultispher® gelatin micro carriers (Percell Biolytica AB, Sweden) are commercially available products and have been widely evaluated as gelatin cell carriers.[57] These micro carriers supported growth of various mammalian cells *in vitro* and have also been used as biodegradable scaffolds for guided tissue regeneration and cell-based therapies *in vivo*.[56]

Other biomaterials employed for cell encapsulation in the form of hydrogels include PEG combined with acrylates and methacrylates, hyaluronic acid, and cellulose sulphate.[58] Despite the fact that none have been characterized and studied as much as alginate, it is still possible to benefit from the advantages that these biomaterials might offer in the development of alternative cell based therapeutic strategies.

Despite the great advances in cell microencapsulation technology providing great promises in clinical trials and even practices, there are still numerous limitations that need to be overcome. First, there is a significant need to enhance the systemic biocompatibility of encapsulated cells. Fibrous tissue tends to proliferate due to activation of host immune response that results in cell death (failure of transplant) through complicated mechanisms including excessive production of free oxygen species. Moreover, cell necrosis may take place as a result of improper encapsulation biomaterials and/or insufficient oxygen and or nutrient supply. Necrotizing cells may compromise the healthy neighboring cells and elicit long-term immunogenic responses.[48] Therefore, satisfactory survival rate of encapsulated cells *in vivo* has to be achieved to ensure successful transplantation. This brings us back to the first point, using systemically biocompatible biomaterials. As well, microcapsules should provide a semi-permeable membrane with balanced porosity to protect the encapsulated cells from host immune system, while ensuring adequate nutrient supply and disposal of metabolic waste products. Secondly, capsules should impart a proper mechanical strength and stability. Therefore, breakage after transplantation is typical for poor microcapsules. Subsequently, leakage of encapsulated cells may lead to serious immune responses and other unexpected consequences. Thirdly, one type of microcapsule system can never be ideal for all cell types. For example, microcapsules made of non-biodegradable materials may not be suitable for applications that aim for integration of the encapsulated cells within the host

tissue. Lastly, when it comes to clinical practice, regulatory considerations of the encapsulated cells should be taken into account. This necessitates comprehensive standardization of microcapsule characterization methodologies, such as surface properties, permeability, mechanical strength to mention a few. However, many other properties has to be characterized and established to ensure systemic biocompatibility and stability of microcapsules.[49]

1.3.2. Bioprinting technology

The bioprinting technology has been introduced to the field of tissue engineering as a powerful potential tool for building tissue and organ-like structures. This technology allows precise assembly of cells and biomolecules in spatially pre-defined spots within the confined three-dimensional (3D) structures. As well, natural and artificial polymers, their mixtures, and peptides are exploited as bioprinting bio inks for regenerative medicine applications.[59] Several bioprinting technologies have been developed for various applications in life sciences, such as; studying cellular mechanisms, constructing tissues and organs for implantation, including heart valves, skin, myocardial tissue, and blood vessels (as summarized in table 3).

The various bioprinting technologies promise a great potential and to be a paramount tool in the field of medicine in the near future. Nevertheless, several challenges remain for building complex tissues composed of various cell types in a confined microarchitecture. Moreover, microstructures manufactured by bioprinters do not exactly match the native mechanical strength of host tissues/organs. Hence, significant improvements are still required to overcome these challenges. Interestingly, 4D bioprinting is an emerging field where time is integrated as a fourth dimension with the usual 3D bioprinting. In such novel 4D bioprinting, printed structures have the ability to change their shapes by time once an external stimulus is introduced. This technology enables the re-organization of biomaterials and cells after printing to improve effective cell

patterning. Nevertheless, this field is still in its infancy, 4D bioprinting may help to overcome many of the current challenges of 3D bioprinting.[60]

Optimal vascularization is one of the main factors that determines the success of an organ transplant since it ensures proper oxygen and nutrient supply. Though several research studies

Table 3: Applications of bioprinting in tissue engineering. [61]

Application	Bio ink	Printing method	Cell type	Inference
Cartilage	Alginate-Polyethylene glycol	Micro-extrusion	Bone marrow-derived hMSCs	Tougher mechanical integrity like native cartilage
	Acrylonitrile butadiene styrene (ABS) and polylactic acid (PLA)	Micro-extrusion	Primary articular chondrocytes and nucleus pulposus	Porous scaffold for cartilage and intervertebral disc tissue engineering
Skin	Layer-by-layer assembled collagen	Micro-extrusion	Human skin fibroblasts and human skin keratinocytes	Skin matrix that resembles structural and biological features of native skin
Bone	DermaMatrix™ human allograft with bone morphogenetic protein 2	Inkjet	Mouse C2C12 progenitor cells	Osteogenic differentiation of C2C12 cells and promotes clavarial bone healing
Nerve	Polyurethane	Micro-extrusion	Neural stem cells	Recovery from CNS neural injury in zebra fish
Heart	Alginate-gelatin	Micro-extrusion	Aortic root sinus smooth muscle cells (SMC) and aortic valve leaflet interstitial cells (VIC)	Cell encapsulated aortic valve retain anatomic complexity
Liver	Alginate	Micro-extrusion	Human induced pluripotent stem cells	Post-print differentiation into hepatocyte lineage

have focused on developing vascularized constructs using bioprinting, further optimizations are required in this area of research. Simple portable bioprinters can also be fabricated in the near future to address various clinical challenges. As well, further improvements in fabrication technologies and bio inks should be aspired to fabricate fully functional tissues/organs for various applications in the realm of regenerative medicine.[62]

1.4. References

1. Polak, J.M. and A.E. Bishop, *Stem cells and tissue engineering: past, present, and future.* Annals of the New York Academy of Sciences, 2006. **1068**(1): p. 352-366.
2. Andrews, P., et al., *Embryonic stem (ES) cells and embryonal carcinoma (EC) cells: opposite sides of the same coin*. 2005, Portland Press Ltd.
3. Wagers, A.J. and I.L. Weissman, *Plasticity of adult stem cells.* Cell, 2004. **116**(5): p. 639-648.
4. Lysaght, T., et al., *Oversight for clinical uses of autologous adult stem cells: lessons from international regulations.* Cell Stem Cell, 2013. **13**(6): p. 647-651.
5. Prockop, D.J., *Marrow stromal cells as stem cells for nonhematopoietic tissues.* Science, 1997. **276**(5309): p. 71-74.
6. Afanasyev, B.V., E.E. Elstner, and A.R. Zander, *AJ Friedenstein, founder of the mesenchymal stem cell concept.* Cell Ther Transplant, 2009. **1**(3): p. 35-38.
7. Chamberlain, G., et al., *Concise review: mesenchymal stem cells: their phenotype, differentiation capacity, immunological features, and potential for homing.* Stem cells, 2007. **25**(11): p. 2739-2749.
8. Le Blanc, K. and M. Pittenger, *Mesenchymal stem cells: progress toward promise.* Cytotherapy, 2005. **7**(1): p. 36-45.
9. Rustad, K.C. and G.C. Gurtner, *Mesenchymal stem cells home to sites of injury and inflammation.* Advances in wound care, 2012. **1**(4): p. 147-152.
10. Hofstetter, C., et al., *Marrow stromal cells form guiding strands in the injured spinal cord and promote recovery.* Proceedings of the National Academy of Sciences, 2002. **99**(4): p. 2199-2204.
11. Iso, Y., et al., *Multipotent human stromal cells improve cardiac function after myocardial infarction in mice without long-term engraftment.* Biochemical and biophysical research communications, 2007. **354**(3): p. 700-706.
12. Mahmood, A., D. Lu, and M. Chopp, *Intravenous administration of marrow stromal cells (MSCs) increases the expression of growth factors in rat brain after traumatic brain injury.* Journal of neurotrauma, 2004. **21**(1): p. 33-39.
13. Wu, G.D., et al., *Migration of mesenchymal stem cells to heart allografts during chronic rejection.* Transplantation, 2003. **75**(5): p. 679-685.
14. Horwitz, E.M., et al., *Isolated allogeneic bone marrow-derived mesenchymal cells engraft and stimulate growth in children with osteogenesis imperfecta: Implications for cell therapy of bone.* Proceedings of the National Academy of Sciences, 2002. **99**(13): p. 8932-8937.
15. Satija, N.K., et al., *Mesenchymal stem cell-based therapy: a new paradigm in regenerative medicine.* Journal of cellular and molecular medicine, 2009. **13**(11-12): p. 4385-4402.
16. Liu, Y. and D.-A. Wang, *Viral vector-mediated transgenic cell therapy in regenerative medicine: safety of the process.* Expert opinion on biological therapy, 2015. **15**(4): p. 559-567.

17. Hamann, A., A. Nguyen, and A.K. Pannier, *Nucleic acid delivery to mesenchymal stem cells: a review of nonviral methods and applications.* Journal of biological engineering, 2019. **13**(1): p. 7.
18. Devine, S.M., et al., *Mesenchymal stem cells distribute to a wide range of tissues following systemic infusion into nonhuman primates.* Blood, 2003. **101**(8): p. 2999-3001.
19. Yap, M.S., et al., *Neural differentiation of human pluripotent stem cells for nontherapeutic applications: toxicology, pharmacology, and in vitro disease modeling.* Stem Cells International, 2015. **2015**.
20. Katoh, M., *Regulation of WNT signaling molecules by retinoic acid during neuronal differentiation in NT2 cells: threshold model of WNT action.* International journal of molecular medicine, 2002. **10**(6): p. 683-687.
21. Almeida, A.S.C., *Carbon Monoxide modulation of neuronal differentiation.* 2016.
22. Spitzer, N.C., *Electrical activity in early neuronal development.* Nature, 2006. **444**(7120): p. 707.
23. Pleasure, S.J., C. Page, and V. Lee, *Pure, postmitotic, polarized human neurons derived from NTera 2 cells provide a system for expressing exogenous proteins in terminally differentiated neurons.* Journal of Neuroscience, 1992. **12**(5): p. 1802-1815.
24. Cheung, W.M., et al., *Production of human CNS neurons from embryonal carcinoma cells using a cell aggregation method.* BioTechniques, 1999. **26**(5): p. 946-954.
25. Podrygajlo, G., *Doctor of Philosophy-Ph. D*. 2009, Citeseer.
26. Newman, M.B., et al., *Tumorigenicity issues of embryonic carcinoma-derived stem cells: relevance to surgical trials using NT2 and hNT neural cells.* Stem cells and development, 2005. **14**(1): p. 29-43.
27. Nguyen, H., et al., *Stem Cell-Paved Biobridge: A Merger of Exogenous and Endogenous Stem Cells Toward Regenerative Medicine in Stroke*, in *Cellular and Molecular Approaches to Regeneration and Repair*. 2018, Springer. p. 153-180.
28. Hara, K., et al., *Neural progenitor NT2N cell lines from teratocarcinoma for transplantation therapy in stroke.* Progress in neurobiology, 2008. **85**(3): p. 318-334.
29. Dunbar, C.E., et al., *Gene therapy comes of age.* Science, 2018. **359**(6372): p. eaan4672.
30. Wirth, T., N. Parker, and S. Ylä-Herttuala, *History of gene therapy.* Gene, 2013. **525**(2): p. 162-169.
31. Anderson, W.F., *The current status of clinical gene therapy*. 2002, Mary Ann Liebert, Inc.
32. Gomez-Puerto, M.C., et al., *Bone morphogenetic protein receptor signal transduction in human disease.* The Journal of pathology, 2019. **247**(1): p. 9-20.
33. LORENTE, E.C., et al., *AAV-Mediated Overexpression of BMP7 in White Adipose Tissue Induces Adipogenesis and Ameliorates Insulin Resistance*. 2018, Am Diabetes Assoc.
34. Wu, M., G. Chen, and Y.-P. Li, *TGF-β and BMP signaling in osteoblast, skeletal development, and bone formation, homeostasis and disease.* Bone research, 2016. **4**: p. 16009.
35. Ning, J., et al., *Opposing roles and potential antagonistic mechanism between TGF-β and BMP pathways: Implications for cancer progression.* EBioMedicine, 2019.
36. Yin, H., et al., *Non-viral vectors for gene-based therapy.* Nature Reviews Genetics, 2014. **15**(8): p. 541-555.
37. Betker, J.L. and T.J. Anchordoquy, *Effect of charge ratio on lipoplex-mediated gene delivery and liver toxicity.* Therapeutic delivery, 2015. **6**(11): p. 1243-1253.
38. Hayat, S.M.G., et al., *Gene delivery using lipoplexes and polyplexes: principles, limitations and solutions.* Critical Reviews™ in Eukaryotic Gene Expression, 2019. **29**(1).
39. del Pozo-Rodríguez, A., M.Á. Solinís, and A. Rodríguez-Gascón, *Applications of lipid nanoparticles in gene therapy.* European Journal of Pharmaceutics and Biopharmaceutics, 2016. **109**: p. 184-193.
40. Keles, E., et al., *Recent progress in nanomaterials for gene delivery applications.* Biomaterials science, 2016. **4**(9): p. 1291-1309.

41. Saffari, M., H.R. Moghimi, and C.R. Dass, *Barriers to liposomal gene delivery: from application site to the target.* Iranian journal of pharmaceutical research: IJPR, 2016. **15**(Suppl): p. 3.
42. Balbino, T.A., et al., *Continuous flow production of cationic liposomes at high lipid concentration in microfluidic devices for gene delivery applications.* Chemical engineering journal, 2013. **226**: p. 423-433.
43. Zylberberg, C., et al., *Engineering liposomal nanoparticles for targeted gene therapy.* Gene therapy, 2017. **24**(8): p. 441.
44. Tang, Y., et al., *Overcoming the Reticuloendothelial System Barrier to Drug Delivery with a "Don't-Eat-Us" Strategy.* ACS nano, 2019.
45. Grijalvo, S., et al., *Cationic niosomes as non-viral vehicles for nucleic acids: challenges and opportunities in gene delivery.* Pharmaceutics, 2019. **11**(2): p. 50.
46. Moghassemi, S. and A. Hadjizadeh, *Nano-niosomes as nanoscale drug delivery systems: an illustrated review.* Journal of controlled release, 2014. **185**: p. 22-36.
47. Muzzalupo, R. and L. Tavano, *Niosomal drug delivery for transdermal targeting: recent advances.* Research and Reports in Transdermal Drug Delivery, 2015. **4**: p. 23.
48. Attia, N., et al., *Behaviour and ultrastructure of human bone marrow-derived mesenchymal stem cells immobilised in alginate-poly-l-lysine-alginate microcapsules.* Journal of microencapsulation, 2014. **31**(6): p. 579-589.
49. Santos, E., et al., *Therapeutic cell encapsulation: ten steps towards clinical translation.* Journal of Controlled Release, 2013. **170**(1): p. 1-14.
50. Choe, G., et al., *Hydrogel biomaterials for stem cell microencapsulation.* Polymers, 2018. **10**(9): p. 997.
51. Thomas, D., T. O'Brien, and A. Pandit, *Toward Customized Extracellular Niche Engineering: Progress in Cell-Entrapment Technologies.* Advanced Materials, 2018. **30**(1): p. 1703948.
52. Chen, F.-M. and X. Liu, *Advancing biomaterials of human origin for tissue engineering.* Progress in polymer science, 2016. **53**: p. 86-168.
53. Valero, C., et al., *Combined experimental and computational characterization of crosslinked collagen-based hydrogels.* PloS one, 2018. **13**(4): p. e0195820.
54. Ahmed, S., A. Ali, and J. Sheikh, *A review on chitosan centred scaffolds and their applications in tissue engineering.* International journal of biological macromolecules, 2018. **116**: p. 849-862.
55. Gazda, L.S., et al., *No evidence of viral transmission following long-term implantation of agarose encapsulated porcine islets in diabetic dogs.* Journal of diabetes research, 2014. **2014**.
56. Acarregui, A., et al., *A perspective on bioactive cell microencapsulation.* BioDrugs, 2012. **26**(5): p. 283-301.
57. Kaur, G., et al., *Biomaterials for Cell Encapsulation: Progress Toward Clinical Applications*, in *Clinical Applications of Biomaterials*. 2017, Springer. p. 425-458.
58. Ahmadian, E., et al., *The Potential Applications of Hyaluronic Acid Hydrogels in Biomedicine.* Drug research, 2019.
59. Zhang, X. and Y. Zhang, *Tissue engineering applications of three-dimensional bioprinting.* Cell biochemistry and biophysics, 2015. **72**(3): p. 777-782.
60. Gao, B., et al., *4D bioprinting for biomedical applications.* Trends in biotechnology, 2016. **34**(9): p. 746-756.
61. Sundaramurthi, D., S. Rauf, and C. Hauser, *3D bioprinting technology for regenerative medicine applications.* 2016.
62. Norotte, C., et al., *Scaffold-free vascular tissue engineering using bioprinting.* Biomaterials, 2009. **30**(30): p. 5910-5917.

Chapter 2

Objectives

Gene therapy based on non-viral gene carriers is a relatively emerging science, and despite the great achievements as yet, scientists still face persistent challenges. Nevertheless, along with the promise of gene editing, non-viral delivery methods are likely to become more efficient and less toxic.

One of the most promising non-viral gene carriers are the niosomes. Though, their use is hampered by the limited gene delivery efficacy. Once transfected, stem cells depict promising features to become, by themselves, a good gene delivery tool. The main objective of this thesis is the use of novel niosome vehicles to transfect stem cells to enhance their potential in regenerative medicine. To accomplish the aim of this thesis, we established different objectives:

1. To develop and characterize a novel niosome formulation based on the cationic lipid 2,3-di(tetradecyloxy)propan-1- amine (D), combined with polysorbate 80 (DP80 niosomes) for hBMP7 gene delivery to mesenchymal stem cells, *in vitro*.
2. To investigate the impact of hBMP7 gene overexpression by the transfected MSCs on their osteogenic differentiation through the analysis of the alkaline phosphatase activity (ALP), Von Kossa staining and ultrastructural analysis by transmission electron microscopy (TEM).
3. To study the effect of the combined use of two nonionic surfactants, poloxamer 188 (P) and polysorbate 80 (P80) into niosomes based on 2,3-di(tetradecyloxy)propan-1-amine cationic lipid (D) as a gene delivery tool (DPP80 niosomes) for NT2 cells, primary cerebral cortex cell culture, and rat *in vivo* cerebral cortex.
4. To explore the potential effect of NT2 cells transfected by DPP80 niosomes, to overexpress the hBMP7, to mitigate the migration of glioblastoma (C6) cells, *in vitro*.

Chapter 3

Nanomedicine: Nanotechnology, Biology and Medicine

Volume 14, Issue 2, February 2018, Pages 521-531

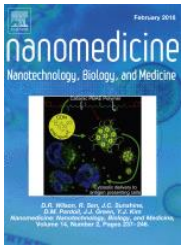

Stem cell-based gene delivery mediated by cationic niosomes for bone regeneration

Noha Attia[a,b,*], Mohamed Mashal[a,*], Santiago Grijalvo[c,d], Ramon Eritja[c,d], Jon Zárate[a,d], Gustavo Puras[a, d] and José Luis Pedraz[a, d].

[a] NanoBioCel Group, Laboratory of Pharmaceutics, School of Pharmacy, University of the Basque Country (UPV/EHU), Paseo de la Universidad 7, 01006 Vitoria-Gasteiz, Spain.
[b] Histology and Cell Biology Department, Faculty of Medicine, University of Alexandria, Alexandria, Egypt.
[c] Institute of Advanced Chemistry of Catalonia (IQAC-CSIC), Spain.
[d] Biomedical Research Networking Centre in Bioengineering, Biomaterials and Nanomedicine (CIBER-BBN), Spain.
* Noha Attia and Mohamed Mashal contributed equally to this work.

Stem cell-based gene delivery mediated by cationic niosomes for bone regeneration

Abstract

Bone morphogenetic protein-7 (BMP7) plays a pivotal role in the transformation of mesenchymal stem cells (MSCs) into bone. However, its impact is hampered due to its short half-life. Therefore, gene therapy may be an interesting approach to deliver BMP7 gene to D1-MSCs. In this manuscript we prepared and characterized niosomes based on cationic lipid 2,3-di(tetradecyloxy)propan-1-amine, combined with polysorbate 80 for gene delivery purposes. Niosomes were characterized and combined initially with pCMS-EGFP reporter plasmid, and later with pUNO1-hBMP7 plasmid to evaluate osteogenesis differentiation. Additionally, specific blockers of most relevant endocytic pathways were used to evaluate the intracellular disposition of complexes. MSCs transfected with niosomes showed increased growth rate, enhanced alkaline phosphatase activity (ALP) and extracellular matrix deposition which suggested the formation of osteoblast-like cells. We concluded that hBMP7-transfected MSCs could be considered not only as an effective delivery tool of hBMP7, but also as proliferating and bone forming cells for bone regeneration.

Key words: bone regeneration; stem cells; gene delivery; niosomes

3.1. Introduction

Bone marrow-derived mesenchymal stem cells (BM-MSCs) have a multi-directional differentiation capacity into bone, cartilage, and epithelial cells when cultured in the appropriate inductive media.[1] Additionally, BM-MSCs are very appealing cells due to their immunomodulatory features, allowing for allogeneic administration.[2,3] When they are genetically modified, their ability to regenerate morbid osseous tissue is notably enhanced, which provides a promising *ex vivo* approach for clinical orthopedic applications.[4,5] Several genes have been delivered and overexpressed in MSCs to promote both proliferation and differentiation into osteoblastic cells.[6]

Bone morphogenetic protein-7 (BMP7) is known to be beneficial for attachment, proliferation, as well as for differentiation of pre-osteoblasts.[6,7] Although the use recombinant human BMP7 protein, also known as osteogenic protein-1 (OP-1) was approved by FDA to improve the

osteogenic differentiation of MSCs, its local stimulatory impact is hampered by diffusion and/or degradation leading to a short half-life.[8] Therefore, MSC-based hBMP7 gene therapy represents an interesting approach since it could boost bone repair by prolonged protein production in a more physiologic manner. Furthermore, MSCs supply can be crucial, especially when the number of MSCs are reduced in osteoporosis.[9]

Non-viral vectors have attracted great attention as safer alternatives of viral-based gene delivery vehicles since they can avoid several concerns such as; immunogenic, mutagenic and oncogenic effects.[10] Additionally, non-viral gene carriers render the ability to deliver large-sized genes and are of low production costs. Consequently, the applications of non-viral vectors in clinical trials have increased considerably since 2004.[11] However, non-viral formulations are still limited, mainly by their modest transfection efficiency. Therefore, this topic demands great efforts of the scientific community.[12]

Niosomes as self-assembled vesicular nano carriers are composed of non-ionic surfactants and cationic lipids.[13] Being chemically stable, easily handled and well-tolerated formulations,[14] niosomes are considered advantageous over liposomes.[15] Our group has recently reported encouraging *in vitro* and *in vivo* gene delivery applications of a liposomal formulation based on the novel cationic lipid 2,3-di(tetradecyloxy)propan-1-amine.[16] In light of such findings, our main goal was the development of a novel niosome formulation based on the aforementioned cationic lipid combined with polysorbate 80 to deliver and transfect hBMP7 plasmid in MSCs. Additionally, the impact of such transfection on MSC *in vitro* osteogenic differentiation was evaluated.

Firstly, niosomes were elaborated by the reverse phase evaporation technique, and characterized in terms of size, superficial charge and morphology. As a proof of concept of successful gene delivery and expression, pCMS-EGFP reporter plasmid was used to obtain nioplexes in order to transfect D1-MSCs, before the transfection efficiency evaluation of nioplexes based on pUNO1-hBMP7 plasmid. Finally, the impact of hBMP7 gene expression on cell osteogenic differentiation was analyzed with alkaline phosphatase activity (ALP), Von Kossa staining and ultrastructural analysis by transmission electron microscopy (TEM).

3.2. Methods

3.2.1. Production of cationic niosomes

The hydrochloride salt of the cationic lipid 2,3-di (tetradecyloxy)propan-1-amine (**DTPA-Cl**) was synthesized by a slight modification of the experimental protocol described previously.[17] Once the cationic lipid was produced, niosomes were elaborated by modified reverse phase evaporation technique.[18] Briefly, 5mg of cationic lipid were dissolved in 1 ml of dichloromethane, and then emulsified in 5 ml of polysorbate 80 (**P80**) (0.5% w/v). The emulsion was obtained by sonication (Branson Sonifier 250®, Branson Ultrasonics Corporation, Danbury, USA) at 45 W for 30 s. Upon dichloromethane evaporation, a dispersion containing the nanoparticles was formed by precipitation of the cationic nanoparticles in the aqueous medium. The resulting niosomes referred as **DP80** contained both **DTPA-Cl** and **P80** at a molar ration of 1:2.

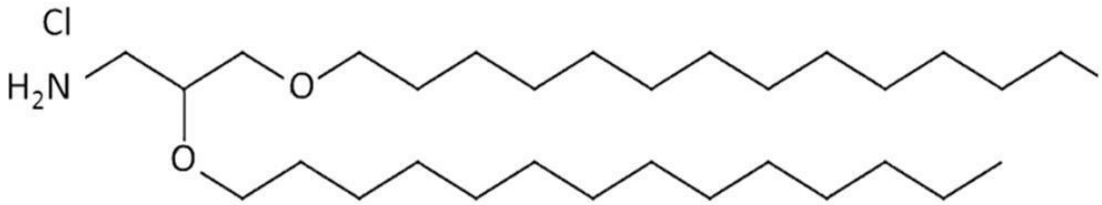

A. 2,3-Di (tetradecyloxy)propan-1-amine (DTPA Chloride salt)

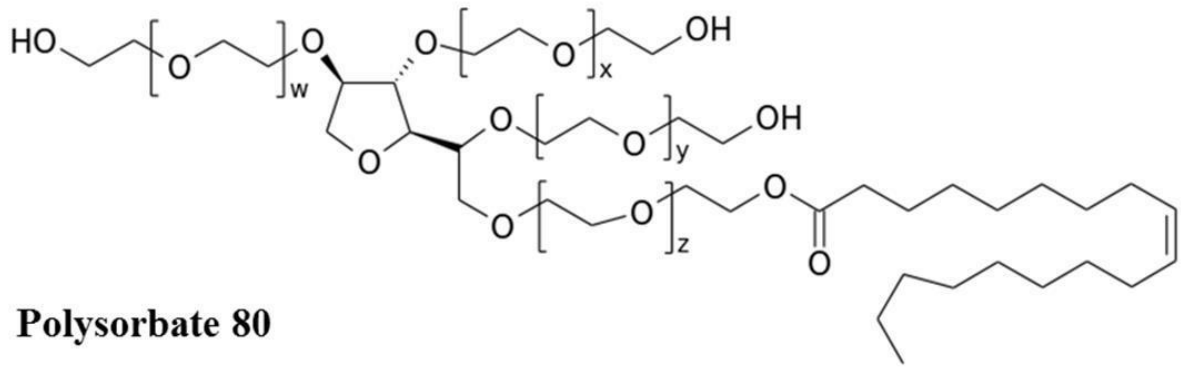

B. Polysorbate 80

Figure 1: Chemical structure of the components of DP80 niosomes (A. Cationic lipid DTPA-Cl, B. Polysorbate 80)

3.2.2. Plasmid propagation and elaboration of nioplexes

pCMS-EGFP reporter plasmid (5541 bp, PlasmidFactory, Bielefeld, Germany), was propagated, purified and quantified as previously described.[19] pUNO1-hBMP7 plasmid (4497 bp) was purchased from InvivoGen (Toulouse, France). Nioplexes (niosome/DNA complexes) were

elaborated by mixing an appropriate volume of a stock solution of pCMS-EGFP/pUNO1-hBMP7 plasmids (0.5 mg/) with different volumes of niosome suspensions (1mg cationic lipid/ml) to obtain different cationic lipid/DNA ratios (w/w). The mixture was left for 30 min at room temperature to enhance electrostatic interaction. Nioplexes were referred as DP80-EFGP or DP80-hBMP7 depending on the plasmid used.

3.2.3. Characterization of niosomes and DP80-EFGP nioplexes

Particle size and zeta potential (ZP) were determined by dynamic light scattering (DLS) and Laser Doppler Velocimetry (LDV) (Zetasizer Nano ZS, Malvern Instruments, UK). Particle size was obtained by cumulative analysis. All measurements were carried out in triplicate. The morphology of nioplexes was assessed by cryo-TEM analysis.[20] Digital images were acquired for samples examined by TEM, TECNAI G2 20 TWIN (FEI), operating at an accelerating voltage of 200 KeV in a bright-field and low-dose image mode.

The capacity of niosomes to condense, release and protect DNA from enzymatic digestion was performed by agarose gel electrophoresis assay using pCMS-EGFP plasmid. Naked DNA (as control) or niosome-complexed DNA samples (200 ng of plasmid/20 µl) were run on agarose gel (0.8% w/v), stained with GelRed™. The gel was immersed in a Tris–acetate–EDTA buffer and exposed for 30 min to 120 V. Bands were visualized by ChemiDoc™ MP Imaging System (Bio-Rad, Madrid, Spain). To analyze DNA release from nioplexes at different cationic lipid/DNA mass ratios, 20µl of a 2% SDS solution (Sigma-Aldrich, Madrid, Spain) was added to each sample. Protection capacity of nioplexes against enzymatic digestion was studied after adding DNase I (Sigma-Aldrich, Madrid, Spain) at a final concentration of 1U DNase I/2.5µg DNA. Afterwards, mixtures were incubated at 37°C for 30 min. Finally, a 2% SDS solution was added to release DNA from nioplexes.

3.2.4. Culture and characterization of D1-MSCs

Mouse mesenchymal stem cells (ATCC®CRL-12424™) (D1-MSCs) were cultured in growth medium (GM) composed of: Dulbecco's modified Eagle's medium (DMEM) (ATCC 30−2002) supplemented with 10% fetal bovine serum (FBS) and 1% penicillin/streptomycin, (both reagents from Gibco, Spain). Cell multipotency was determined by differentiation into osteogenic and adipogenic lineages as reported in previous work.[1] After two weeks, cells were stained with Alizarin Red S (osteogenic differentiation) and Oil Red O (adipogenic differentiation).

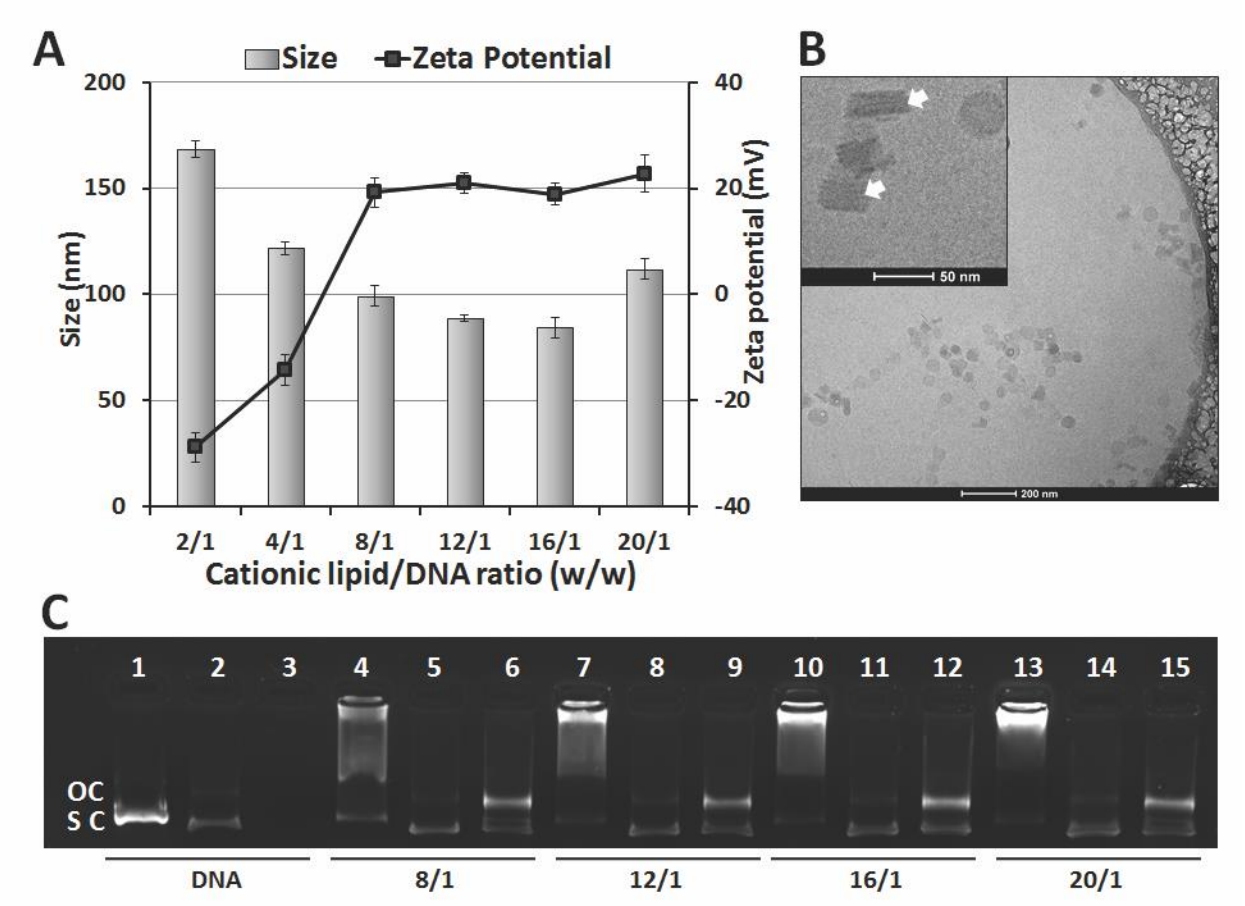

Figure 2: Physicochemical characterization of DP80-EGFP nioplexes (A) Effect of cationic lipid/DNA ratio (w/w) on both particle size (bars) and ZP (line), n = 3. (B) Cryo-TEM micrographs of nioplexes at 16/1 cationic lipid/DNA ratio (w/w). Arrows indicate lamellar pattern. Scale bar =200 nm (inset scale bar =50 nm). (C) Binding, SDS-induced release and protection of DNA at different cationic lipid/DNA ratios (w/w) of DP80-EGFP- nioplexes visualized by agarose electrophoresis. Nioplexes were treated with SDS (lanes 2, 5, 8, 11 and 14) and DNase I + SDS (lanes 3, 6, 9, 12 and 15). OC: open circular form, SC: supercoiled form.

3.2.5. Reporter EGFP plasmid *in vitro* transfection

D1-MSCs were seeded at a density of 9×10^4 cells/well in 24-well plates. 24 h later, GM was removed, and cells were washed with serum-free Opti-MEM® solution (Gibco®, California, USA). Then, cells were exposed to DP80-EFGP nioplexes (1.25 µg DNA) at different cationic lipid/DNA ratios (w/w), and incubated in serum-free Opti-MEM® solution for 4 h at 37°C. Subsequently, transfection medium was replaced with GM, and cells were allowed to grow for further 48 h until fluorescence microscopy imaging (Nikon TSM) and FACSCalibur flow cytometer analysis (BD Biosciences, USA). To analyze cell viability, cells were stained with Propidium Iodide (Sigma-

Aldrich, Madrid, Spain) prior to flow cytometer analysis. Experiments with uncomplexed DNA was considered as negative control. Regarding to positive control, both TransIT® 2020 (Mirus, Madrid, Spain) (at a ratio of 3µl of reagent/1µg of DNA) and Lipofectamine® 2000 (L2000) (Invitrogen, California, USA) were used. A minimum of 10.000 events were acquired and analyzed for each sample in triplicate.

3.2.6. Endocytosis uptake mechanism for nioplexes

Several uptake inhibitors were used to determine the endocytosis mechanism by nioplexes. Genistein and chlorpromazine hydrochloride were used as inhibitors for caveolae-mediated endocytosis (CvME) and clathrin-mediated endocytosis (CME), respectively. Methyl-β-cyclodextrin was used to simultaneously inhibit CvME and CME. Additionally, wortmannin, was employed to inhibit macropinocytosis (MPC).

D1-MSCs were transfected as mentioned in the previous **3.2.5** section, but in this case, nioplexes were prepared with FITC-labeled EGFP plasmid (DareBio, Madrid, Spain). Cells were incubated for 30 min with genistein 200 µM, methyl- β -cyclodextrin 5 mM and wortmannin 50 nM, and for 60 min with chlorpromazine hydrochloride 5 µg/ml prior to addition of nioplexes. After 4 h of incubation with nioplexes, cells were washed thoroughly with PBS, detached, and analyzed by FACSCalibur flow cytometer (BD Biosciences, USA). For each sample, 10.000 events were collected and analyzed. Cellular uptake data were expressed as the percentage of FITC-positive cells. Naked DNA was used as a negative control. Each sample was analyzed in triplicate.

3.2.7. Characterization of DP80-hBMP7 nioplexes, *in vitro* transfection and proliferation/cytotoxicity assay

DP80-hBMP7 nioplexes were characterized at different mass ratios as previously described in the section **3.2.3.** Subsequently, transfection of D1-MSCs was performed using DP80-hBMP7 nioplexes using the transfection protocol described in section **3.2.5**. After 48 h post-transfection, conditioned media was collected, filtered (0.22 µm filters) and preserved at - 80°C until ELISA was performed (R&D, UK) to determine the hBMP7 secreted. CCK-8 viability/proliferation assay (Sigma Aldrich, Spain) was performed according to manufacturer's instructions. Color development was read at 450 nm (Tecan M200 microplate reader), corrected with reference wavelength at 690 nm and normalized against mean value of three blank wells (GM).

3.2.8. *In vitro* assessment of osteogenesis

Transfection protocol of DP80-hBMP7 nioplexes was applied as mentioned in section **3.2.5.** On day 2 post-transfection, both cell cultures in transfected and untransfected (control) wells were allowed to continue in growth medium/ osteogenic medium (GM/OM) to determine the impact of hBMP7 transfection on the osteogenesis potential of D1-MSCs. Therefore, cells were classified in four different groups: untransfected culture in GM/OM, transfected culture in GM/OM. After 2 weeks, the following *in vitro* assays were performed.

3.2.8.1. Alkaline Phosphatase (ALP) activity assay

D1-MSCs from the four groups were washed and 500 µl of GM were added. After 24h of incubation, conditioned media were collected, filtered (0.22 µm filters) and ALP activity assay was performed according to manufacturer's instructions. ALP activity of each sample was read at 405 nm (Tecan M200 microplate reader) and normalized to 100.000 cells.

3.2.8.2. Von Kossa Staining

For qualitative assessment of calcium deposits, Von Kossa staining (Abcam, UK) was performed as previously reported.[21] Micrographs were digitally processed using NIH Fiji© program.

3.2.8.3. Transmission electron microscopy (TEM)

D1-MSCs from both untransfected and transfected groups cultured in GM for two weeks were detached and pellets were fixed with 2% gluteraldehyde (pH 7.4) for 24h at 4˚C, processed as previously reported[1] and examined with Philips EM208S TEM.

3.2.9. Statistical analysis

Statistical differences between groups at significance levels of >95% were calculated by ANOVA and Student's *t* test. In all cases, *P* values <0.05 were regarded as significant. Normal distribution of samples was assessed by the Kolmogorov- Smirnov test and the homogeneity of the variance by the Levene test. Numerical data were presented as mean ± SD.

3.3. Results

3.3.1. Physicochemical characterization of niosomes and DP80-EGFP nioplexes

The size of niosomes was 54.0±0.9 nm with PDI vales of 0.5±0.1 and ZP values of 41.9±7.1mV. Figure 2-A depicts size and ZP values of nioplexes at mass ratios from 2/1 to 20/1. The size of nioplexes (bars) decreased from 168 nm to 84 nm at cationic lipid/DNA mass ratios of 2/1 and 16/1, respectively, then increased slightly to 111 nm at 20/1 mass ratio. PDI of all nioplexes were less than 0.3 (Table 1, supplementary data). Concerning ZP, readings were clearly increasing from -28.9mV at 2/1 mass ratio to +19.2mV at 8/1 mass ratio, while afterwards depicted no notable

change. As illustrated in Fig. 2-B, the cryo-TEM-assessed nioplexes (16/1 mass ratio) exhibited a discrete imperfectly spherical morphology with no aggregates. Some nioplexes depicted lamellar pattern at higher magnification (arrows, Fig 2-B inset). More pictures at lower magnification can be observed in Figure 1, on supplementary data. Figure 2-C represents gel retardation assay of DP80-EGFP nioplexes prepared at different cationic lipid/ DNA ratios (8/1, 12/1, 16/1 and 20/1). Partial condensation of DNA was seen since faint SC bands were observed on 4, 7, 10 and 13 lanes. However, condensed DNA was released upon the addition of SDS, as can be observed on lanes 5, 8, 11 and 14. Moreover, complexed DNA was protected against DNase I enzymatic digestion, since clear OC (open circular) and SC (supercoiled) bands were detected on lanes 6, 9, 12 and 15 compared to the absence of OC/SC bands in lane 3 (free DNA).

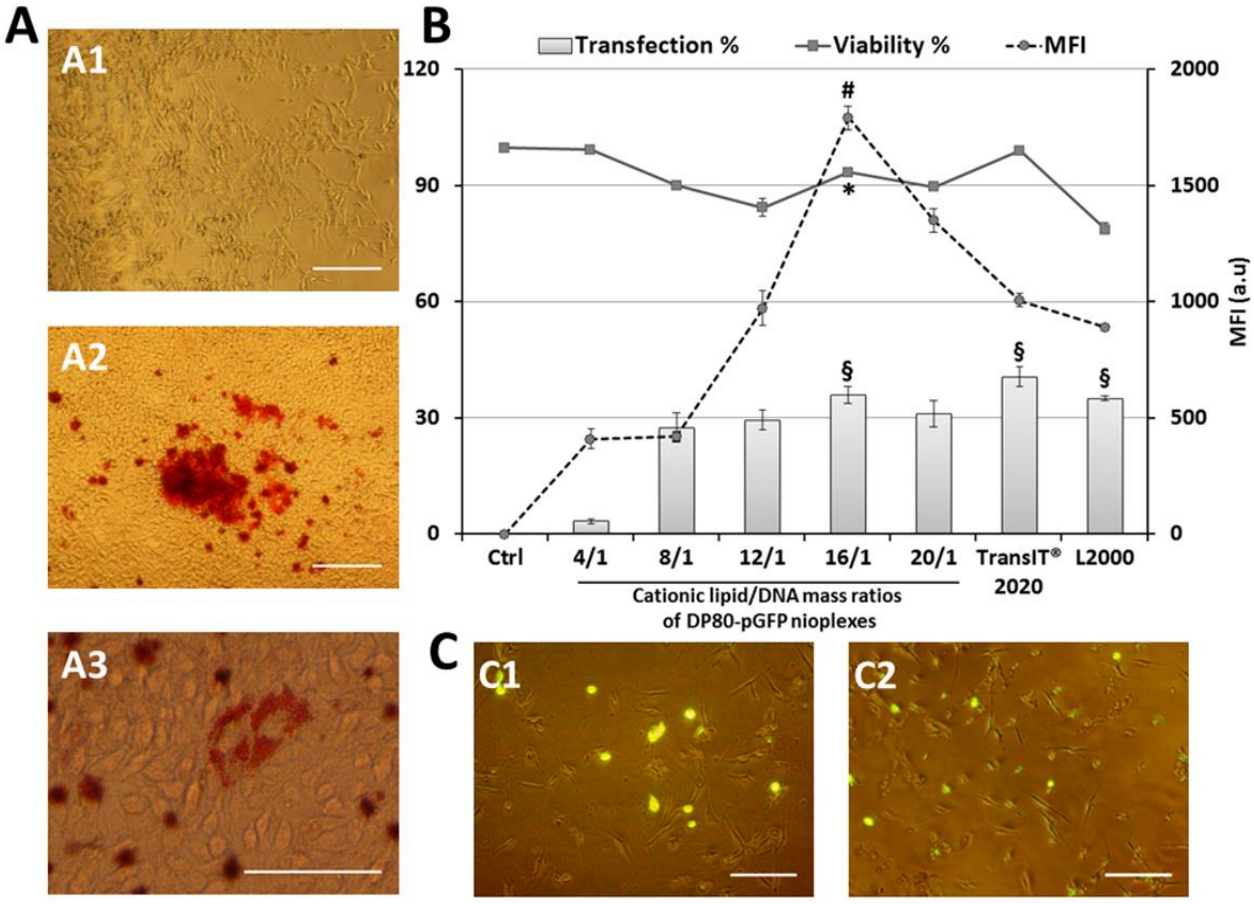

Figure 3: D1-MSCs culture (A1), osteogenic (A2) and adipogenic differentiation (A3). (B) Cell transfection efficiency and viability at different cationic lipid/DNA ratios (w/w). Percentage of EGFP-positive cells (bars), percentage of viable cells (line) and MFI (dashed line), (n = 3). Similar symbol (§) indicate insignificant differences among three bars (P>0.05). $^{*}P < 0.05$ vs. TransIT® 2020 and L2000 viability. $^{\#}P < 0.05$ vs. TransIT® 2020 and L200 MFI. (C) Representative overlay

micrographs of D1-MSCs 48 h post-transfection via (C1) DP80-EGFP nioplexes (16/1 cationic lipid/DNA mass ratio) and (C2) TransIT® 2020. Scale bars: A1, A2, B1 and B2 = 50 μm and A3= 25 μm.

3.3.2. *In vitro* culture, transfection and viability of MSCs by reporter EGFP plasmid

Cultured D1-MSCs were spindle-shaped adherent, colony forming cells (Fig 3-A1). Upon culture in osteogenic or adipogenic media, they demonstrated calcific deposits by Alizarin Red S (Fig 3-A2) and Oil red O-stained cytoplasmic lipid vacuoles (Fig 3-A3), respectively. In figure 3-B, all cationic lipid/DNA ratios (w/w) studied above 4/1 showed considerable percentages of transfection. Meanwhile, naked DNA (control) did not elicit any transfection. The mass ratio of 16/1 represented the best transfection results of 35.9±1.9%, which did neither differ significantly from that obtained by TransIT 2020® (40.7±2.5%) nor by L2000 (35.06±0.5%). On the other hand, cell viability was higher with TransIT 2020® ($p < 0.05$) compared to mass ratio of 16/1 (99.1±0.5% and 93.6±1.2%, respectively). Regarding mean fluorescence intensity (MFI) obtained by our nioplexes at 16/1 as mass ratio, it was markedly higher than that obtained by TransIT 2020® (1792 a.u. and 1006 a.u, respectively). Similar finding was observed in figure 3-C. L2000 had least viability (78.7± 1.3%) and low MFI (891.3± 2.7 a.u.), therefore excluded from further experiments.

3.3.3. Endocytosis uptake mechanism of nioplexes

The uptake of nioplexes at 16/1 mass ratio was determined compared to naked DNA (negative control). Figure 4-A showed representative dot plots for uptake of both free DNA and DP80 nioplexes (0.32% and 83%, respectively). Interestingly, we observed that the selective inhibition of caveolae-mediated (genistein) or clathrin-mediated (chlorpromazine hydrochloride) uptake pathway had significant effects on cellular uptake of nioplexes ($p< 0.05$). However, there was no statistically significant difference between both inhibitors.

When both previously mentioned endocytosis mechanisms were simultaneously inhibited by prior treatment with methyl-β-cyclodextrin, an extremely significant difference was observed when compared to control group ($p< 0.0001$). Nevertheless, wortmannin, an inhibitor of MPC, did not affect the nioplexes internalization ($p> 0.05$).

3.3.4. Physicochemical characterization of DP80-hBMP7-nioplexes

Figure 5-A depicts size and ZP values of nioplexes at different mass ratios (from 2/1 to 20/1). The size of nioplexes (bars) decreased gradually from 217nm at 2/1 cationic lipid/DNA mass ratio to 69 nm at 20/1 mass ratio with PDI values less than 0.3 (Table 1, supplementary data). Regarding ZP values, readings were clearly increasing from -11.1 mV at 2/1 mass ratio to +26.2mV at 8/1

mass ratio, while afterwards, slowly decreased to +18.3 mV at mass ratio of 20/1. As illustrated in figure 5-B, nioplexes, assessed by cryo-TEM, exhibited a discrete spherical/ovoid morphology with no notable clumps. Some nioplexes appeared lamellar at higher magnification (arrows, Fig. 5-B inset). More pictures at lower magnification can be observed in Figure 1, on supplementary data. Figure 5-C illustrated that DNA was partially condensed at mass ratio of 4/1, though complete capture was discerned at mass ratios of 8/1, 12/1, and 16/1, since no SC bands were observed on lanes 7, 10 and 13. Complexed DNA was released after the addition of SDS, as it could be observed on lanes 5, 8, 11 and 14. Except for mass ratio of 4/1, captured DNA was protected against DNase I enzymatic digestion since clear OC/ SC bands were detected on lanes 9, 12 and 15 in comparison to lane 3 (free DNA) due to the unopposed lytic action of the enzyme.

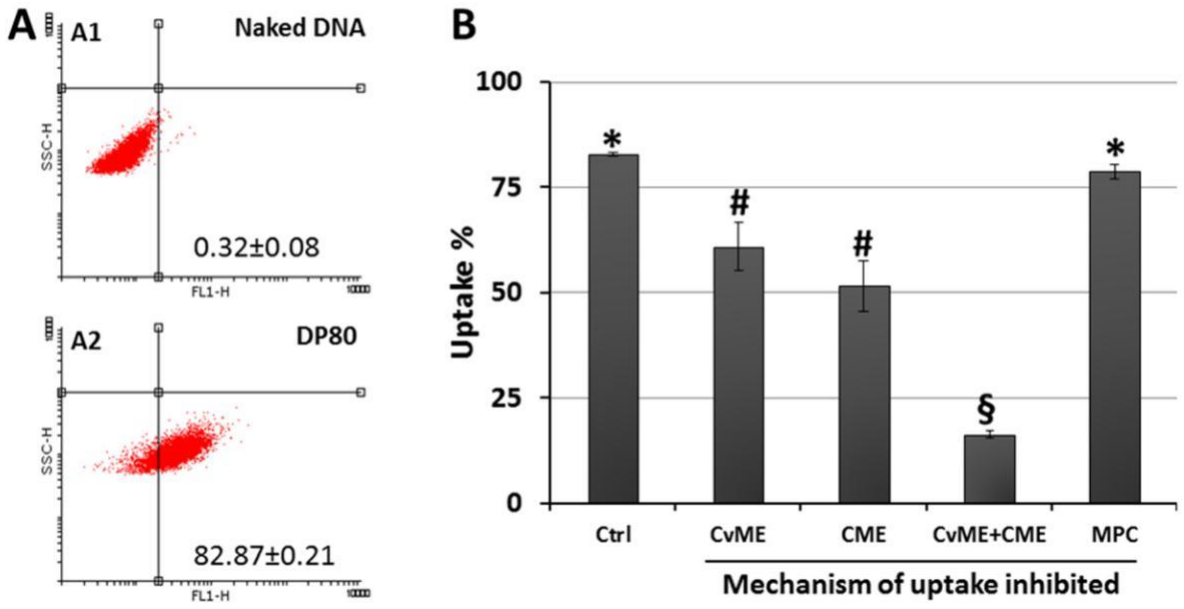

Figure 4: Uptake study of D1-MSCs 4 h post-incubation with FITC-labeled nioplexes. (A) Representative dot plots for cellular uptake, (A1) naked DNA (no carrier), (A2) DP80 nioplexes. (B) Uptake % (FITC-positive cells) in the presence/absence of endocytosis inhibitors. (Ctrl) represents the uptake with no inhibitors. Mean ± SD; n = 3. ($^{*}p<0.05$, $^{***}p< 0.0001$)

3.3.5. Transfection of MSCs by pUNO1 -hBMP7 plasmid

As can be observed in figure 6 (bars), all studied cationic lipid/DNA ratios (w/w) demonstrated significant secretion of hBMP7 protein in comparison to the untransfected cells (controls). The mass ratios of 4/1, 8/1 and 12/1 demonstrated the best transfection results (1460 pg/ml), without

significant differences observed among them ($p > 0.05$), but was still less than secretion obtained by TransIT 2020® transfection (2111 pg/ml) ($p < 0.05$). On the other hand, cell counting assay (CCK8) performed immediately after conditioned media was collected (48h post-transfection) demonstrated that transfection by nioplexes at ratios of 8/1, 12/1, and 16/1 induced significant cell proliferation (164%, 137% and 122%, respectively) compared to control and TransIT 2020® groups (100% and 23%, respectively) (Fig 6, line). Nevertheless, cell viability decreased significantly to 65% at 20/1 cationic lipid/DNA mass ratio.

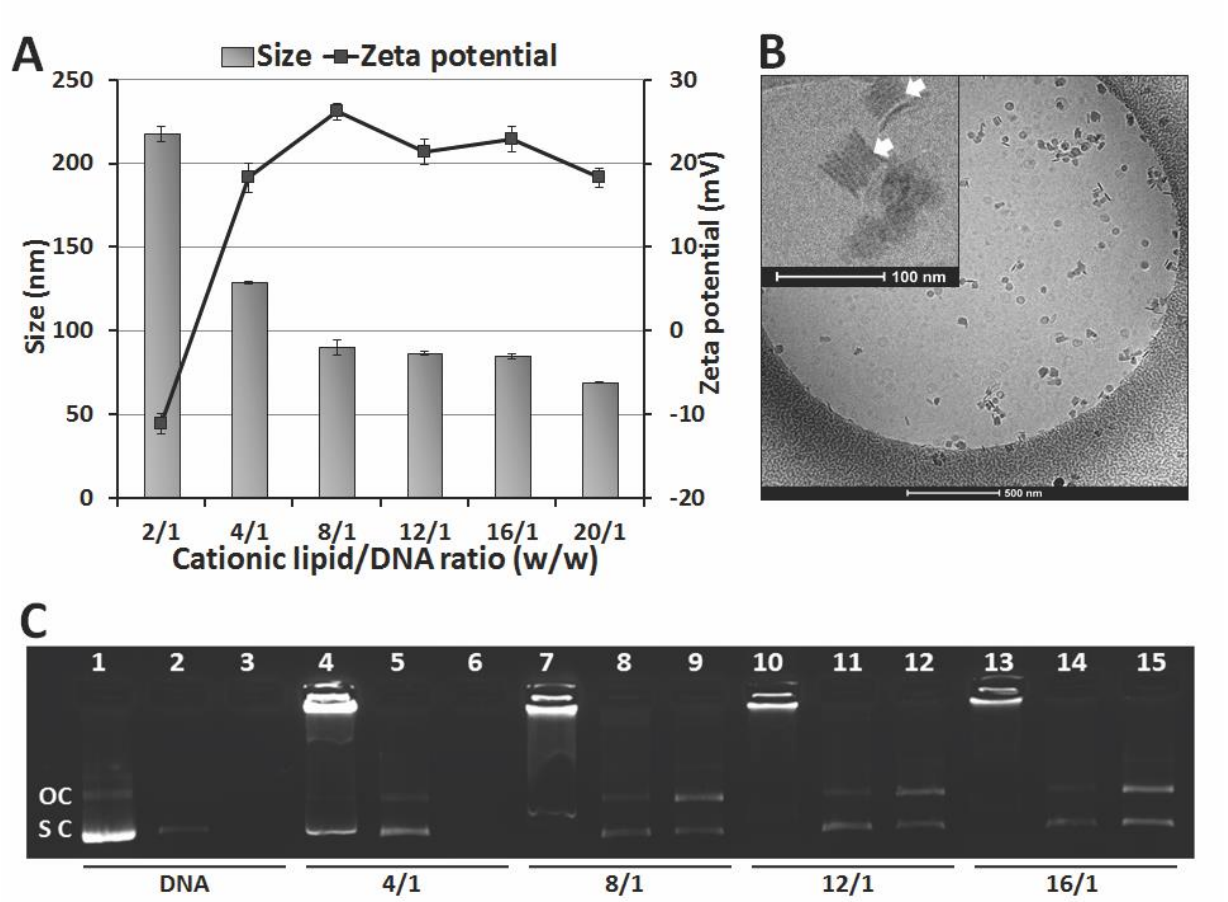

Figure 5: Physicochemical characterization of DP80-hBMP7 nioplexes. (A) Effect of cationic lipid/DNA ratio (w/w) on particle size (bars) and zeta potential (line), n = 3. (B) Cryo-TEM micrographs of nioplexes at ratio of 8/1 cationic lipid/DNA ratio (w/w). Arrows indicate lamellar pattern. Scale bar = 500 nm (inset scale bar =100 nm). (C) Binding, SDS-induced release and protection of DNA at different cationic lipid/DNA ratios (w/w) of DP80-hBMP7 nioplexes visualized by agarose electrophoresis. Nioplexes were treated with SDS (lanes 2, 5, 8, 11 and 14) and DNase I + SDS (lanes 3, 6, 9, 12 and 15). OC: open circular form, SC: supercoiled form.

3.3.6. *In vitro* assessment of osteogenesis

3.3.6.1. Alkaline Phosphatase (ALP) activity assay

As observed in figure 7-A, ALP activity in transfected cell culture was significantly higher whether cells were cultured in GM or OM. Although ALP activity of all groups was superior to untransfected cells cultured in GM ($p < 0.05$), no significant differences were discerned among those groups ($p > 0.05$).

3.3.6.2. Von Kossa Staining

After Von Kossa staining, no calcium deposits were observed in the control group (Fig 7-B1). However, mineralized bone nodules were observed in D1-MSCs cultured in OM (Fig 7-B2). Similar nodules were noticed in culture plates of D1-MSCs transfected with hBMP7, whether cultured in GM or OM (Figs 7-B3 and 7-B4, respectively).

3.3.6.3. Transmission electron microscopy (TEM)

TEM was applied to detect the ultrastructure of untransfected (7-C1) vs. transfected (7-C2) D1-MSCs cultured for two weeks in GM. Electron micrographs of both groups showed large euchromatic nuclei (N) with prominent nucleoli (n). The chromatin was dispersed except for a thin dense layer located immediately inside the nuclear envelope. Although cytoplasmic organelles depicted no obvious change, Golgi complex (arrowhead) was evident in many cells of transfected group (7-C2). In addition, deposition of amorphous extracellular matrix was noticed (arrows).

3.4. Discussion

Our novel niosomes were formulated with cationic lipid salt (DTPA-HCl) and the non-ionic surfactant polysorbate 80 (Fig 1). The cationic lipid, DTPA, has been used for gene delivery applications,[22] though it was not tested neither in salt form, nor as a niosome formulation. Structurally, DTPA-HCl is composed of the four crucial elements that govern the process of gene transfection. Namely, the polar head, backbone, linker and two non-polar tails.[23]During niosome elaboration, we endeavored to circumvent the potential cytotoxicity of the ether linker of DTPA-HCl by decreasing its molar ratio compared to P80 (DTPA-Cl to P80 as 1:2, respectively).

Once synthesized, DP80 niosomes showed appropriate nano-scaled size for gene delivery purposes. High positive ZP values (> +25 mV) would ensure long-lasting stability[24] and spontaneous electrostatic interaction with plasmid DNA. Additionally, it could enhance proper

binding of the resulting nioplexes to the negatively charged cell coat prior to nioplexes internalization.[23]

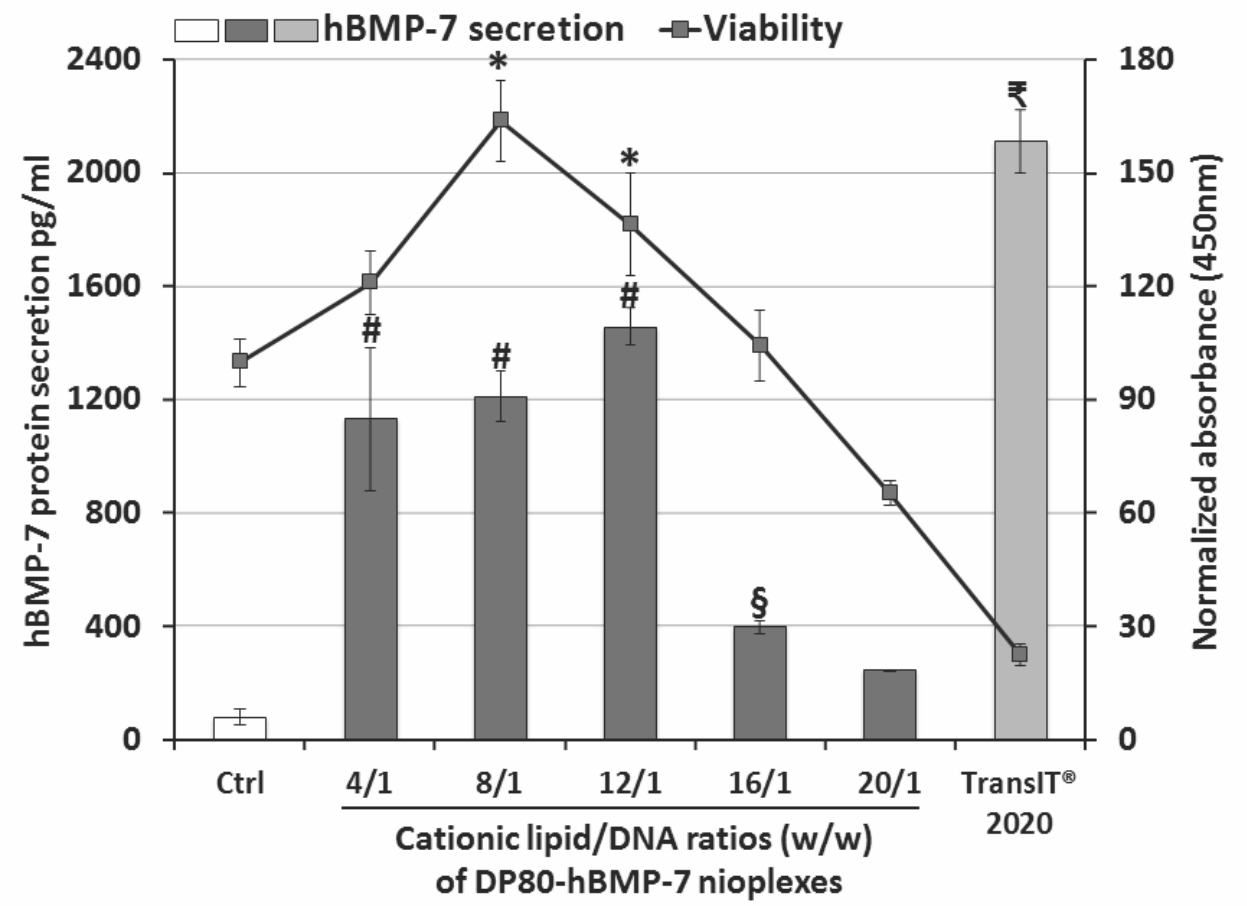

Figure 6: hBMP7 secretion (pg⁄mL) compared to untransfected cells (Ctrl) and TransIT® 2020-transfected cells (Bars). CCK-8 viability assay (line). Values represent mean ± SD (n = 3). Different symbols above bars indicate statistically significant differences. *P < 0.05 compared to all data points of line graph.

To probe the behavior of our niosomes we elaborated, as a proof of concept, DP80-EGFP-nioplexes by adding pCMS-EGFP reporter plasmid to DP80 niosomes at different cationic lipid/DNA mass ratios. Such sequence was adopted to ensure better complex assembly.[25] A gradual decrease in the size of nioplexes was observed (168 - 84 nm, Fig.2-A), at mass ratios studied up to 16/1. Such decline in size is governed by balanced events in a delicate multistep self-assembly process of complex formation, such as: electrostatic interaction, further membrane merging, lipid mixing and aggregate growth.[25] The size of nioplexes is of great importance to grant proper interactions with cell components (organelle membranes and cytoskeletal filaments). The

small size of nioplexes might be advantageous to improve the rate of cellular uptake.[26] In addition, nioplexes would be able to navigate the mammalian cytoskeleton with mesh size about 200 nm.[27] Regarding the ZP values, the gradual initial increase of superficial charge along with cationic lipid/DNA ratios (w/w), followed by a plateau phase, demonstrated the ability of cationic niosomes to bind to and neutralize the negatively charged phosphate groups in plasmid DNA.[28] At small cationic lipid/DNA mass ratios (2/1 and 4/1), the ZP readings were negative and shifted to the positive territory (around +20 mV) at 8/1, 12/1, 16/1, and 20/1 mass ratios. At higher ratios, nioplexes were figured to function as gene delivery carriers taking advantage of their positive surface charge that facilitates proper electrostatic interaction with the anionic glycocalyx during the early steps of the endocytosis.[29]

The shape of complexes has a marked effect on their performance as a gene delivery candidate,[30] albeit, the effect of particle shape on biological interactions is not yet understood. As reviewed by Champion et al,[30] vast observations proved the complexity of cell-particle interactions and revealed the ability of cells to respond differently to varied particle shapes. For instance, non-spherical particles were reported to be internalized faster than the perfectly spherical ones.[26, 31] Cryo-TEM micrographs illustrated that most of the DP80-EGFP complexes were not perfectly spherical (Fig 2-B). Additionally, the discerned discrete morphology of nioplexes with no aggregates (Fig 2-B) could be attributed to the moderately positive surface charge. Interestingly, the lamellar pattern observed in several nioplexes is believed to occur during the process of complex formation by the complete topological transformation of both lipid and DNA into compact quasi-spherical complex particles with diameter around 200 nm, that form string-like colloidal aggregates, inside of which, the complexes have an ordered multi-lamellar planar structure (Fig 2-B, arrows).[32] The regular lamellar spacing of almost 5.5-6 nm (Fig 2-B inset) was similar to that reported by LeBihan and colleagues, denoting that the repetitive motif corresponded to DNA strands complexed with cationic lipid bilayers.[33]

Among other factors that can influence on the transfection process, the electrostatic interactions between the negatively charged phosphate groups of DNA and the positively charged amine groups of the cationic niosomes merits special attention.[20, 28, 34, 35] We observed by agarose gel electrophoresis assay that at all cationic lipid/DNA ratios evaluated, niosomes were able to capture, release and protect the DNA from enzymatic digestion (Fig 2-C).

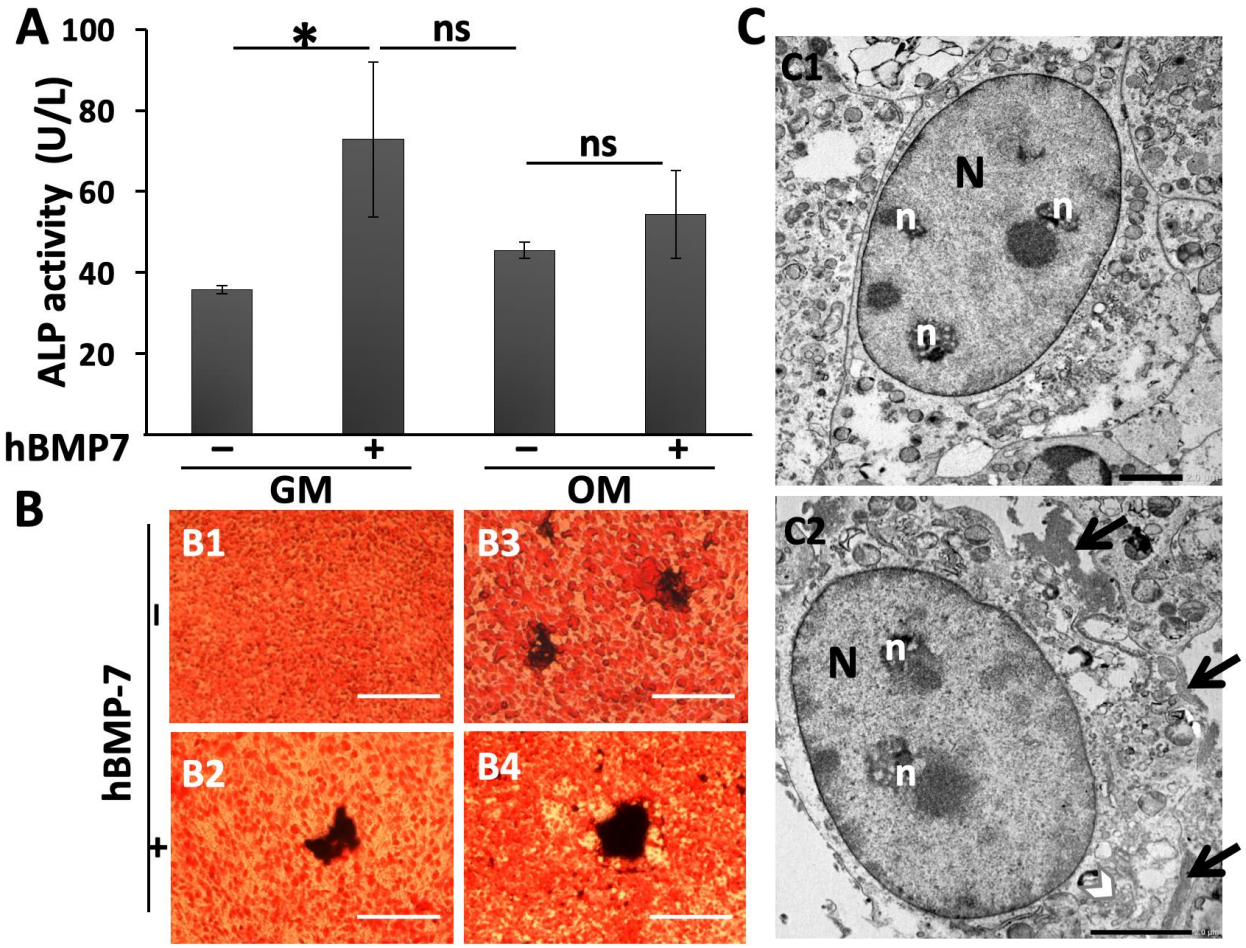

Figure 7: Osteogenic differentiation *in vitro* (A) Validation of ALP activity of the conditioned media of D1-MSCs, n=5. * indicated statistically significant differences ($P < 0.05$). ns indicated no statistically significant differences ($P \geq 0.05$). (B) Representative light micrographs of D1-MSCs culture after Von Kossa staining for calcium deposition. Scale bars = 40µm. GM= Growth Medium, OM = Osteogenic Medium. (C) TEM micrographs for cell ultrastructure in both untransfected (C1) and transfected (C2) cultures. Arrowhead points at Golgi complex, arrows point at extracellular matrix deposits. N = nucleus, n= nucleolus. Scale bars = 2 µm.

Once we evaluated that DP80-EGFP nioplexes would be suitable for gene delivery purposes, we proceeded to evaluate their biological performance *in vitro*. BM-MSCs are of vital importance in adult bone repair as they home to the fracture site, proliferate and serve as a source of osteochondral progenitors. Hence, bone marrow-derived D1-MSCs were selected for the current study. In accordance to our results (Fig 3-A) they were known to represent a multipotent MSC platform holding potential of osteogenic fate determination *in vitro*.[36, 37] Moreover, their

phenotypic characteristics and osteogenic differentiation potential were reported to be consistent with primary human MSCs.[36, 38]

There is a general belief that niosomes are well tolerated both *in vitro* and *in vivo* conditions.[19] Our results (Fig 3-B) illustrated that DP80 (16/1) induced transfection efficiency similar to that obtained by TransIT® 2020 and L2000 commercial reagents (35.8 %, 40.6% and 35.1%, respectively). However, the MFI of the transfected cells (Figs 3-B and 3-C) were significantly higher with DP80 (1791 a.u.) compared to TransIT® 2020 (1006 a.u). Interestingly, cell viability reported with DP80-EGFP nioplexes was significantly higher than that with L2000, while inferior to that reported by TransIT® 2020 commercial reagents. Such cytotoxicity might be induced, even in part, by GFP-induced apoptosis that might result from GFP aggregations or free radicals.[39] In general, the main aim of gene delivery is to attain overexpression of the transfected gene to express the protein in super physiological doses. Thereafter, transfection efficiency is not only a matter of how many cells were transfected, but also the amount of gene expression by the transfected cells. The high transfection efficiency values observed were preceded by a great percentage of nioplexes uptake as shown for best transfection efficiency (16/1) (Fig 4-A). Despite the reported high uptake percentage (almost 83%), the performance of non-viral vectors is known to be clearly affected by their distinct cellular internalization pathway, taking into account the variable effectiveness of every pathway in the release of DNA into the cytoplasm, which is one of the critical steps in the eventual transgene expression.[19] Therefore, we further analyzed intracellular trafficking of our nioplexes by blocking three of the most important endocytosis pathways in mammalian cells,[26,10] namely, caveolae-mediated endocytosis (CvME), clathrin-mediated endocytosis (CME) and macropinocytosis (MPC).

The results observed in figure 4-B suggested that internalization of DP80-EGFP was mainly through CvME and CME with no significant difference between them. Although a robust consensus does not exist, it is widely accepted that the endolysosomal fate is the hallmark feature of CME.[40, 41] Oppositely, CvME and/or MPC routes could be advantageous to avoid lysosomal degradation, which could ensure a better plasmid delivery and integrity.[10,42] Consequently, the relevant contribution of the clathrin-mediated endocytosis pathway, which directs nioplexes to the lysosomes, could explain the relatively low transfection efficiency values observed (35.8%, Fig 3-B), despite the fact that high number of cells (83%, Fig 4-A) captured the complexes.

The promising results obtained with the reporter EGFP plasmid encouraged us to explore hBMP7 gene transfection. As done before with DP80-EGFP nioplexes, we characterized DP80-hBMP7 nioplexes regarding their physicochemical features. As noted in figure 5-A, gradual decline of size correlated to the increased cationic lipid/DNA mass ratio (bars). Starting from mass ratio of 4/1, ZP values observed were in the positive territory that fluctuated between 18.3 and 26.2 mV. Particles were of no perfect shape and mostly acquired the planar lamellar pattern (Fig 5-B). Similar to what has been reported in figure 2-C, DP80-hBMP7 nioplexes were able to bind, release and protect plasmid DNA against DNase I enzymatic digestion (Fig 5-C). These findings suggested that DP80-hBMP7nioplexes could transfect D1-MSCs *in vitro*. The hBMP7 protein secreted after 48 h of transfection (Fig 6) reached its highest value at the ratios of 4-12/1(up to 1460 pg/ml). These results showed that the mass ratios of best transfection efficiency changed with different plasmids used (EGFP at 16/1).

The CCK-8 assay interestingly depicted that cells seemed to proliferate more significantly when transfection was the best at mass ratios of 8/1 and 12/1. This phenomenon might be due to two main factors; first, the negligible cytotoxicity effect of our nioplexes on D1-MSCs at such ratios compared to the higher ratios (16/1 and 20/1), and second, a direct enhancement of mitotic activity of such cells by the released hBMP7 protein[43].

Although TransIT® 2020 induced significantly efficient transfection (2111.5 pg/ml, Fig. 6), it extremely hampered cell viability (23%). This might be referred to the cytotoxic impact of the hBMP7- based TransIT® 2020 complexes that seemed to badly attenuate the initial population of hBMP7secreting cells.[46] Since ELISA assay was performed as early as 48 h post-transfection, the number of cells in TransIT® 2020 samples was not obviously enhanced by the putative mitogenic effect of hBMP7 protein.

Noteworthy that results (shown in figs. 3-B and 6) elucidated the fact that different plasmids could behave differently in regard to transfection efficiency or cell viability. In the current study, both EGFP and hBMP7 plasmids had a different length (5541 and 4497 bp, respectively) and promotors. Therefore, the obtained nioplexes rendered different physicochemical characteristics and thus demonstrated discrepant behavior regarding to transfection efficiency or cell tolerance. [44,45]

We further assessed the effectiveness of hBMP7 overexpression to induce osteogenesis *in vitro* using the alkaline phosphatase activity (Fig 7-A). ALP is considered an important

parameter to assess osteoblastic phenotype as it is required for mineralization, thus induced early during osteoblast differentiation.[46] Both ALP assay and Von Kossa staining (Fig 7-B) of the mineralized bone nodules denoted that hBMP7 expression induced spontaneous osteoblastic differentiation and calcified matrix deposition under standard culture in GM. The amorphous extracellular matrix deposition was further shown at the ultrastructural level in figure 7-C2. During this process, secreted hBMP7 was anticipated to interact with cell membrane receptors, which could induce a signaling cascade that lead to osteoblastic differentiation in autocrine and/or paracrine mode.[47] Nevertheless, BMP7 transfection did not manifest significant difference when cells were cultured in OM for two weeks (Fig 7-B3 vs. 7-B4).

Our results suggest that hBMP7-transfected D1-MSCs could be considered not only as an effective delivery tool of hBMP7, but also as proliferating and bone forming cells for bone regeneration purpose, which offers reasonable hope to use stem cell-based gene delivery by niosomes approach to target sites where bone regeneration is needed. To validate that hypothesis, additional *in vivo* experiments and an optimization process of the niosomes formulations would be required, since biological conditions are different and not always exists a consistent correlation between *in vitro* and *in vivo* experiments.

3.5. References

1. Attia N, Santos E, Abdelmouty H, Arafa S, Zohdy N, Hernández RM, et al. Behaviour and ultrastructure of human bone marrow-derived mesenchymal stem cells immobilised in alginate-poly-l-lysine-alginate microcapsules. Journal of microencapsulation. 2014;31(6):579-89.
2. Vadalà G, Sowa G, Hubert M, Gilbertson LG, Denaro V, Kang JD. Mesenchymal stem cells injection in degenerated intervertebral disc: cell leakage may induce osteophyte formation. Journal of tissue engineering and regenerative medicine. 2012;6(5):348-55.
3. Yang X, Zhu T-Y, Wen L-C, Cao Y-P, Liu C, Cui Y-P, et al. Intraarticular Injection of Allogenic Mesenchymal Stem Cells has a Protective Role for the Osteoarthritis. Chinese medical journal. 2015;128(18):2516.
4. Hodgkinson CP, Gomez JA, Mirotsou M, Dzau VJ. Genetic engineering of mesenchymal stem cells and its application in human disease therapy. Human gene therapy. 2010;21(11):1513-26.
5. Saeed H, Ahsan M, Saleem Z, Iqtedar M, Islam M, Danish Z, et al. Mesenchymal stem cells (MSCs) as skeletal therapeutics–an update. Journal of biomedical science. 2016;23(1):41.
6. Fischer J, Kolk A, Pautke C, Warnke P, Plank C, Smeets R. Future of local bone regeneration–protein versus gene therapy. Journal of Cranio -Maxillofacial Surgery. 2011;39(1):54-64.
7. Zhang Y, Fan W, Ma Z, Wu C, Fang W, Liu G, et al. The effects of pore architecture in silk fibroin scaffolds on the growth and differentiation of mesenchymal stem cells expressing BMP7. Acta biomaterialia. 2010;6(8):3021-8.
8. Mont MA, Ragland PS, Biggins B, Friedlaender G, Patel T, Cook S, et al. Use of bone morphogenetic proteins for musculoskeletal applications. J Bone Joint Surg Am. 2004;86(suppl 2):41-55.
9. Kanakaris NK, Petsatodis G, Tagil M, Giannoudis PV. Is there a role for bone morphogenetic proteins in osteoporotic fractures? Injury. 2009;40: S21-S6.

10. Xiang S, Tong H, Shi Q, Fernandes JC, Jin T, Dai K, et al. Uptake mechanisms of non-viral gene delivery. J Control Release. 2012 Mar 28;158(3):371-8.
11. Ramamoorth M, Narvekar A. Non-viral vectors in gene therapy-an overview. J Clin Diagn Res. 2015;9(1):GE01-GE6.
12. Oliveira AV, Marcelo A, da Costa AMR, Silva GA. Evaluation of cystamine-modified hyaluronic acid/chitosan polyplex as retinal gene vector. Materials Science and Engineering: C. 2016;58:264-72.
13. Marianecci C, Di Marzio L, Rinaldi F, Celia C, Paolino D, Alhaique F, et al. Niosomes from 80s to present: the state of the art. Adv Colloid Interface Sci. 2014 Mar;205:187-206.
14. Rajera R, Nagpal K, Singh SK, Mishra DN. Niosomes: a controlled and novel drug delivery system. Biol Pharm Bull. 2011;34(7):945-53.
15. Kazi KM, Mandal AS, Biswas N, Guha A, Chatterjee S, Behera M, et al. Niosome: A future of targeted drug delivery systems. J Adv Pharm Technol Res. 2010 Oct;1(4):374-80.
16. Ochoa GP, Sesma JZ, Díez MA, Díaz-Tahoces A, Avilés-Trigeros M, Grijalvo S, et al. A novel formulation based on 2, 3-di (tetradecyloxy) propan-1-amine cationic lipid combined with polysorbate 80 for efficient gene delivery to the retina. Pharmaceutical research. 2014;31(7):1665-75.
17. Kokotos G, Verger R, Chiou A. Synthesis of 2-Oxo Amide Triacylglycerol Analogues and Study of Their Inhibition Effect on Pancreatic and Gastric Lipases. Chemistry–A European Journal. 2000;6(22):4211-7.
18. Ojeda E, Agirre M, Villate-Beitia I, Mashal M, Puras G, Zarate J, et al. Elaboration and Physicochemical Characterization of Niosome-Based Nioplexes for Gene Delivery Purposes. Non-Viral Gene Delivery Vectors: Methods and Protocols. 2016:63-75.
19. Mashal M, Attia N, Puras G, Martínez-Navarrete G, Fernández E, Pedraz JL. Retinal gene delivery enhancement by lycopene incorporation into cationic niosomes based on DOTMA and polysorbate 60. Journal of Controlled Release. 2017.
20. Ojeda E, Puras G, Agirre M, Zárate J, Grijalvo S, Pons R, et al. Niosomes based on synthetic cationic lipids for gene delivery: the influence of polar head-groups on the transfection efficiency in HEK-293, ARPE-19 and MSC-D1 cells. Organic & biomolecular chemistry. 2015;13(4):1068-81.
21. Rahman F, Al Frouh F, Bordignon B, Fraterno M, Landrier J-F, Peiretti F, et al. Ascorbic acid is a dose-dependent inhibitor of adipocyte differentiation, probably by reducing cAMP pool. Frontiers in cell and developmental biology. 2014;2:29.
22. Song YK, Liu D. Free liposomes enhance the transfection activity of DNA/lipid complexes in vivo by intravenous administration. Biochim Biophys Acta. 1998 Jun 24;1372(1):141-50.
23. Balazs DA, Godbey W. Liposomes for use in gene delivery. Journal of drug delivery. 2010;2011.
24. Szunerits S, Boukherroub R. Introduction to Plasmonics: Advances and Applications: CRC Press;2015.
25. Wasungu L, Hoekstra D. Cationic lipids, lipoplexes and intracellular delivery of genes. J Control Release. 2006 Nov 28;116(2):255-64.
26. Singh J, Michel D, Chitanda JM, Verrall RE, Badea I. Evaluation of cellular uptake and intracellular trafficking as determining factors of gene expression for amino acid-substituted gemini surfactant-based DNA nanoparticles. Journal of nanobiotechnology. 2012;10(1):7.
27. Majzoub RN, Ewert KK, Safinya CR. Cationic liposome–nucleic acid nanoparticle assemblies with applications in gene delivery and gene silencing. Phil Trans R Soc A. 2016;374(2072):20150129.
28. Puras G, Mashal M, Zarate J, Agirre M, Ojeda E, Grijalvo S, et al. A novel cationic niosome formulation for gene delivery to the retina. J Control Release. 2014 Jan 28;174:27-36.
29. Sakurai F, Inoue R, Nishino Y, Okuda A, Matsumoto O, Taga T, et al. Effect of DNA/liposome mixing ratio on the physicochemical characteristics, cellular uptake and intracellular trafficking of plasmid DNA/cationic liposome complexes and subsequent gene expression. J Control Release. 2000 May 15;66(2-3):255-69.
30. Champion JA, Katare YK, Mitragotri S. Particle shape: a new design parameter for micro-and nanoscale drug delivery carriers. Journal of Controlled Release. 2007;121(1):3-9.

31. Gratton SE, Ropp PA, Pohlhaus PD, Luft JC, Madden VJ, Napier ME, et al. The effect of particle design on cellular internalization pathways. Proceedings of the National Academy of Sciences. 2008;105(33):11613-8.
32. Ma B, Zhang S, Jiang H, Zhao B, Lv H. Lipoplex morphologies and their influences on transfection efficiency in gene delivery. Journal of Controlled Release. 2007;123(3):184-94.
33. Le Bihan O, Chèvre R, Mornet S, Garnier B, Pitard B, Lambert O. Probing the in vitro mechanism of action of cationic lipid/DNA lipoplexes at a nanometric scale. Nucleic acids research. 2011;39(4):1595-609.
34. Ojeda E, Puras G, Agirre M, Zarate J, Grijalvo S, Eritja R, et al. The role of helper lipids in the intracellular disposition and transfection efficiency of niosome formulations for gene delivery to retinal pigment epithelial cells. International journal of pharmaceutics. 2016;503(1):115-26.
35. Puras G, Martinez-Navarrete G, Mashal M, Zarate J, Agirre M, Ojeda E, et al. Protamine/DNA/Niosome Ternary Nonviral Vectors for Gene Delivery to the Retina: The Role of Protamine. Mol Pharm. 2015 Oct 5;12(10):3658-71.
36. Honda Y, Ding X, Mussano F, Wiberg A, Ho C-m, Nishimura I. Guiding the osteogenic fate of mouse and human mesenchymal stem cells through feedback system control. Scientific reports. 2013;3:3420.
37. Hsiong SX, Boontheekul T, Huebsch N, Mooney DJ. Cyclic arginine-glycine-aspartate peptides enhance three-dimensional stem cell osteogenic differentiation. Tissue Engineering Part A. 2008;15(2):263-72.
38. Garate A, Ciriza Js, Casado JG, Blazquez R, Pedraz JL, Orive G, et al. Assessment of the behavior of mesenchymal stem cells immobilized in biomimetic alginate microcapsules. Molecular pharmaceutics. 2015;12(11):3953-62.
39. Jensen EC. Use of fluorescent probes: their effect on cell biology and limitations. The Anatomical Record. 2012;295(12):2031-6.
40. El-Sayed A, Harashima H. Endocytosis of gene delivery vectors: from clathrin-dependent to lipid raft-mediated endocytosis. Molecular Therapy. 2013;21(6):1118-30.
41. Bareford LM, Swaan PW. Endocytic mechanisms for targeted drug delivery. Adv Drug Deliv Rev. 2007 Aug 10;59(8):748-58.
42. Kou L, Sun J, Zhai Y, He Z. The endocytosis and intracellular fate of nanomedicines: Implication for rational design. Asian Journal of Pharmaceutical Sciences. 2013;8(1):1-10.
43. Xu J, Wang NX, Wang MN, Xie HX, Cao YH, Sun LH, et al. BMP7 enhances the effect of BMSCs on extracellular matrix remodeling in a rabbit model of intervertebral disc degeneration. The FEBS journal. 2016;283(9):1689-700.
44. Hornstein BD, Roman D, Arévalo-Soliz LM, Engevik MA, Zechiedrich L. Effects of Circular DNA Length on Transfection Efficiency by Electroporation into HeLa Cells. PloS one. 2016;11(12):e0167537.
45. Yin W, Xiang P, Li Q. Investigations of the effect of DNA size in transient transfection assay using dual luciferase system. Analytical biochemistry. 2005;346(2):289-94.
46. Scarfì S. Use of bone morphogenetic proteins in mesenchymal stem cell stimulation of cartilage and bone repair. World journal of stem cells. 2016;8(1):1.
47. Dorman L, Tucci M, Benghuzzi H. In vitro effects of bmp-2, BMP7, and bmp-13 on proliferation and differentation of mouse mesenchymal stem cells. Biomedical sciences instrumentation. 2011;48:81- 7.

Chapter 4

Drug Design, Development and Therapy **Dovepress**

November 2018 Volume 2018:12 Pages 3937-3949

Gene transfer to rat cerebral cortex mediated by polysorbate 80 and poloxamer 188 nonionic surfactant vesicles

Noha Attia,[1–3,*] Mohamed Mashal,[1,*] Cristina Soto-Sánchez,[4,5] Gema Martínez-Navarrete,[4,5] Eduardo Fernández,[4,5] Santiago Grijalvo,[4,6] Ramón Eritja,[4,6] Gustavo Puras,[1,4] Jose Luis Pedraz[1,4,*]

[1]NanoBioCel Group, Laboratory of Pharmaceutics, School of Pharmacy, University of the Basque Country (UPV/EHU), Vitoria-Gasteiz, Spain; [2]Medical Histology and Cell Biology Department, Faculty of Medicine, University of Alexandria, Alexandria, Egypt; [3]Department of Basic Sciences, The American University of Antigua-College of Medicine, Coolidge, Antigua and Barbuda; [4]Networking Research Centre of Bioengineering, Biomaterials and Nanomedicine (CIBER-BBN), Vitoria-Gasteiz, Spain; [5]Neuroprothesis and Neuroengineering Research Group, Miguel Hernández University, Elche, Spain; [6]Institute of Advanced Chemistry of Catalonia (IQAC-CSIC), Barcelona, Spain.

* Noha Attia and Mohamed Mashal contributed equally to this work.

Gene transfer to rat cerebral cortex mediated by polysorbate 80 and poloxamer 188 nonionic surfactant vesicles

Abstract

Background: Gene therapy can be an intriguing therapeutic option in wide-ranging neurological disorders. Though non-viral gene carriers represent a safer delivery system to their viral counterparts, a thorough design of such vehicles is crucial to enhance their transfection properties.
Purpose: This study evaluated the effects of combined use of two nonionic surfactants, poloxamer 188 (P) and polysorbate 80 (P80) into nanovesicles–based on 2,3-di(tetradecyloxy)propan-1-amine cationic lipid (D) – destined for gene delivery to central nervous system cells.
Methods: Niosome formulations without and with poloxamer 188 (DP80 and DPP80, respectively) were prepared by the reverse-phase evaporation technique and characterized in terms of size, surface charge, and morphology. After the addition of pCMS-EGFP plasmid, the binding efficiency to the niosomes was evaluated in agarose gel electrophoresis assays. Additionally, transfection efficiency of complexes was also evaluated *in vitro* and *in vivo* conditions.
Results: *In vitro* experiments on NT2 cells revealed that the complexes based on a surfactant combination (DPP80) enhanced cellular uptake and viability when compared with the DP80 counterparts. Interestingly, DPP80 complexes showed protein expression in glial cells after administration into the cerebral cortices of rats.
Conclusion: These data provide new insights for glia-centered approach for gene therapy of nervous system disorders using cationic nanovesicles, where nonionic surfactants play a pivotal role.
Keywords: gene therapy, non-viral gene vectors, poloxamer 188, niosomes, cationic lipids

4.1. Introduction

The genetic base of many central nervous system (CNS) diseases along with the recent advances in the nanotechnology fields makes gene therapy an attractive therapeutic option.[1] Gene therapy can improve the quality of life in patients with major brain diseases, including Parkinson, Alzheimer, or epilepsy.[2–4] Successful delivery of DNA– vector hybrids that can correct such CNS disorders was probed.[5–7] Although many phase-I clinical trials of CNS gene therapy are

documented, only a few have reached phase-II.[5] Such modest improvement is due mainly to the lack of optimal vehicles able to deliver the genetic material in an efficient way.[8]

Being easier in large-scale production with lower production cost, non-immunogenic and non-oncogenic, non-viral approach offers several advantages in delivering pDNA and siRNA.[9,10] However, their main drawback is the lower transfection efficiency compared with virus-based vectors.[11] Therefore, further research in the design of such formulations is necessary before they become a realistic medical option to treat CNS disorders.

Among the different available gene delivery systems such as liposomes or micelles, niosomes have attracted a great amount of attention.[12] Nonionic surfactant lipid vesicles, such as niosomes, are synthetic vesicles with high drug-delivery potential.[13] Niosomes can deliver both water- and lipid-soluble molecules. In addition, and depending on their chemical structure, they can also control the release of such molecules.[14] However, niosomes are more stable and cheaper systems, compared with liposomes.[15] Among several factors, the nonionic surfactants are known to provide stability to the formulation. Other components, such as cationic lipids, can interact with negatively charged genetic material to form niocomplexes, in gene delivery context.[16,17]

Recently, some encouraging results have been obtained with niosomes based on the hydrochloride salt of the cationic lipid 2,3-di(tetradecyloxy)propan-1-amine (DTPA-Cl) and polysorbate 80 (P80) nonionic surfactant to transfect retinal cells.[16] DTPA-Cl is a fairly water-soluble lipid that can efficiently condense DNA. In addition, other cationic niosome formulations have been able to transfect neuronal cells after intracranial administration in the brain of rats.[18] Considering such results, we explored the impact of adding poloxamer 188 nonionic surfactant (P) to niosomes that contained the hydrochloride salt of cationic lipid DTPA (D) and P80 to obtain two kinds of niosomes, with only one surfactant (DP80 formulation) or with a mixture of them (DPP80 formulation). Previous studies showed that poloxamer 188, a biocompatible copolymer, could be well tolerated by cells.[19] Moreover, P has been successfully used in several gene-delivery studies when combined with different lipid components.[20,21]

In addition, other reports in the literature highlight the advantage of combining two surfactants in the same formulation.[22,23] Particle size, polydispersity index (PDI), and zeta potential (ZP) of both niosomes were analyzed for comparison purposes. When the pCMS-EGFP plasmid was added at different cationic lipid/DNA ratios (w/w), the resulted nioplexes were physicochemically analyzed. *In vitro* experiments were performed to evaluate the behavior of both vectors in NT2

cells regarding their cellular uptake, protein expression efficiency, and cell viability. Afterwards, the formulation that showed better results was administered to primary neuronal culture, and then, into rat cerebral cortex in order to evaluate protein expression in *in vivo* conditions.

4.2. Methods

4.2.1. Elaboration of cationic niosomes

The hydrochloride salt of the cationic lipid DTPA-Cl was synthesized as indicated in previous work.[24] Once the cationic lipid (D) was produced, it was used to elaborate niosomes that were elaborated by modified reverse-phase evaporation technique.[25] An amount of 5 mg of D was dissolved in 1 mL of dichloromethane organic solvent, and sonicated in 5 mL of surfactant (either P80 alone or equal weights of both P and P80). The details of chemical structure of each component of the niosome formulations are represented in Figure 1. The emulsions were obtained after a sonication process (Branson Sonifier 250®; Branson Ultrasonics Corporation, Danbury, CT, USA) at 45 W for 30 seconds. When dichloromethane was evaporated, dispersions of niosome vesicles were obtained in the aqueous phase. Then, niosome formulations were named as DP80 and DPP80 both of them containing DTPA-Cl (D) cationic lipid and P80 or P+P80 as nonionic surfactants at a cationic lipid/nonionic surfactant ratio of 1/5 (Table 1).

Table 1 Components (in mg) and physical characterization of niosome formulations regarding particle size (nm), PDI, and zeta potential (mV).

Niosomes	**Components (mg)**			**Characterization**		
	DTPA (D)	**Poloxamer 188 (P)**	**Polysorbate 80 (P80)**	**Size (nm)**	**PDI**	**Zeta potential (mV)**
DP80	5	–	25	54.02±0.94	0.52±0.10	41.9±7.10
DPP80	5	12.5	12.5	90.41±0.65	0.42±0.01	44.1±4.39

Note: Data represent mean±SD (n=3).

Abbreviations: DTPA, 2,3-di(tetradecyloxy)propan-1-amine; PDI, polydispersity index.

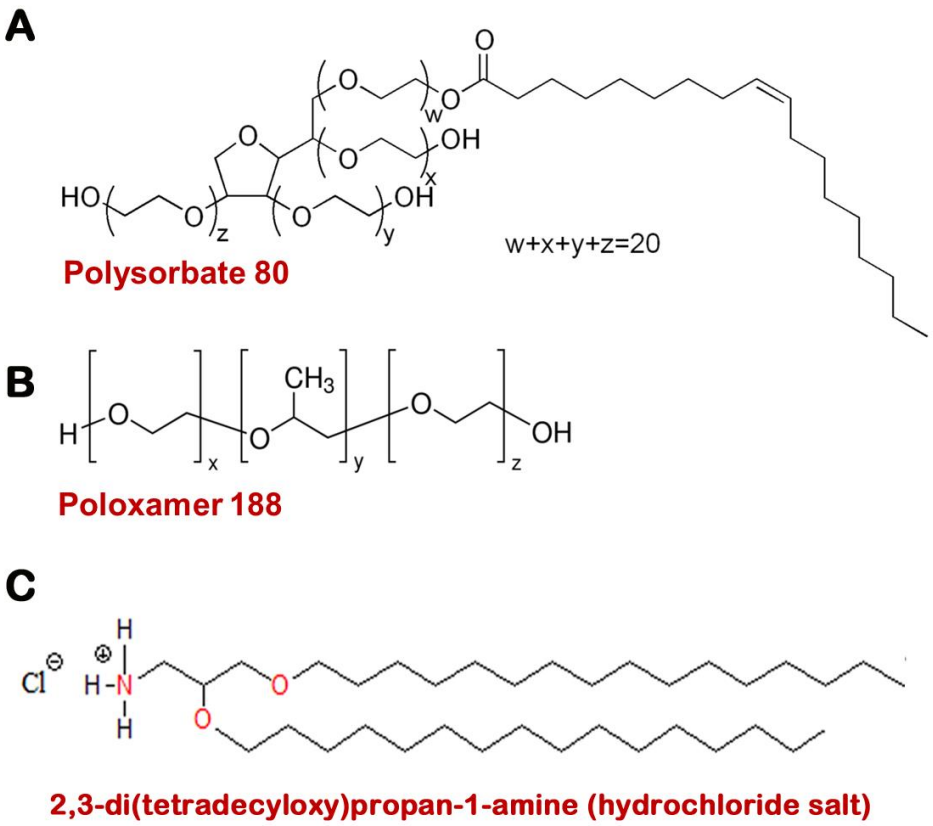

Figure 1 Chemical structure of: (A) polysorbate 80, (B) poloxamer 188, and (C) cationic lipid DTPA. **Abbreviation: DTPA,** 2,3-di(tetradecyloxy)propan-1-amine.

4.2.2. Plasmid propagation and elaboration of complexes

The pCMS-EGFP plasmid (5,541 bp; PlasmidFactory, Bielefeld, Germany), was propagated, as previously described.[14] Nioplexes were obtained after mixing a stock solution of pCMS-EGFP plasmids (0.5 mg/mL) with different volumes of suspensions where niosomes were dispersed (1 mg cationic lipid/mL) to obtain nioplexes at different cationic lipid/DNA ratios (w/w).

4.2.3. Physicochemical analysis of niosomes and complexes

The particle size, superficial charge (ZP), and morphology of lipid formulations were analyzed as described previously.[24,26] To evaluate the interactions between the niosomes and the genetic material, an agarose gel electrophoresis assay was performed.[24]

4.2.4. *In vitro* transfection in NT2 cells

NT2 cells (ATCC®–CRL, 1973) were cultivated and processed as previously described.27 Cells were exposed to complexes (1.25 µg of pCMS-EGFP/well). After 4 hours of incubation, transfection medium was removed and refreshed with complete medium. Cells were allowed to

grow for 24 hours until being analyzed by fluorescence microscopy (EclipseTE2000-S; Nikon Instruments, Melville, NY, USA) and flow cytometry (FACSCalibur; BD, San Jose, CA, USA) as described previously.[14] Positive control (Lipofectamine® 2000 [L2K], Gibco®; Life Technologies S.A., Madrid, Spain) was prepared following the manufacturer's protocol.

4.2.5. Cellular uptake and intracellular disposition of complexes

NT2 cells were cultured as previously mentioned in Section "*In vitro* transfection in NT2 cells." After 4 hours of incubation with complexes, the transfection medium was removed and cells were washed thoroughly with PBS, trypsinized, and analyzed by FACSCalibur flow cytometer to evaluate cellular uptake. In total, 10,000 events were collected and analyzed for each sample. Each sample was analyzed in triplicate.

The intracellular distributions of the complexes were analyzed by confocal laser scanning microscopy (CLSM, Olympus Fluoview 500). Specific fluorescence-labeled commercial reagents were used to evaluate co-localization with Fluorescein isothiocyanate (FITC)-pCMS-EGFP plasmid by Mander's co-localization coefficient (M) as previously reported.[27]

4.2.6. Primary cortical neuron culture

Experimental procedures for *in vitro* isolation and culture of primary cortex cells were carried out according to the directive 2010/63/EU of the European Parliament and of the Council, and the RD 53/2013 Spanish regulation on the protection of animals use for scientific purposes. Additionally, all procedures were approved by the Miguel Hernandez University Committee for Animal Use in Laboratory. Dissociated cultures of primary cortical neurons were obtained from E17–E18 rat embryos (Sprague–Dawley) and preserved in Hanks' Balanced Salt Solution during extraction. Then, trypsin was added to the medium and incubated at 37°C for chemical dissociation. Subsequently, the tissue was dissociated in neurobasal medium/FBS and cell density was determined using a hemocytometer. Cells were seeded on glass coverslips following the same transfection protocol previously described for cellular uptake and trafficking studies. Then, the samples were incubated overnight at 4°C with the primary antibodies and rabbit anti-glial fibrillary acidic protein (GFAP) (1:300), as a marker of glial cells and mouse anti-GFP (1:100) diluted in PBS containing TritonX100 (0.5%). Later, coverslips were washed in PBS and incubated for 1 hour with specific Alexa Fluor 555 and Alexa Fluor 488 conjugated secondary antibodies (Thermo Fisher Scientific, Madrid, Spain). Hoechst 33342 was used to label the nuclei. Finally, coverslips were mounted for imaging and analyzed with a Leica TCS SPE fluorescence microscope.

4.2.7. *In vivo* studies in rat brain

Adult male Sprague–Dawley rats were used for *in vivo* experiments. All procedures were carried out in accordance with the Spanish and European Union regulations for the use of animals in research and supervised by the Miguel Hernandez University Standing Committee for Animal Use in Laboratory. Pretreatment of rats and injection of the complexes were performed as previously reported.[18]

4.2.8. Analysis of protein expression in brain

About 72 hours after surgery, animals were sacrificed and perfusion with PBS followed by paraformaldehyde (4%) was performed for fixation. Then, rat brains were preserved in paraformaldehyde (4%) and cryoprotected in sucrose solution (30%) with PBS before slicing. A cryostat (HM 550; Microm International GmbH, Walldorf, Germany) was used to obtain slices of 20 μm from coronal frozen sections close to the area of injection. Next, slices were mounted for immunohistochemistry analysis with rabbit anti-NeuN (1:100) to label neurons and with mouse anti-GFP (1:100) diluted in PBS containing TritonX100 (0.5%) and incubated at 4°C over-night. Thereafter, slices were washed in PBS and incubated for 1 hour in dark with specific Alexa Fluor 555 and Alexa Fluor 488 conjugated secondary antibodies for visualization. Nuclei were counterstained with Hoechst 33342.[18]

4.2.9. Statistical analysis

Statistical differences between groups at significance levels of .95% were calculated by ANOVA and Student's *t*-test. In all cases, *P*-values ,0.05 were regarded as significant. Normal distribution of samples was assessed by the Kolmogorov–Smirnov test and the homogeneity of the variance by the Levene test. Numerical data were presented as mean±SD.

4.3. Results

4.3.1. Physicochemical characterization of niosomes/complexes

Table 1 shows the characterization of both DP80 and DPP80 niosome formulations. The niosomes prepared only with P80 (DP80) had sizes around 54 nm. Interestingly, when equal weights of both tensioactives, P and P80, were incorporated, the size obtained was significantly larger (90.4 nm)

with a slight decrease in PDI (0.42, instead of 0.52). Regarding the surface charge, all niosomes were in the positive territory ranging from 42 to 44 mV.

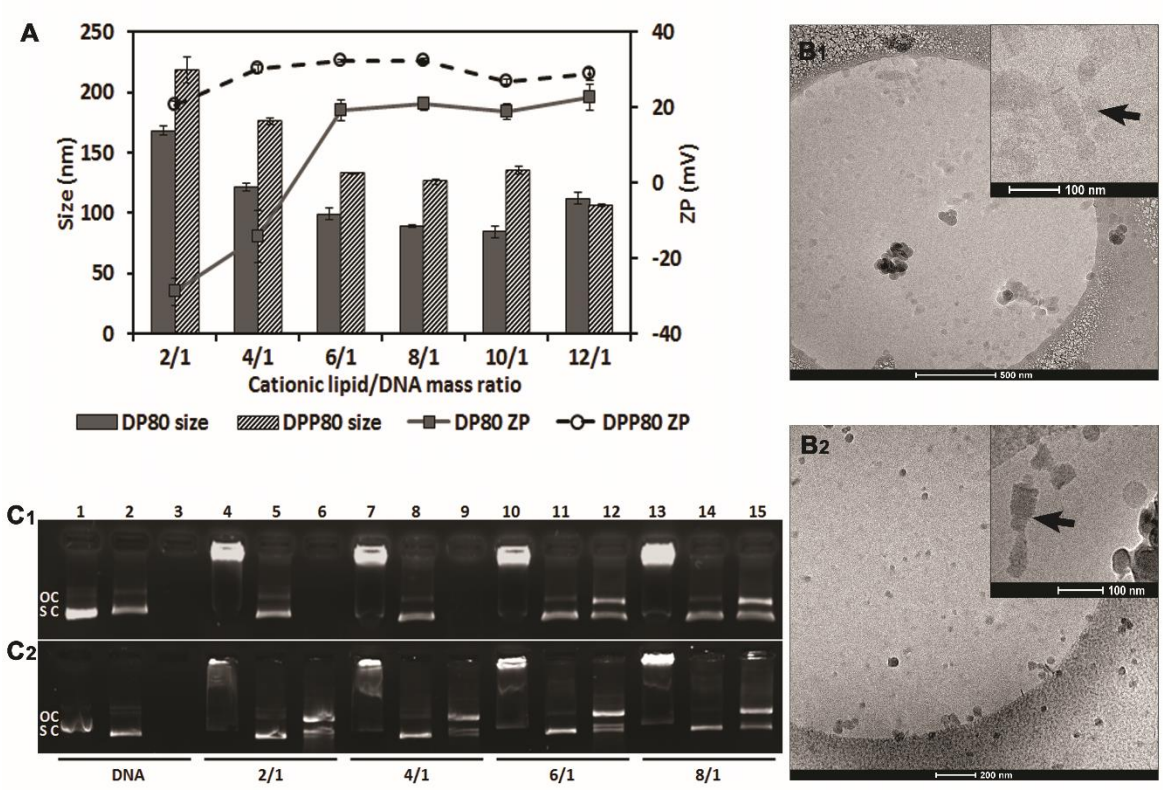

Figure 2 characterization of DP80 and DPP80 complexes. Notes: (A) Particle size (nm) and ZP (mV). The data represent mean±SD (n=3). (B1, B2) Cryo-TEM pictures of nioplexes. Arrows in both insets point to the multi-lamellar pattern. (C) agarose gel electrophoresis assay at different cationic lipid/DNA ratios of DP80 and DPP80 complexes (upper and lower panels, respectively), based on both formulations. lanes are shown as: 1–3, uncomplexed DNA; 4–6, mass ratio 2/1; 7–9, mass ratio 4/1; 10–12, mass ratio 6/1; and 13–15, mass ratio 8/1. lanes 2, 5, 8, 11, and 14 depict niocomplexes treated with SDS, while lanes 3, 6, 9, 12, and 15 were treated with DNase I+ SDS. OC and SC (open circular and supercoiled forms, respectively). **Abbreviations**: SDS, sodium dodecyl sulphate; ZP, zeta potential.

Figure 2 summarizes some parameters of DP80 and DPP80 complexes in terms of size, superficial charge (ZP), morphology, and plasmid-binding capacity. DPP80 complexes depicted sizes larger than DP80 (*P*,0.05), except for 12/1 ratio (where no true difference was noticed, *P*.0.05). For both formulations, complexes gradually tended to decrease in size while ratio increased. In general, values of size/charge were significantly affected by the DNA incorporated into these complexes. Starting with the mass ratio of 2/1, the sizes of DP80 and DPP80 complexes were around 168 and 219 nm, respectively. A gradual reduction was discerned to become almost 106 and 111 nm at 12/1 ratio. The PDI values of both nioplexes were around 0.2 (as depicted in Table S1). Regarding

ZP of DP80 complexes (Figure 2A, lines), it started with negative values at 2/1 and 4/1 ratios (−29 and −14 mV, respectively) which gradually increased towards the positive territory to remain around +20 mV. The behavior of DPP80 complexes was different. In this case, all ZP values were positive. In addition, ZP values increased from 20 mV at 2/1 ratio to 32.5 mV at 8/1 ratio, then decreased in the last two ratios (10/1 and 12/1) (Figure 2A). When assessed by cryo-TEM (Figure 2B), both DP80 and DPP80 complexes at 6/1 (w/w) ratio appeared as electron dense particles with a discrete distribution. Interestingly, DPP80 (Figure 2B3) depicted less tendency to form aggregates compared with DP80 (Figure 2B1). At a higher magnification (Figure 2B2 and B4), complexes were mostly elongated with a lamellar morphology (arrows). Agarose gel electrophoresis assays (Figure 2C) revealed the capacity of DP80 niosomes to bind efficiently to DNA (lanes 4, 7, 10, and 13 that corresponded to 2/1, 4/1, 6/1, and 8/1 ratios, respectively). On the other hand, the ability of DPP80 niosomes to capture DNA increased proportionally with the increase in the ratio (Figure 2C). Upon addition of sodium dodecyl sulphate (SDS) the DNA bound to the niosomes was released from all studied complexes. The absence of white bands in wells 5, 8, 11, and 14 (2/1, 4/1, 6/1, and 8/1 ratios) confirmed this fact. Interestingly, the supercoiled (SC) bands observed in lanes 6, 9, 12, and 15 (Figure 2C, lower panel) confirmed that the plasmid DNA released from the DPP80 niosome formulation was protected from degradation at all ratios tested. However, DP80-released DNA was not protected at ratios of 2/1 and 4/1 (Figure 2C, upper panel).

4.3.2. Protein expression and viability studies

Figure 3A shows a peak of 28.8% of transfected cells when DP80 was used at 6/1 mass ratio. Regarding DPP80 formulation, the best transfection percentage (30.1%) was observed again at 6/1 mass ratio, followed by a gradual decline. No protein expression was observed on cells when free “uncomplexed” DNA was analyzed (data not shown). The viability of transfected cells (Figure 3A, lines) depicted a clear negative relationship with the cationic lipid/DNA mass ratio. DPP80 (dashed line) showed higher cell viability results compared with DP80 formulation (continuous line) at all ratios studied, unless at 2/1 ratio, where cell viability was around 100% in both formulations. At 6/1 ratio, cell viability value was 85.4%, significantly higher (*P*,0.05) than that of DP80 at the same 6/1 ratio and Lipofectamine 2000 positive control (80.4% and 80%, respectively). Figure 3B2–B4 revealed fluorescence overlay and phase contrast micrographs of NT2 cells at 24 hours post-transfection of both formulations at 6/1 ratios as well as L2K positive control. In all cases, NT2 cells retained their normal morphology compared with the untransfected

(control [Ctrl]) cells (Figure 3B1). Mean fluorescence intensity (MFI) of cells transfected by complexes based on DPP80 niosomes at a ratio of 6/1 had markedly higher values (*P*,0.05) compared with those obtained by complexes based on DP80 niosomes (Figure 3C).

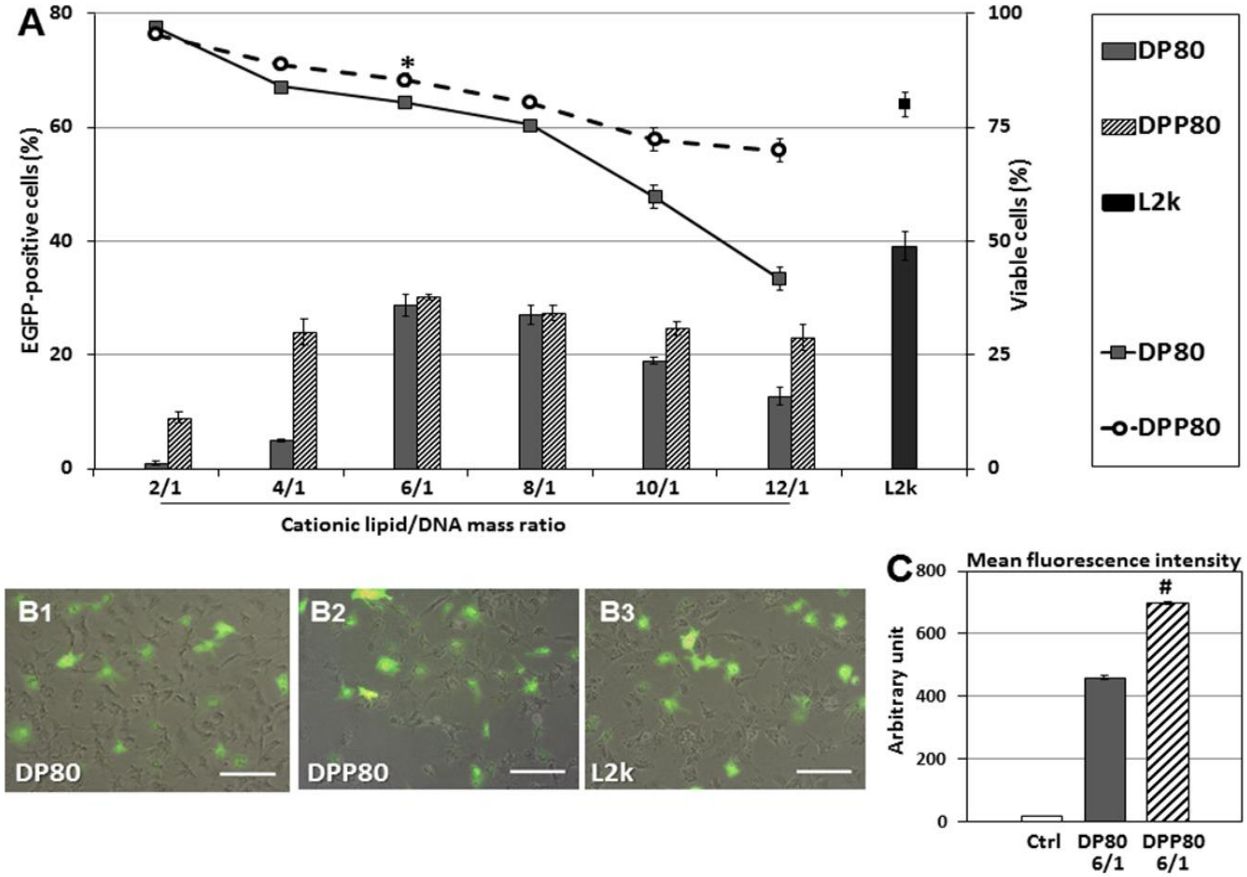

Figure 3 Transfection studies in NT2 culture cells.
Notes: (A) Flow cytometry analysis of percentage of cells that express EGFP (bars) and percentage of live cells (lines) at different cationic lipid/DNA ratios (w/w). Values represent mean±SD (n=3). *P,0.05 compared with DP80 at 6/1 and L2K at 2/1. Overlay of fluorescence and DIC pictures of control cells (B1), DP80 at 6/1 (B2), DPP80 at 6/1 (B3), and L2K at 2/1 mass ratios (B4). scale bars=100 µm. (C) Mean fluorescence intensity (a.u.). **Abbreviations**: a.u., arbitrary unit; ctrl, control; DIC, digital image correlation; L2K, lipofectamine® 2000.

4.3.3. Trafficking studies

Both FITC-labeled complexes were applied at the cationic lipid/DNA (w/w) mass ratio that depicted the best transfection percentage (6/1; as shown in Figure 3A). With an uptake percentage of about 95%, DPP80 complexes exceeded the other two formulations (DP80 and L2K of 84% and 85%, respectively). Control cells transfected with DNA alone did not show any uptake (Figure 4A and B1). However, when FITC-labeled DP80 and DPP80 complexes were used, some fluorescence signal within the cytoplasm of most of the cells in the field was observed, as shown

in Figure 4B2 and B3. The internalization studies of FITC-labeled DPP80 complexes at 6/1 ratio are represented in figure 4. At 4 hours after incubation of FITC-labeled complexes with fluorescence markers of CME [(clathrin mediated endocytosis); AlexaFluor 546-Transferrin; Figure 4C1], CvME [(caveolae mediated endocytosis); AlexaFluor 555-Cholera Toxin; Figure 4C2], MPC ([macropinocytosis]; AlexaFluor 594-Dextran;Figure 4C3), and late endosome/lysosome(LysoTracker red DND-99; Figure 4C4), Mander's M1 co-localization coefficient was 0.39, 0.88, 0.75, 0.81, respectively.

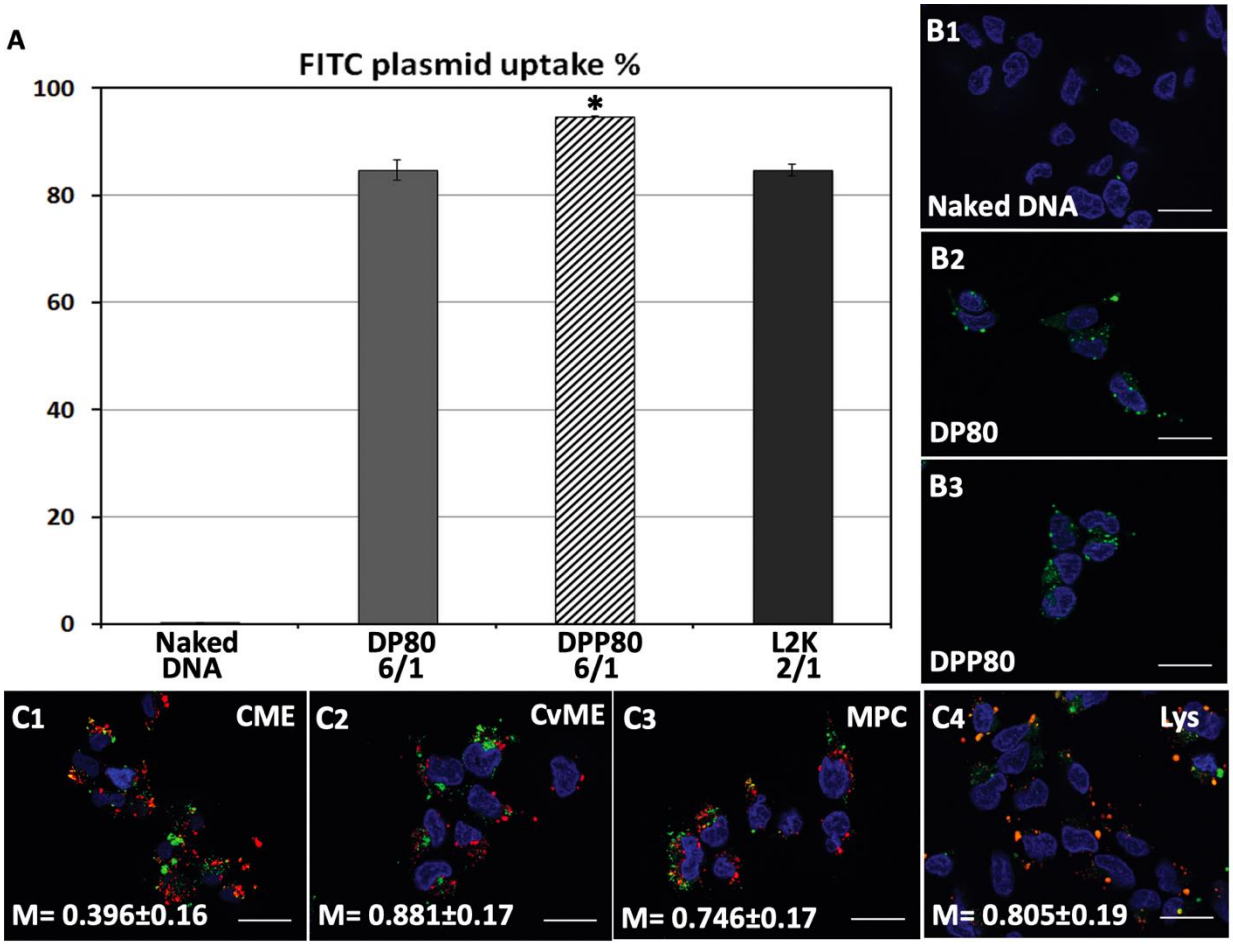

Figure 4 Trafficking studies in NT2 culture cells. **Notes:** (A) Flow cytometry measurement of the percentage of cells that captured plasmid labeled with FITC. error bars represent SD (n=3). *P,0.05 compared with other groups. (B1–B3) Fluorescence micrographs with FITC-labeled naked plasmids, and DP80 and DPP80 niocomplexes (at 6/1 mass ratios), respectively (scale bar=25 µm). (C) confocal micrographs showing intracellular distribution of DPP80 complexes, where plasmid is labeled in green color, and AlexaFluor 546-Transferrin (C1), AlexaFluor 555-Cholera Toxin (C2), AlexaFluor 594-Dextran (C3), and LysoTracker red DND-99 markers (C4), all in red. Nuclei of cells were stained with DAPI-fluoromount G (blue) (scale bar=25 µm). **Abbreviations:** CME, clathrin mediated endocytosis; CvME, caveolae mediated endocytosis; FITC, fluorescein isothiocyanate; M, Mander's co-localization coefficient; MPC, macropinocytosis.

4.3.4. Protein expression in primary cortical neuron and rat brain

Protein expression was observed in primary cortical cultures of cells transfected with DPP80 complexes at 6/1 ratio (w/w) and is shown in Figure 5A1. In any case, none of those cells were $GFAP^{+ve}$ (Figure 5A2). Interestingly, 72 hours after intracortical administration of complexes, $NeuN^{-}$ve (non-neuronal) positive cells with glial morphology were observed expressing EGFP in their dendrites (Figure 5B). Other pictures of brain experimented with different injections and the corresponding contralateral sections are shown in Figure S1.

4.4. Discussion

Considering the recently shown promising results of cationic niosomes to transfect stem cells[17] and neurons in both brain and retina,[18,28] and the reports on literature that highlights the benefits of combining two surfactants in the same formulation,[22,23] we explored in the present manuscript, the impact of combining P and P80 nonionic surfactants in the same niosome gene-delivery system based on the cationic lipid DTPA.

Our data showed that a particle was affected depending on the type of surfactant used (Table 1). The difference in size could be due to the different hydrophilic–lipophilic balance (HLB) value of surfactant used. P80 (lower HLB value) gave rise to nanovesicles of smaller sizes.[29] However, the interaction between surfactant(s) and cationic lipid in niosomes should not be excluded as another influential factor that could also affect the vesicle size.[30]

Prior to performing transfection experiments, we characterized complexes at different mass ratios of cationic lipid and DNA content (Figure 2). There is no general rule in the scientific community about the optimal size of non-viral vector particles for gene-delivery applications. In any case, it is clear that this parameter affects their transfection efficiency,[31] and in the case of niosome vesicles, it strongly depends on the mass ratio between both the cationic lipid and the DNA. As can be observed in Figure 2A, when DNA was bound to obtain both DP80 and DPP80 nioplexes at 2/1 ratio, the size exceeded 150 and 200 nm, respectively. In any case, when the ratio increased, the size of nioplexes decreased, probably due to the condensation of DNA plasmid on the surface of niosome vesicles in a more efficient multi-lamellar pattern by interaction between opposite charges, as discerned in the cryo-TEM examination (Figure 2B2 and B4, arrows). The shape of complexes has a marked effect on their final performance as a gene-delivery carrier.[32] Interestingly, the lamellar pattern discerned in several complexes is believed to occur during the process of complex formation. The complete topological transformation of both lipid and DNA

into complex particles would form string-like aggregates, in which complexes have a multi-lamellar pattern. The discrete morphology of complexes at 6/1 mass ratio (Figure 2B) could be attributed to the moderately positive surface charge (20 mV).[16] DPP80 complexes had a higher ZP (30 mV), and thus depicted less aggregates as they tend to repel each other.[33] Another crucial parameter that influences the transfection process is the electrostatic interactions between the negatively charged phosphate groups of DNA and the positively charged amine groups of the cationic niosomes.[34] Such parameter was analyzed in agarose gel electrophoresis assays (Figure 2C). For DPP80 niosomes, all ratios analyzed released and protected plasmid DNA against degradation. However, complexes based on DP80 niosomes (Figure 2C, upper panel) failed clearly to protect the DNA at low cationic lipid/DNA rates. Despite the fact that DP80 niosomes condensed and released properly the DNA after the addition of SDS at all analyzed mass ratios, the protective capacity of DNA against enzymatic digestion is a mandatory issue for efficient gene-delivery vectors. We hypothesize that electrostatic interactions between the DP80 niosomes and DNA at low cationic lipid/DNA ratios (2/1 and 4/1) were efficient to condense the DNA, but were not strong enough to protect the DNA,24 that might be attributed to the net negative surface charge of the complexes at the aforementioned ratios.

Afterward, both complexes were evaluated *in vitro* conditions to analyze protein expression and cytotoxic effect of formulations in NT2 culture cells. This cell line has been reported to be a promising human cell source for *in vivo* therapeutic application in many CNS disorders.[35,36] Their therapeutic importance lies in the fact that, following retinoic acid treatment, NT2 cells undergo an irreversible commitment to terminally differentiate into stable post-mitotic neurons, even long time after transplantation in animal brain.[37] Moreover, NT2-mediated functional recovery in preclinical stroke models has endorsed their application in clinical trials.[38] NT2 cells are stable, easy to cultivate, amenable to scale-up for cell production, and represent a CNS-like delivery vehicle for glioblastoma therapy.[38–40] NT2 cells can be differentiated into both neuronal and glial cells.[41] Therefore, these cells represent an appealing model to evaluate transfection efficiency by non-viral vectors based on cationic niosomes.

The data of transfection efficiency (Figure 3A) revealed the impact of the surfactant included in the formulation. When DP80 was used, the values of transfection started to increase at the 6/1 mass. Complexes at the lower ratios (2/1 and 4/1) had previously shown an inability to protect DNA against enzymatic digestion (Figure 2C), which could justify low transfection efficiencies at

these ratios. However, the incorporation of P in DPP80 formulation markedly enhanced transfection at the lower ratios (2/1 and 4/1) and maintained sufficient transfection at the higher ratios. The addition of P in DPP80 complexes shifted the ZP (Figure 2A) from negative to positive values at small mass ratios (2/1 and 4/1), which would enhance uptake, and thus transfection (Figure 3A).[42] Interestingly, DPP80 depicted higher MFI compared with DP80 at the cationic lipid/DNA mass ratio of 6/1 (maximum transfection). Actually, one of the most relevant concerns of gene therapy is to attain enough expression of the protein to reach physiological levels. Thus, the amount of protein expression by the transfected cells needs to be also considered along with the percentage of transfected cells when designing non-viral vectors for gene-delivery purposes.[26] Regarding cell viability, DPP80 niosomes showed less toxic effect on NT2 cells than DP80 counterpart at all mass ratios analyzed, being cell viability at 6/1 mass ratio significantly superior to that reported by liposome-based L2K transfection reagent. These promising data encouraged us to perform further *in vivo* studies, where not only gene-delivery efficiency but also cytotoxicity needs to be considered. The higher cationic lipid/DNA mass ratios resulted in a clear toxic effect on cells which were more accused in the case of DP80 niosomes, without the increase of transfection efficiency.

The fact that both the type of surfactant and the amount of such surfactant influence the biological function of nano-vesicles [43] could explain the low percentage of transfected cells and viability results observed when only P (Figure S2) or P80 (Figure 3A) surfactant was used in niosome formulations (DP and DP80, respectively). Additionally, when liposome vesicles were elaborated in the absence of any kind of surfactant (referred to as D; Figure S2), both transfection efficiency and cell viability values were also lower than the values obtained with DPP80 niosomes. To analyze more deeply the complex transfection mechanism of DPP80 complexes in NT2 culture cells, we performed some trafficking studies to investigate both the cellular uptake of complexes and the posterior cytoplasmic disposition inside the cells, since it has been previously reported on the literature that those parameters could markedly influence the gene-delivery properties of vectors.[14] Cellular uptake values were compared with DP80 niosomes as well as L2K transfection reagent. As can be observed in Figure 4A, the uptake of DPP80 complexes exceeded that of their DP80 counterparts that could be due to their higher surface charge (Figure 2A) or to more specific interactions of such nioplexes with some lipid components present on the cell membrane.[44] Additionally, it has been reported that variations in the length of surfactant carbon chains and/or

in the number of unsaturated bonds (inside their carbon chains) can affect the permeability of nanovesicles across membranes.[29] However, the great difference observed on DPP80 complexes between cellular uptake (95%; Figure 4A) and percentage of transfected cells (30%; Figure 3A) suggests that other biological processes involved on the transfection process should also be evaluated.[45] Therefore, we analyzed as well the endocytosis mechanism and the co-localization with the late endosome. Despite the absence of consensus on the most efficient endocytosis pathway, we analyzed the endocytosis processes mediated by clathrin, caveolae, and macropinocytosis, which could affect the fate of internalized complexes.[46]

The observed results in Figure 4C suggested that internalization of DPP80 complexes was mediated, mainly by caveolae and macropinocytosis. Such endocytosis pathways, normally, are connected with the lysosomes. In such compartments, the acid pH value, normally, degrades the genetic material, which in turn could reduce the percentage of transfected cells.[45] Therefore, the co-localization of complexes with the late endosome/lysosome (Figure 4C4) could explain why out of 95% of NT2 that captured DPP80 complexes (Figure 4A), only around 30% of them were successful to eventually express EGFP (Figure 3).[47]

Next, and before proceeding for *in vivo* studies in rat brain, we analyzed the transfection efficiency of DPP80 complexes in primary cortical cultures of rat embryos, where different kinds of neurons and glial cells are interconnected to set up complex neuronal–glial networks. Results showed some positive EGFP cells (Figure 5A1). Next, the lack of $GFAP^{+ve}$ reactivity in immunohistochemical assays confirmed that such EGFP-positive cells could be neurons (Figure 5A2). After observing these promising results obtained in neurons, we proceeded to evaluate in rat brain the protein expression of DPP80 complexes after intracranial injection. We did not observe any sign of toxicity in the cortical tissue after injection (data not shown). Unlike the primary culture observations, the $NeuN^{-ve}$ cells (neuroglia) were the only transfected cells (Figure 5B). The discrepancies between *in vitro* and *in vivo* assays are widely recognized and could be probably due to the fundamental difference in the mechanism of gene delivery in both biological contexts.[48]

The preference of DPP80 complexes to transfect mainly glial cells instead of neurons could be explained by the fact that glial cells have a higher mitotic and phagocytic activity.[49] Therefore, transfection process could be enhanced in such circumstances.

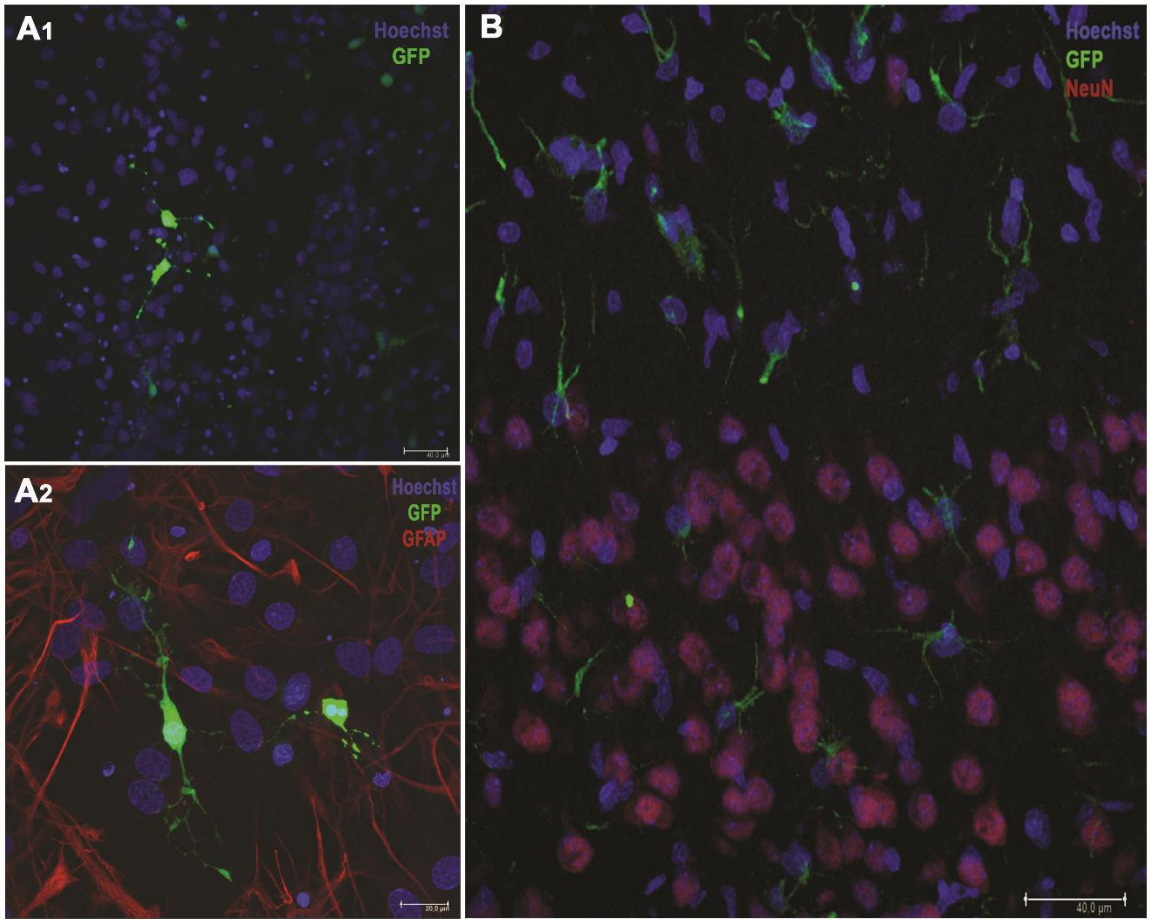

Figure 5 EGFP gene expression in primary neuronal cell cultures (A1 and A2). $GFAP^{+ve}$ neuroglia (red) and nuclei were stained in blue color with Hoechst 33342 (scale bars=40 and 20 µm, respectively). (B) *in vivo* expression green protein (scale bar=40 µm). **Note:** nuclei are shown in blue color (Hoechst), while neurons in red ($neuN^{+ve}$).

By contrast, the lack of protein expression observed in neurons of rat cortex exposed to DPP80 complexes could be explained by the particular biological processes of these kind of cells where both endocytosis and posterior intracellular disposition are severely hampered.[50] Considering these encouraging *in vivo* results, DPP80 complexes could be used as non-viral vectors to deliver genetic material into glial cells in the CNS, in order to tackle neurological disorders that affect these kind of cells.51 Alterations of glial cells are commonly found in many devastating neurological disorders such as Alzheimer and Parkinson, to name just the most relevant ones.[51,52]

4.5. Conclusion

Our results showed that physicochemically characterized DPP80 niosomes elaborated with a mixture of both P and P80 nonionic surfactants were able to transfect efficiently NT2 cells without

compromising their viability after cellular uptake mainly mediated by CME and MPC. Such novel biocompatible nanocarriers were able to induce *in vivo* transfection into glial cells of rats after intracortical administration. Interestingly, DPP80 gene carriers not only represent a promising tool for direct *in vivo* transfection, but also for cell-based gene delivery applications, since transfected NT2 cells or their derived neurons could be used as a delivery tool of therapeutic genes for different neurologic disorders.[53,54]

4.6. Acknowledgments

This project was supported by the Basque Country Government (CGIC10/172), Spanish Ministry of Education (Grant CTQ2017-84415-R, MAT2015-69967-C3-1R), the Generalitat de Catalunya (2014/SGR/624), and the Instituto de Salud Carlos III (CB06_01_0019, CB06_01_1028). The authors also wish to thank the intellectual and technical assistance from the ICTS "NANBIOSIS", more specifically by the Drug Formulation Unit (U10) of the CIBER in Bioengineering, Biomaterials, and Nanomedicine (CIBER-BBN) at the University of Basque Country (UPV/EHU). Technical and human support provided by SGIker (UPV/EHU) is gratefully acknowledged. Jose Luis Pedraz and Gustavo Puras are corresponding authors for this study.

Disclosure

The authors report no conflicts of interest in this work.

4.7. References

1. Tardieu M, Zérah M, Gougeon ML, et al. Intracerebral gene therapy in children with mucopolysaccharidosis type IIIB syndrome: an uncontrolled phase 1/2 clinical trial. *Lancet Neurol*. 2017;16(9):712–720.
2. Kaplitt MG, Feigin A, Tang C, et al. Safety and tolerability of gene therapy with an adeno-associated virus (AAV) borne GAD gene for Parkinson's disease: an open label, phase I trial. *Lancet*. 2007; 369(9579):2097–2105.
3. Tuszynski MH, Thal L, Pay M, et al. A phase 1 clinical trial of nerve growth factor gene therapy for Alzheimer disease. *Nat Med*. 2005; 11(5):551–555.
4. Krook-Magnuson E, Armstrong C, Oijala M, Soltesz I. On-demand optogenetic control of spontaneous seizures in temporal lobe epilepsy. *Nat Commun*. 2013;4:1376.
5. Jayant RD, Sosa D, Kaushik A, et al. Current status of non-viral gene therapy for CNS disorders. *Expert Opin Drug Deliv*. 2016;13(10): 1433–1445.
6. Palfi S, Gurruchaga JM, Ralph GS, et al. Long-term safety and tolerability of ProSavin, a lentiviral vector-based gene therapy for Parkinson's disease: a dose escalation, open-label, phase 1/2 trial. *Lancet*. 2014; 383(9923):1138–1146.
7. Rafii MS, Baumann TL, Bakay RA, et al. A phase1 study of stereotactic gene delivery of AAV2-NGF for Alzheimer's disease. *Alzheimers Dement*. 2014;10(5):571–581.
8. Pluvinage JV, Wyss-Coray T. Microglial Barriers to Viral Gene Delivery. *Neuron*. 2017;93(3):468–470.
9. Li J, Liang H, Liu J, Wang Z. Poly (amidoamine) (PAMAM) dendrimer mediated delivery of drug and pDNA/siRNA for cancer therapy. *Int J Pharm*. 2018;546(1–2):215–225.

10. Liu J, Li J, Liu N, et al. In vitro studies of phospholipid-modified PAMAM-siMDR1 complexes for the reversal of multidrug resistance in human breast cancer cells. *Int J Pharm*. 2017;530(1–2): 291–299.
11. Vanderwall AG, Noor S, Sun MS, et al. Effects of spinal non-viral interleukin-10 gene therapy formulated with d-mannose in neuropathic interleukin-10 deficient mice: Behavioral characterization, mRNA and protein analysis in pain relevant tissues. *Brain Behav Immun*. 2018;69:91–112.
12. Torchilin VP. *Nanoparticulates as Drug Carriers*. London: Imperial College Press; 2006.
13. Kazi KM, Mandal AS, Biswas N, et al. Niosome: A future of targeted drug delivery systems. *J Adv Pharm Technol Res*. 2010;1(4):374–380.
14. Mashal M, Attia N, Puras G, Martínez-Navarrete G, Fernández E, Pedraz JL. Retinal gene delivery enhancement by lycopene incorporation into cationic niosomes based on DOTMA and polysorbate 60. *J Control Release*. 2017;254:55–64.
15. Allam A, Fetih G. Sublingual fast dissolving niosomal films for enhanced bioavailability and prolonged effect of metoprolol tartrate. *Drug Des Devel Ther*. 2016;10:2421–2433.
16. Puras G, Mashal M, Zárate J, et al. A novel cationic niosome formulation for gene delivery to the retina. *J Control Release*. 2014;174: 27–36.
17. Puras G, Martínez-Navarrete G, Mashal M, et al. Protamine/DNA/ Niosome Ternary Nonviral Vectors for Gene Delivery to the Retina: The Role of Protamine. *Mol Pharm*. 2015;12(10):3658–3671.
18. Ojeda E, Puras G, Agirre M, et al. The influence of the polar head-group of synthetic cationic lipids on the transfection efficiency mediated by niosomes in rat retina and brain. *Biomaterials*. 2016;77:267–279.
19. Gu JH, Ge JB, Li M, Xu HD, Wu F, Qin ZH. Poloxamer 188 protects neurons against ischemia/reperfusion injury through preserving integrity of cell membranes and blood brain barrier. *PLoS One*. 2013; 8(4):e61641.
20. Yuan H, Zhang W, du YZ, Hu FQ, Yz D, Fq H. Ternary nanoparticles of anionic lipid nanoparticles/protamine/DNA for gene delivery. *Int J Pharm*. 2010;392(1–2):224–231.
21. Law SL, Chuang TC, Kao MC, Lin YS, Huang KJ. Gene transfer mediated by sphingosine/dioleoylphosphatidylethanolamine liposomes in the presence of poloxamer 188. *Drug Deliv*. 2006;13(1):61–67.
22. Wang Y, Li X, Wang L, Xu Y, Cheng X, Wei P. Formulation and pharmacokinetic evaluation of a paclitaxel nanosuspension for intravenous delivery. *Int J Nanomedicine*. 2011;6:1497–1507.
23. Muzzalupo R, Tavano L, Lai F, Picci N. Niosomes containing hydroxyl additives as percutaneous penetration enhancers: effect on the transdermal delivery of sulfadiazine sodium
salt. *Colloids Surf B Biointerfaces*. 2014;123:207–212.
24. Ojeda E, Puras G, Agirre M, et al. Niosomes based on synthetic cationic lipids for gene delivery: the influence of polar head-groups on the transfection efficiency in HEK-293, ARPE-19 and MSC-D1 cells. *Org Biomol Chem*. 2015;13(4):1068–1081.
25. Ojeda E, Agirre M, Villate-Beitia I, et al. Elaboration and Physicochemical Characterization of Niosome-Based Nioplexes for Gene Delivery Purposes. *Methods Mol Biol*. 2016;1445:63–75.
26. Attia N, Mashal M, Grijalvo S, et al. Stem cell-based gene delivery mediated by cationic niosomes for bone regeneration. *Nanomedicine*. 2018;14(2):521–531.
27. Mashal M, Attia N, Soto-Sánchez C, et al. Non-viral vectors based on cationic niosomes as efficient gene delivery vehicles to central nervous system cells into the brain. *Int J Pharm*. 2018;552(1–2):48–55.
28. Ochoa GP, Sesma JZ, Díez MA, et al. A novel formulation based on 2,3-di(tetradecyloxy)propan-1-amine cationic lipid combined with polysorbate 80 for efficient gene delivery to the retina. *Pharm Res*. 2014; 31(7):1665–1675.
29. Basha M, Abd El-Alim SH, Shamma RN, Awad GE. Design and optimization of surfactant-based nanovesicles for ocular delivery of Clotrimazole. *J Liposome Res*. 2013;23(3):203–210.
30. Bnyan R, Khan I, Ehtezazi T, et al. Surfactant Effects on Lipid-Based Vesicles Properties. *J Pharm Sci*. 2018;107(5):1237–1246.

31. Pezzoli D, Giupponi E, Mantovani D, Candiani G. Size matters for in vitro gene delivery: investigating the relationships among complexation protocol, transfection medium, size and sedimentation. *Sci Rep*. 2017;7:44134.
32. Le Bihan O, Chèvre R, Mornet S, Garnier B, Pitard B, Lambert O. Probing the in vitro mechanism of action of cationic lipid/DNA lipoplexes at a nanometric scale. *Nucleic Acids Res*. 2011;39(4):1595–1609.
33. Mady MM, Darwish MM, Khalil S, Khalil WM. Biophysical studies on chitosan-coated liposomes. *Eur Biophys J*. 2009;38(8):1127–1133.
34. Eastman SJ, Siegel C, Tousignant J, Smith AE, Cheng SH, Scheule RK. Biophysical characterization of cationic lipid: DNA complexes. *Biochim Biophys Acta*. 1997;1325(1):41–62.
35. Jain KK. Cell therapy for CNS trauma. *Mol Biotechnol*. 2009;42(3):367–376.
36. Cacciotti I, Ceci C, Bianco A, Pistritto G. Neuro-differentiated Ntera2 cancer stem cells encapsulated in alginate beads: First evidence of biological functionality. *Mater Sci Eng C Mater Biol Appl*. 2017;81: 32–38.
37. Hara K, Yasuhara T, Maki M, et al. Neural progenitor NT2N cell lines from teratocarcinoma for transplantation therapy in stroke. *Prog Neurobiol*. 2008;85(3):318–334.
38. Hao S, Wang B. Editorial: Review on Intracerebral Haemorrhage: Multidisciplinary Approaches to the Injury Mechanism Analysis and Therapeutic Strategies. *Curr Pharm Des*. 2017;23(15):2159–2160.
39. Frosina G. Stem cell-mediated delivery of therapies in the treatment of glioma. *Mini Rev Med Chem*. 2011;11(7):591–598.
40. Ahmed AU, Alexiades NG, Lesniak MS. The use of neural stem cells in cancer gene therapy: predicting the path to the clinic. *Curr Opin Mol Ther*. 2010;12(5):546–552.
41. Ferrari A, Ehler E, Nitsch RM, Götz J. Immature human NT2 cells grafted into mouse brain differentiate into neuronal and glial cell types. *FEBS Lett*. 2000;486(2):121–125.
42. Midoux P, Monsigny M. Efficient gene transfer by histidylated polylysine/pDNA complexes. *Bioconjug Chem*. 1999;10(3):406–411.
43. Taymouri S, Varshosaz J. Effect of different types of surfactants on the physical properties and stability of carvedilol nano-niosomes. *Adv Biomed Res*. 2016;5:48.
44. Ma B, Zhang S, Jiang H, Zhao B, Lv H. Lipoplex morphologies and their influences on transfection efficiency in gene delivery. *J Control Release*. 2007;123(3):184–194.
45. Goldshtein M, Forti E, Ruvinov E, Cohen S. Mechanisms of cellular uptake and endosomal escape of calcium-siRNA nanocomplexes. *Int J Pharm*. 2016;515(1–2):46–56.
46. Zhao F, Zhao Y, Liu Y, Chang X, Chen C, Zhao Y. Cellular uptake, intracellular trafficking, and cytotoxicity of nanomaterials. *Small*. 2011;7(10):1322–1337.
47. Ruiz de Garibay AP, Solinís Aspiazu MÁ, Rodríguez Gascón A, Ganjian H, Fuchs R. Role of endocytic uptake in transfection efficiency of solid lipid nanoparticles-based nonviral vectors. *J Gene Med*. 2013; 15(11–12):427–440.
48. Puras G, Zarate J, Díaz-Tahoces A, Avilés-Trigueros M, Fernández E, Pedraz JL. Oligochitosan polyplexes as carriers for retinal gene delivery. *Eur J Pharm Sci*. 2013;48(1–2):323–331.
49. Schafer DP, Stevens B. Phagocytic glial cells: sculpting synaptic circuits in the developing nervous system. *Curr Opin Neurobiol*. 2013; 23(6):1034–1040.
50. Bergen JM, Park IK, Horner PJ, Pun SH. Nonviral approaches for neuronal delivery of nucleic acids. *Pharm Res*. 2008;25(5):983–998.
51. Barres BA. The mystery and magic of glia: a perspective on their roles in health and disease. *Neuron*. 2008;60(3):430–440.
52. Milligan ED, Watkins LR. Pathological and protective roles of glia in chronic pain. *Nat Rev Neurosci*. 2009;10(1):23–36.
53. Watson DJ, Longhi L, Lee EB, et al. Genetically modified NT2N human neuronal cells mediate long-term gene expression as CNS grafts in vivo and improve functional cognitive outcome following experimental traumatic brain injury. *J Neuropathol Exp Neurol*. 2003;62(4):368–380.

54. Longhi L, Watson DJ, Saatman KE, et al. Ex vivo gene therapy using targeted engraftment of NGF-expressing human NT2N neurons attenuates cognitive deficits following traumatic brain injury in mice. *J Neurotrauma*. 2004;21(12):1723–1736.

4.8. Supplementary materials

Table S1 Polydispersity index (PDI) of DP80 and DPP80 niocomplexes at different cationic lipid/DNA mass ratios.

Nioplexes	**2/1**	**4/1**	**6/1**	**8/1**	**10/1**	**12/1**
DP80	0.296±0.016	0.222±0.014	0.211±0.013	0.193±0.020	0.229±0.009	0.234±0.012
DPP80	0.208±0.031	0.211±0.017	0.230±0.014	0.217±0.003	0.258±0.032	0.202±0.005

Note: Data represent mean±SD (n=3).

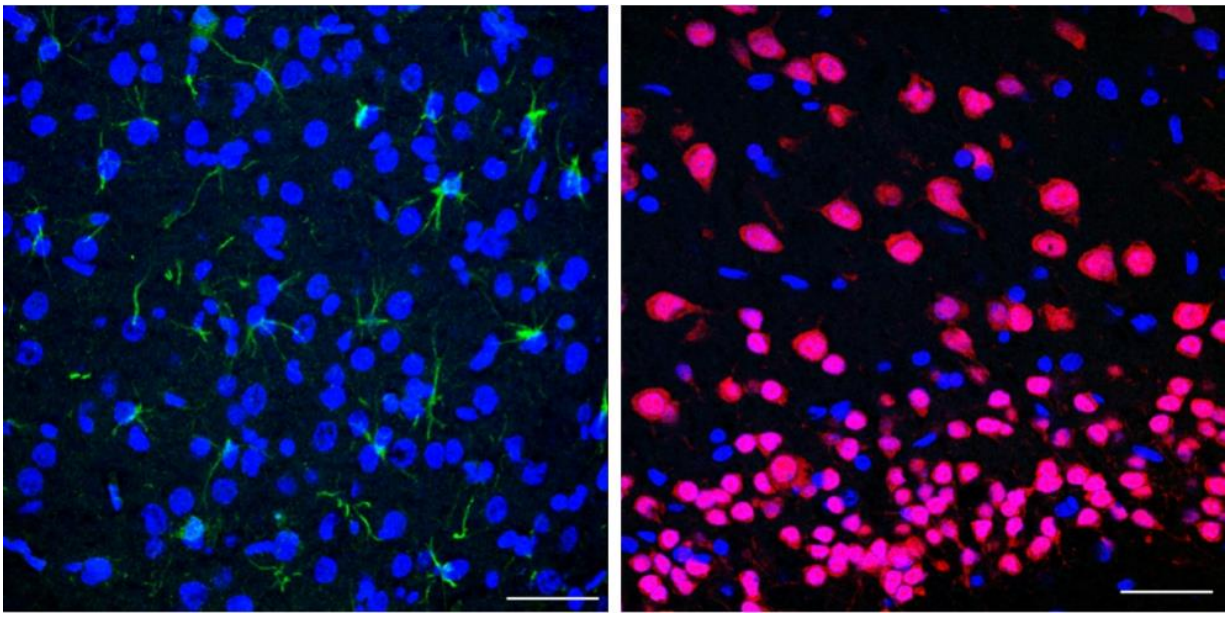

Figure S1 (A) EGFP expression in rat cortex. nuclei are shown in blue (Hoechst); scale bar=40 µm. (B) contralateral picture. nuclei are shown in blue (Hoechst), and neurons in red ($neuN^{+ve}$); scale bar=40 µm.

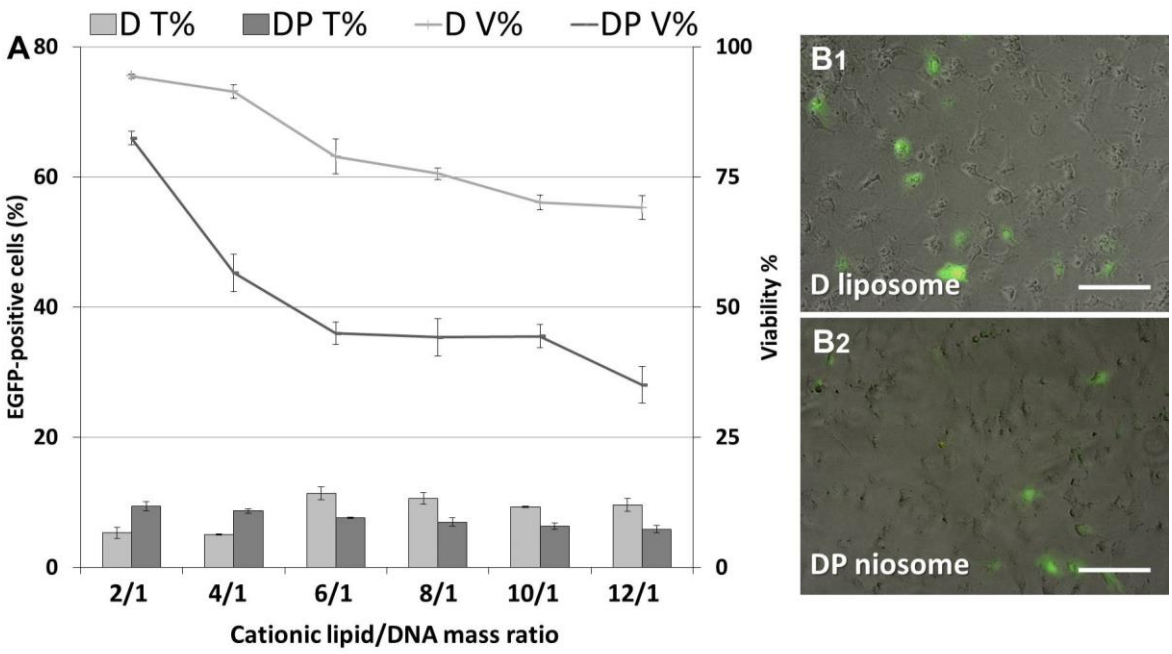

Figure S2 (A) Transfection efficiency of D liposomes and DP niosomes in NT2 cells. Percentages of cells that express green protein (bars) and live cells (lines). Values represent mean±SD (n=3). (B1 and B2) Overlay of fluorescence and DIC pictures of NT2 cells with D liposomes (6/1) and DP niosomes (2/1), respectively (scale bar=100 μm). **Abbreviations:** DIC, digital image correlation; T, transfection; V, viability.

Chapter 5

Volume 53, October 2019, 101219

Journal of Drug Delivery Science and Technology

journal homepage: www.elsevier.com/locate/jddst

Cationic niosome-based hBMP7 gene transfection of neuronal precursor NT2 cells to reduce the migration of glioma cells *in vitro*

Noha Attia[a,b,c,1], Mohamed Mashal[a,1], Santiago Grijalvo[d,e], Ramón Eritja[d,e], Gustavo Puras[a,d], Jose Luis Pedraz[a,d,]

[e] NanoBioCel Group, Laboratory of Pharmaceutics, School of Pharmacy, University of the Basque Country (UPV/EHU), Paseo de la Universidad 7, 01006, Vitoria-Gasteiz, Spain
[f] Histology and Cell Biology Department, Faculty of Medicine, University of Alexandria, Alexandria, Egypt
[g] Department of Basic Sciences, The American University of Antigua-College of Medicine, Coolidge, Antigua and Barbuda
[h] Networking Research Centre of Bioengineering, Biomaterials and Nanomedicine (CIBER-BBN), Vitoria-Gasteiz, Spain
[i] Institute for Advanced Chemistry of Catalonia (IQAC-CSIC), Spain
[1] Noha Attia and Mohamed Mashal contributed equally to this work.

Cationic niosome-based hBMP7 gene transfection of neuronal precursor NT2 cells to reduce the migration of glioma cells *in vitro*

ABSTRACT

This study explores interesting complementary approaches in cell-based hBMP7 gene delivery in order to mitigate the migration of glioblastoma cells based on the idea that this human bone morphogenetic protein (hBMP7) has enormous therapeutic potential in curing brain injuries as well as malignancies. After physicochemical characterization, the non-viral cationic niosomes were complexed with pUNO1-hBMP7 plasmids and used to transfect neuronal precursor NT2 cells. Subsequently, the transfected cells were co-cultured with glioma C6 cells to determine their antitumor effect in vitro. However, the co-culture with either untransfected/transfected NT2 cells may reduce the viability of C6 glioma cells, the hBMP7-overexpressing NT2 cells hamper the migration of C6 glioma cells. These results highlight the potential of NT2 cell-based delivery of hBMP7 for impeding the metastasis of glioma cells.

Key words: Glioblastoma; Gene therapy; hBMP7; Niosomes; NT2 cells

5.1. Introduction

Glioblastoma multiforme (GBM), the most aggressive primary intracranial tumor, is well-known for its high mortality rate and poor treatment outcomes [1]. The average survival time of patients following surgery combined with chemotherapy and/or radiotherapy, is less than 12 months. Therefore, therapeutic approaches are still needed to fight this devastating disease. During glioma genesis, the tumor-suppressive activity of transforming growth factor-β (TGF-β) signaling pathway is generally perturbed, leading to malignant progression [2].

The human bone morphogenetic protein 7 (hBMP7), a member of the transforming growth factor β superfamily, plays a pivotal role in the development of bone, kidney and nervous tissues [3]. Interestingly, exposure to BMP7 can induce canonical BMP signaling in stem-like glioblastoma cells, *in vitro* [4]. The ability of BMP7 to induce the differentiation of brain tumor stem cells is accompanied by the attenuation of stem-like marker expression and reduction of self-renewal. Currently, the *in vivo* delivery methods of BMP7 are basically through multiple local and/or intravenous injections of the recombinant hBMP7. Unlike some other growth factors, BMPs have a short half-life, are not particularly soluble and seem to act locally, so the aforementioned delivery

routes are often ineffective [5], and need multiple injections. Nevertheless, in sensitive tissues such as brain tissue, repeated injections could lead to inevitable tissue damage. Therefore, alternative approaches for supplying BMP7 to glioma cells are needed to circumvent the negative aspects of conventional therapies. Amongst those promising alternatives are those based on cell/gene delivery. More specifically, human neuronal precursor NT2 cells exhibit two ideal characteristics for cancer gene therapy; they have tumor-selective migratory capacity and they can be genetically manipulated to express selected therapeutic genes [6].

As gene delivery systems, non-viral vectors have gained attention over the years, in comparison to their counterparts, the viral-based vectors [7,8]. Non-viral gene carriers are not as limited by the size of the transferred genes and they have a lower immunogenicity and oncogenic profile. These appealing features make the non-viral gene carriers potential candidates for commercialization because of how easy it is to produce them and also because there are less hurdles to overcome in terms of meeting the regulatory standards.

As non-viral gene carriers, cationic niosomes are osmotically active self-assembled vesicles made up of cationic lipids and non-ionic surfactants. They are better than liposomes in terms of cost effectiveness and chemical stability, and have received increasing attention over time as potential gene delivery vehicles [9,10].

In our recent study [11], we developed a novel cationic niosome gene carrier based on chemical compounds (the cationic lipid 2,3-di-tetradecyloxypropan-1amine, the non-ionic surfactants poloxamer 188 and polysorbate 80) demonstrating flattering properties for gene delivery applications [12]. Our previous results obtained with reporter GFP plasmids, in vitro/vivo, have encouraged us to proceed with the current study in which we aimed to provide a proof-of-concept of whether NT2 cells could be used as a model for hBMP7 gene expression in order to combat glioma cell migration. We initially transfected NT2 cells with DPP80- hBMP7 nioplexes and then we investigated their potential "combined" antitumor effect on C6 glioma cell line, *in vitro*.

5.2. Material and methods

5.2.1. Material

Human teratocarcinoma NTERA2/D1(NT2) (ATCC®−CRL, 1973) and the rat glioma cell line (C6, CCL-107) were purchased from the American Type Culture Collection (ATCC, Manassas, VA, USA). C6 cells were grown in the ATCC-formulated F-12K Medium (Catalog No. 30-2004).

Dulbecco's Modified Eagle's Medium (DMEM, ATCC 30 −2002), trypsin, Fetal bovine Serum (FBS) were purchased from Gibco® (San Diego, California, US). Opti-MEM® reduced medium, Lipofectamine® 2000 transfection reagent, antibiotics [100 U/ml penicillin and 100 μg/ ml streptomycin (Pen/Strep)] were acquired from Gibco® (Life Technologies S.A., Madrid, Spain). Cell counting (CCK-8) viability/ proliferation assay and crystal violet were obtained from Sigma Aldrich (Madrid, Spain). GelRed® solution was obtained from Biotium (Hayward, California, USA), while other materials for gel electrophoresis were obtained from Bio-Rad (Madrid, Spain). pUNO1-hBMP7 plasmid (0.5 mg/ml) was obtained from InvivoGen (Toulouse, France). Sodium dodecyl sulfate (SDS), DNase I, polysorbate 80, poloxamer 188, and PBS were purchased from Sigma Aldrich (Madrid, Spain). Uncoated Transwell® 24 well microplates with 8.0 μm pore size (Costar-Corning, Corning, NY).

5.2.2. Preparation of niosome vesicles

The cationic lipid 2,3-di (tetradecyloxy)propan-1-amine hydrochloride (D) was synthesized by slightly modifying the experimental protocol previously described [13]. Afterward, niosomes were manufactured by modifying the reverse phase evaporation technique as discussed earlier [14]. Briefly, the cationic lipid (5 mg) was dissolved in dichloromethane (1 ml), and then emulsified in 5 ml of non-ionic surfactant “equal weight % of polysorbate 80 (P80) and poloxamer 188 (P). The emulsion was obtained by sonication (Branson Sonifier 250®, Branson Ultrasonics Corporation, Danbury, USA) at 45 W for 30 s. After evaporating the dichloromethane, the resulting niosomes were referred to as DPP80 (components shown in Fig. 1).

5.2.3. Preparation of DPP80-hBMP7 nioplexes

The niosome/DNA complexes (nioplexes) were obtained by mixing an appropriate volume of a stock solution of pUNO1-hBMP7 plasmid (0.5 mg/ml) with different volumes of niosome suspensions (1 mg cationic lipid/ml) in order to obtain different cationic lipid/DNA ratios (w/w). The mixture was incubated for 30 min at room temperature to ensure electrostatic interactions.

5.2.4. Assessment of DPP80-hBMP7 nioplexes’ features

Dynamic light scattering (DLS) and Laser Doppler Velocimetry (LDV) (Zetasizer Nano ZS, Malvern Instruments, UK) were used to determine the particle size and zeta potential (ZP), respectively. Particle size was obtained using cumulative analysis where all measurements were carried out in triplicate.

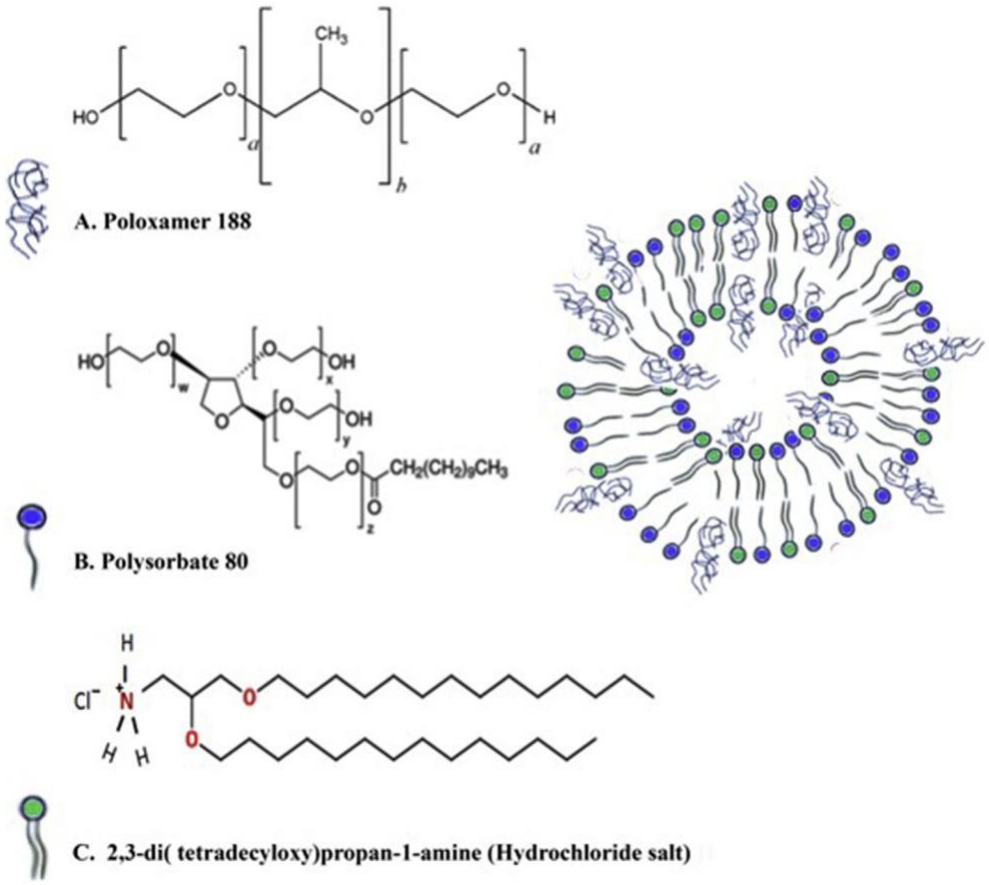

Fig. 1. Chemical structure of: A) Poloxamer 188 (P), B) Polysorbate 80 (P80), and C) Cationic lipid [2,3-di(tetradecyloxy)propan-1-amine] (D).

Nioplexes were examined by via cryo-TEM (TECNAI G2 20 TWIN), operating at an accelerated voltage of 200 KeV in a bright-field and low-dose image mode [15]. The acquired digital images were used to assess the nioplexes' morphology. The niosomes' potential to condense, liberate and protect the pUNO1-hBMP7 plasmid DNA against enzymatic digestion was evaluated using an agarose gel retardation assay. The naked and niosome-complexed DNA samples (200 ng of plasmid/20 µl) were run on an agarose gel (0.8% w/v). The tris–acetate–EDTA buffer-immersed gel was later exposed to 120 V for 30 min. In order to analyze the release of DNA from nioplexes at different cationic lipid/DNA mass ratios, 20 µl of the SDS solution (2%) were added/sample. The supposed nioplexes-induced protection for DNA against DNase I enzymatic digestion was assessed by adding 1U DNase I/2.5 µg DNA. Subsequently, mixtures were incubated at 37 °C for 30 min followed by adding an SDS solution (like above) to release DNA from the nioplexes. The resulting bands were stained with GelRed™ and visualized by ChemiDoc™ MP Imaging System (Bio-Rad, Madrid, Spain).

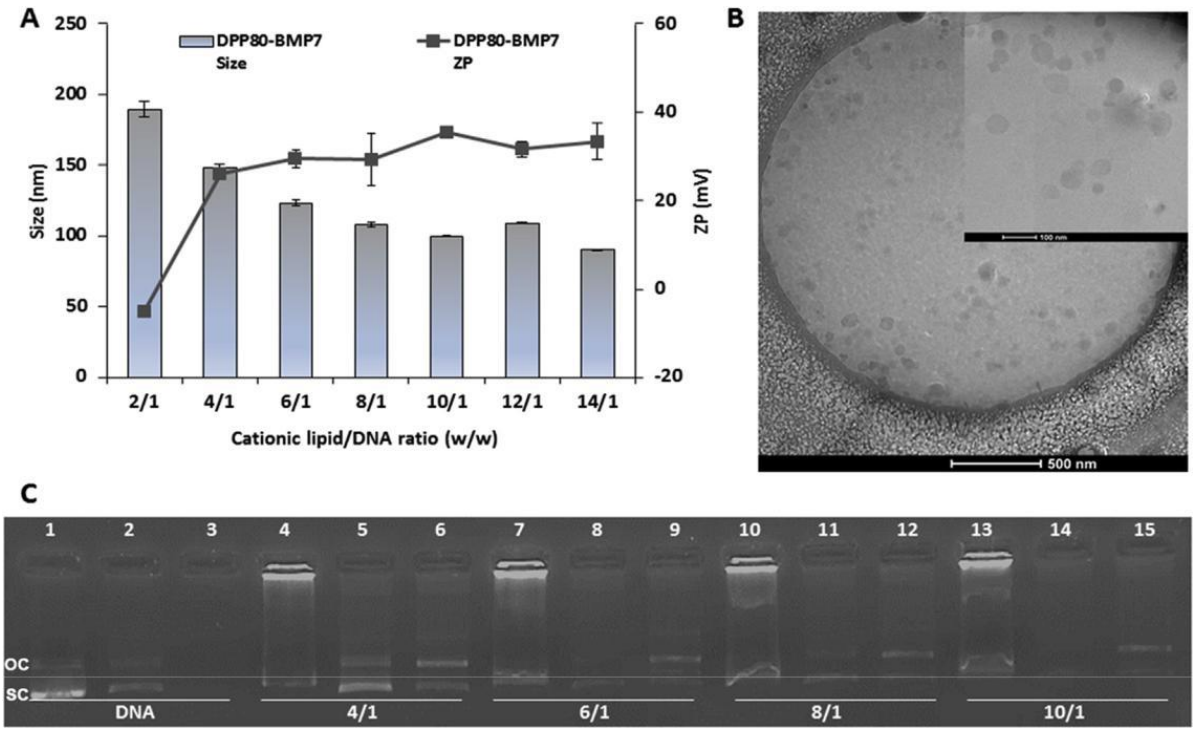

Fig. 2. A) Particle size (nm) and Zeta potential (mV). Data represent mean ± SD (n = 3). B) Cryo-TEM micrographs of nioplexes at 6/1 cationic lipid/DNA mass ratio. Scale bar 500 nm (inset, 100 nm). C) Gel retardation assay of nioplexes. Lanes 2, 5, 8, 11 and 14 depict nioplexes treated with SDS, while lanes 3, 6, 9, 12 and 15 correspond to DNase I- and SDS-treated nioplexes. OC and SC: open circular and supercoiled forms, respectively.

5.2.5. In vitro culture and transfection of NT2 cells

NT2 cells (ATCC®−CRL, 1973) were cultured in a growth medium composed of; Dulbecco's Modified Eagle's Medium (DMEM), 10% fetal bovine serum (FBS) and antibiotics (100 U/ml penicillin and 100 μg/ml streptomycin. The night before transfection, NT2 cells were seeded in 24-well plates at an initial density of 8×10^4 cells/well and allowed to proliferate up to 70−80% confluence. The medium was then replaced with serum-free Opti-MEM, and cells were exposed to the nioplexes at a concentration of 1.25 μg of pUNO1-hBMP7/well. After 4 h of incubation, the serum-free transfection medium was replaced with the growth medium. 24 h later, conditioned media (NT2-CM) was collected, filtered (0.22 μm filters) and preserved at −80 °C until ELISA was performed to determine the hBMP7 secreted. Cell counting (CCK-8) viability/proliferation assay was carried out as previously reported [16]. The color development was read at 450 nm (Tecan M200 microplate reader), corrected with reference wavelength at 690 nm, and normalized

against blank wells. The positive control, Lipofectamine® 2000 was prepared following the manufacturer's transfection protocol.

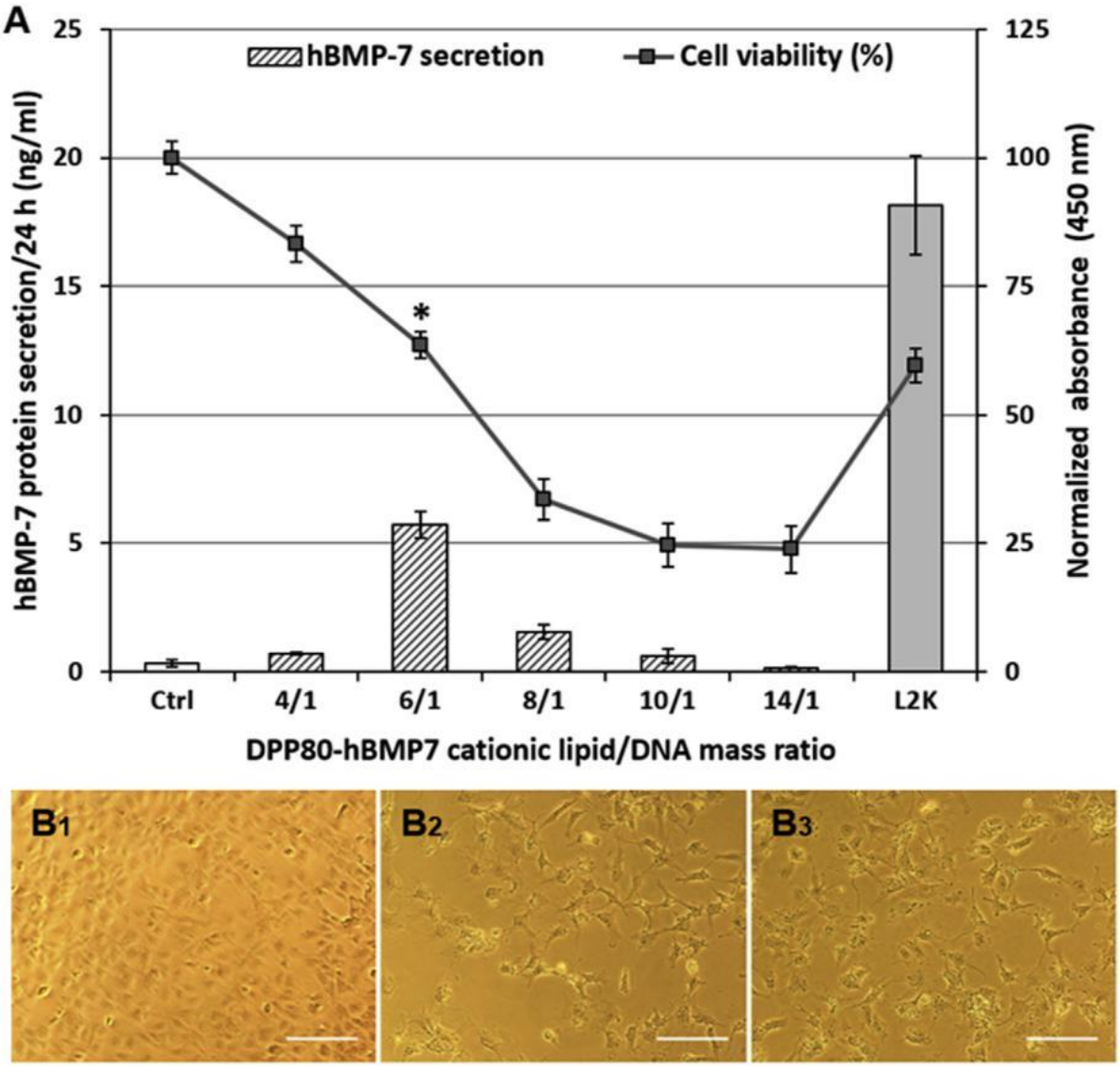

Fig. 3. (A) hBMP7 secretion (ng⁄ml) at 24 h (bars). Values represent mean ± SD (n = 3). $P < 0.05$ versus L2K. (B) Phase contrast micrographs of NT2 cells 24 h post-transfection (B1) control, (B2) hBMP7-DPP80-transfected, (B3) hBMP7-L2K-transfected cells. (Scale bars = 50 μm).

5.2.6. In vitro culture and proliferation assay of C6 glioma cells

The rat glioma cell line (C6, CCL-107) was grown in the ATCC-formulated F-12K Medium (Catalog No. 30-2004). To make the growth medium (GM), fetal bovine serum was added to a final concentration of 2.5%, horse serum to a final concentration of 15%, 100 U/ml of penicillin,

and 100 μg/ml of streptomycin. Cells were maintained at a humidified atmosphere at 37 °C with 5% CO_2 and were used at the third passage.

In 24 multiple-well culture plates, C6 cells were seeded (100.000 cells/well) overnight. The next day, GM was replaced with NT2-CM, both untransfected ($^{+}$NT2) and transfected ($^{+}$NT2-hBMP7). The C6-CM was prepared as mentioned in section **5.2.4**. After 24 h, cell proliferation was determined using CCK8 assay according to the manufacturer's instructions. The wells where NT2-CM was added were compared to "control" C6 glioma cells wells grown on C6-CM.

5.2.7. Co-culture and Transwell migration assays

The glioma cell migration assay was carried out using uncoated Transwell® 24 well microplates with 8.0 μm pore size. About 80.000 NT2 cells (of untransfected/transfected cultures (24 h post-transfection) were seeded in the lower chambers and incubated at 37 °C for 4 h to ensure cell attachment. Then, C6 glioma cells (in 200 μl serum free media) were seeded in the upper Transwell insert (100.000 cells/insert). 16 h later, the medium was aspirated, and non-migratory cells were removed by swabbing the interior of the insert wells using cotton-tipped swabs. The migrating C6 cells on the lower surface of the Transwell® membranes were fixed in methanol, stained with crystal violet (0.09% crystal violet) and counted under an inverted optical microscope (Nikon TSM). Five random fields were counted for each membrane, and the mean values from three independent experiments, performed in triplicate, were used.

5.2.8. Statistical analysis

Statistical differences between groups (significance levels of >95%) were calculated using ANOVA and Student's t-test. The values of $p < 0.05$ were regarded to be significant. Samples' normal distribution and homogeneity of the variance were evaluated with the Kolmogorov-Smirnov and the Levene tests, respectively. All numerical data were presented as mean ± SD.

5.3. Results

5.3.1. Physicochemical features of niosomes/nioplexes

Fig. 2-A depicts both size and ZP assessment of DPP80-hBMP7nioplexes at mass ratios 2/1 through 14/1. The size of nioplexes (bars) gradually decreased from 190 nm to 90 nm at cationic lipid/DNA mass ratios of 2/1 and 14/1, respectively. With regard to surface charge, ZP readings gradually increased from −5.2 mV at 2/1 mass ratio to +35.5 mV at 10/1 mass ratio without any notable change thereafter. As illustrated in Fig. 2-B, the cryo-TEM-examined nioplexes (6/1 mass ratio) depicted imperfect spherical particles. Fig. 2-C represents gel retardation assay of nioplexes

prepared at different cationic lipid/DNA ratios (4/1, 6/1, 8/1 and 10/1). Such nioplexes demonstrated satisfactory ability to hold DNA, since most of the DNA signal was observed in the corresponding wells (4, 7, 10 and 13 lanes), and only faint SC bands were observed. Interestingly enough, the restrained DNA was liberated upon adding SDS, since no clear bands were observed in wells 5, 8, 11 and 14. Moreover, the DNA was protected from the DNase I enzyme, since clear OC (open circular) and SC (supercoiled) bands were detected in the 6th, 9th, 12th and 15th lanes, compared to the 3rd lane (free DNA).

5.3.2. *In vitro* transfection of NT2 cells

The secretion of hBMP7 by transfected/untransfected NT2 cells at 24 h post transfection is observed in Fig. 3-A (bars). Throughout the studied cationic lipid/DNA mass ratios, the ratios of 6/1 and 8/1 depicted significant secretion of hBMP7 in comparison to the un-transfected "ctrl" cells ($p < 0.05$). The ratio of 6/1 was the highest transfection results (5.7 ng/ml), although it was still inferior to the secretion obtained by L2K transfection (18 ng/ml, $p < 0.05$). On the other hand, CCK8 assay demonstrated that cell viability was almost inversely related to the mass ratio of cationic lipid/DNA (Fig. 3, line graph). At the mass ratio of 6/1, peak of hBMP7 secretion, cell viability was still higher than that of L2K (63.6% and 59.5%, respectively, $p < 0.05$). Control NT2 cells were epithelial-like adherent cells (Fig. 3-B_1). One-day post-transfection, cells treated with DPP80 or L2K formulations, appeared more polyhedral with elongated processes (Fig. 3-B_2 and 3-B_3, respectively).

5.3.3. In vitro proliferation assay of C6 glioma cells

In order to measure the functionality of secreted hBMP7 on glioma cells, rat C6 glioma cells were treated with the conditioned media of untransfected (NT2-CM) and transfected (NT2-hBMP7-CM) cells. The NT2-CM significantly inhibited the cell growth of C6 cells, whether transfected ($^{+}$NT2-hBMP7-CM) or untransfected ($^{+}$NT2-CM) when compared to the C6-CM (*$P < 0.05$) (Fig. 4). However, the anti-proliferative effect of the CM retrieved from transfected and untransfected NT2 cells was almost the same ($P > 0.05$).

5.3.4. Transwell migration assay of C6 glioma cells

Subsequently, the effect of hBMP7 secretion on C6 glioma cell migration was evaluated. As seen in Fig. 5, the migration of C6 cells was notably less (*$P < 0.05$) when co-cultured with transfected NT2 cells ($^{+}$NT2-hBMP7) compared to the untransfected cells ($^{+}$NT2).

5.4. Discussion

The high mortality rate and aggressiveness in GBM patients has necessitated the search for novel, safe, and effective therapeutic approaches. Over the past few years, both cell and gene therapies have offered great promise in this realm.

In this study, we aimed to investigate the effectiveness of the newly synthesized cationic niosomes (DPP80) for transfecting NT2 cells, thus obtaining hBMP7-overexpressing NT2 cells. Such cationic niosomes were electrostatically complexed with the negatively charged pUNO1-hBMP7 plasmid rendering nioplexes at different cationic lipid/DNA mass ratios. Despite the lack of consensus over the optimal size of non-viral gene carriers, it is widely accepted that the particle size clearly affects their performance. In the current work, the size of nioplexes was clearly affected by the cationic lipid/DNA mass ratio (Fig. 2-A). At the mass ratio of 2/1, the size was almost 190 nm. Alongside higher mass ratios, the size gradually decreased, and this was most likely due to the electrostatic interactions that condense DNA plasmids more tightly. Not only their size, but the shape of non-viral complexes can also affect their final performance in gene delivery [3]. Our complexes were not perfectly regular in shape (Fig. 2-B) which could be due to the in-corporation of non-ionic surfactants on the surface of niosomes. As well, the discrete morphology of nioplexes at 6/1 mass ratio (Fig. 2-B) may be attributed to the high positive surface charge (> 29 mV), which in turn evades the particles' aggregation through electrostatic repulsion [17]. The electrostatic interactions between the DNA (negatively charged phosphate groups) and the cationic niosomes (positively charged amine groups) play a crucial role during the transfection process as a precise balance between DNA capture and release needs to be achieved [18]. To investigate that parameter, gel retardation assay was carried out (Fig. 2-C). We selected nioplexes at cationic lipid/DNA mass ratios higher than 2/1 since the values of ZP were within the positive range (Fig. 2-A, lines). Interestingly, at all studied cationic lipid/DNA ratios, the niosomes were not only able to partially condense and totally release DNA upon adding SDS in all the cationic lipid/DNA mass ratios tested, but also to protect DNA against the enzymatic digestion, which is of significance in relevant in vivo applications.

Thanks to the previously mentioned desirable characteristics of DPP80-hBMP7 nioplexes, we went on to carry out an in vitro transfection study in order to evaluate the capacity of nioplexes to deliver pUNO1-hBMP7 plasmid into NT2 cells. Besides being regarded as a stable cell line suitable for transfection studies, NT2 cells have been reported to be a promising source of human

cells in CNS-targeted cell therapy applications [19].

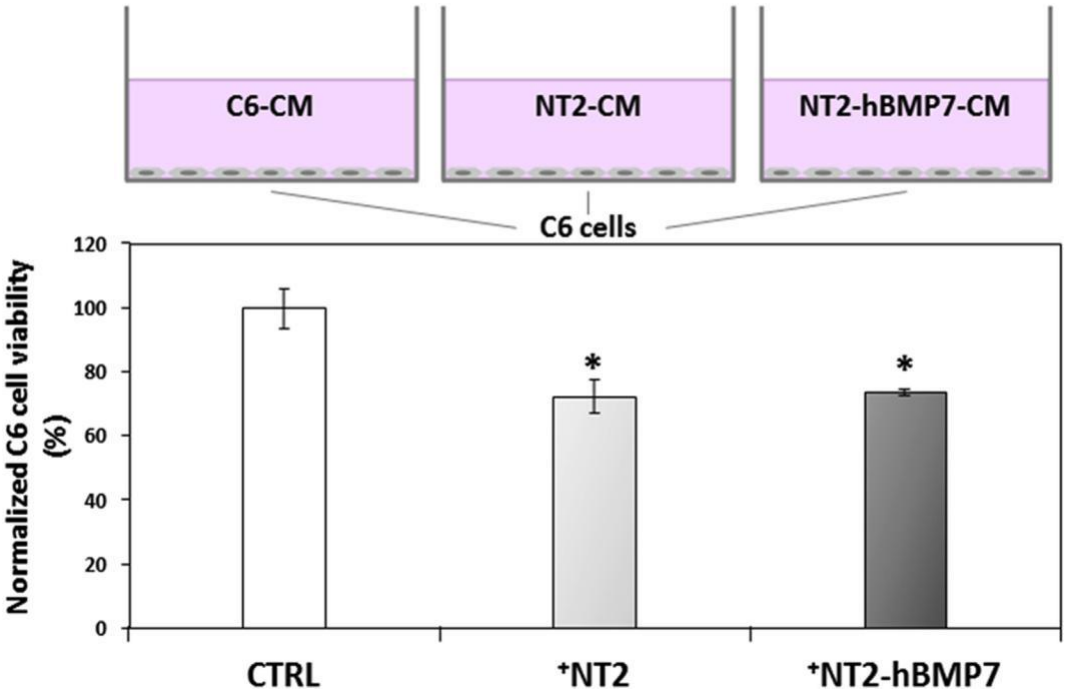

Fig. 4. In vitro viability assay of C6 glioma cells after incubation with; C6-CM, untransfected NT2 cells and transfected NT2 cells. (*P < 0.05).

Interestingly, NT2 cells have successfully induced recovery in pre-clinical stroke models. Therefore, they have been endorsed in several clinical trials [20]. In particular, their intrinsic glioma-tropism has opened up new avenues for brain malignancy therapeutics. NT2 cells are advantageously amenable to scale-up cell production, thus might represent a delivery vehicle for cancer therapy [21]. The transfection data (Fig. 3) revealed the release of significant amount of hBMP7 (5.7 ng/ml) at the mass ratio of 6/1 (cationic lipid/ DNA) where the cytotoxicity on NT2 cells was less compared to positive control L2K ($p < 0.05$).

These results suggest that the BMP7-secreting NT2 cells could be used as an interesting platform for further *in vivo* studies on the nervous tissue as well as other tissues where the production of BMP7 is desired. Despite the comparatively low level of hBMP7 secretion (5.7 ng/ml) by transfected NT2 cells, a markedly low dose of hBMP7 (1 ng/ml) could increase SMAD phosphorylation 5–6 fold, thus having a significant therapeutic effect [5]. A low, yet continuous dose of hBMP7 expression could be both neuroprotective and differentiation-inductive [22]. Similarly, our research team has recently reported a marked impact of hBMP7 production, even at much lower expression values, to induce spontaneous osteogenic differentiation of mesenchymal stem cells [3].

Interestingly, a dose of 1.3 ng/ml of hBMP7 was enough to enhance the alkaline phosphatase activity and osteogenic matrix deposition, suggesting the effectiveness of such low concentrations of hBMP7 to achieve appropriate biological activities [5]. We then proceeded to evaluate the outcome of NT2-expressed hBMP7 on glioma cells. C6 glioma cells are stable, in vitro and in vivo, and express glioma-specific markers [23]. Thereafter, they are widely used in experimental studies for the treatment of gliomas [24]. An in-direct co-culture system by culturing tumor C6 cells in the CM of NT2 cells was adopted to avoid the drawbacks of the direct co-culture system. In particular, the difficulty to evaluate the effect of one type of cells on another type.

The overexpression of hBMP7 can alter the NT2 gene expression and suppress their own tumorigenesis, making them a safe candidate for in vivo studies [25]. Moreover, activation of BMP7 signaling in glioma cells could render them more vulnerable, and thereby more sensitive to low doses of chemotherapeutic drugs [26].

In accordance with Li and colleagues [27], the anti-glioma effect of NT2-CM could be mediated by the inactivation of mitogen activated protein kinase (MAPK) pathway. On the other hand, we observed (Fig. 4) that the overexpression of hBMP7 “per se” did not add any inhibitory effect on the viability of C6 cells. This effect could most probably be attributed to the presence of anti-BMP signals in the remaining serum content of NT2-CM, such as cytokines, noggin or chordin. The main goal of most antitumor drugs is to reduce cancer cell viability. However, because of the hyper-mutability of GBM cells, adjuvant anti-migration strategies are also desirable.

Among others, Chirasani and co-workers [28] have reported, in agreement with our findings, the ability of BMP7-expressing neural precursor cells to attenuate the tumorigenicity of glioblastoma cells as well as to induce glioma stem cell differentiation [29]. Regarding the observed suppression of migration effect, it should be noted that BMP7 may have contradictory effects depending on the cell line being investigated [30]. The discerned anti-migratory effects of hBMP7-transfected NT2 cells (Fig. 5) could be attributed to the negative effect of hBMP7 on cell motility (across uncoated Transwell filters) [31] or to the induction of tumor stem cell differentiation/senescence [26]. Thus, further studies on the exact mechanism are still required. This study represents a proof of concept that NT2 cells could be transfected with hBMP7 expression plasmids using the DPP80 cationic niosome gene carrier. Subsequently, the tumor-suppressive effect of hBMP7-expressing NT2 cells were investigated on the glioma cell line C6. The current preliminary data suggest that the NT2 cell-based gene delivery of hBMP7 could be further explored in animal models as a novel

therapeutic approach to inhibit the proliferation and migration of gliomas. Adequate understanding of the underlying mechanisms is necessary for the development of effective cellular delivery vehicles for glioma therapy.

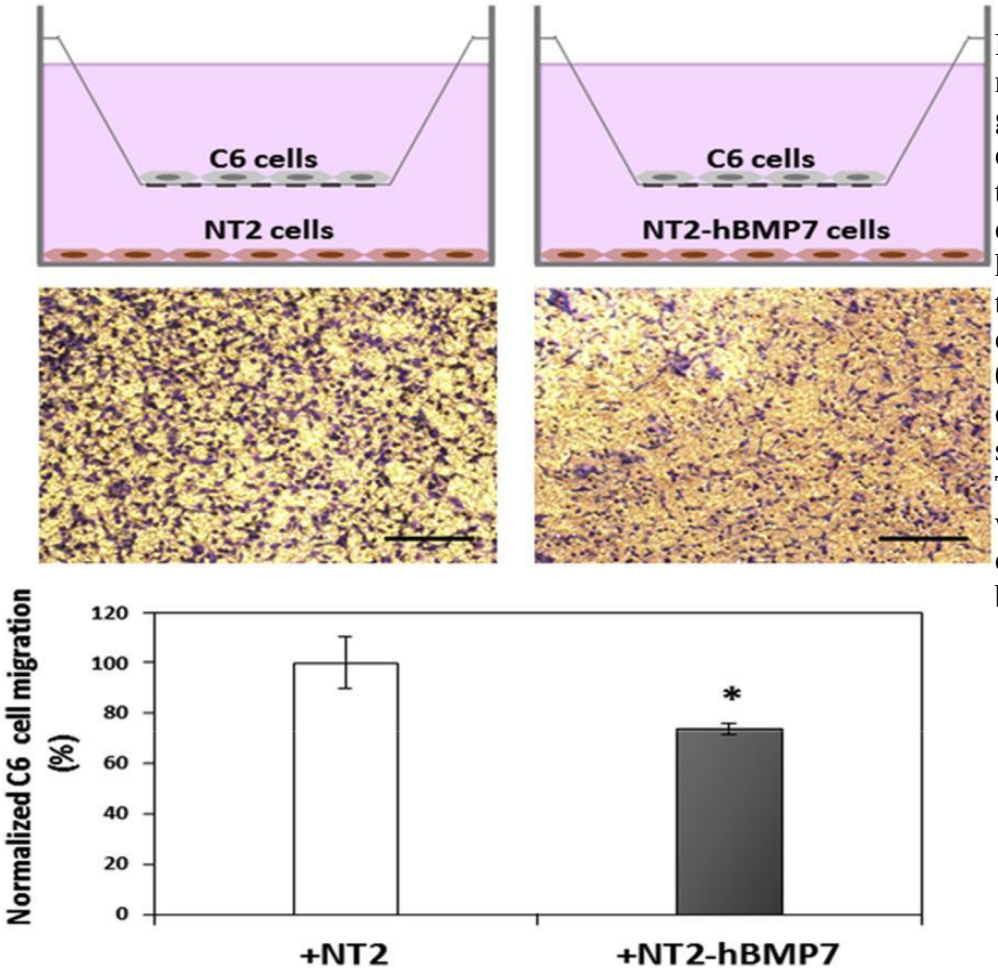

Fig. 5. Transwell migration assay of glioma C6 cells co-cultured with transfected NT2 cells (+NT2-hBMP7) compared to the untransfected cells (+NT2) (*P < 0.05). C6 glioma cells on the lower surface of Transwell inserts were stained with crystal violet (scale bar = 50 μm).

Conflicts of interest

The authors report no conflicts of interest in this work.

5.5. Acknowledgements

This project was supported by the Basque Country Government (CGIC10/172), The Spanish Ministry of Education (Grant CTQ2014-52588-R), the Generalitat de Catalunya (2014/SGR/624) and the Instituto de Salud Carlos III (CB06_01_0019, CB06_01_1028).The authors also wish to thank the intellectual and technical assistance from the ICTS “NANBIOSIS”, more specifically by the Drug Formulation Unit (U10) of the CIBER at Bioengineering, Biomaterials, and Nanomedicine (CIBER-BBN) at the University of Basque Country (UPV/EHU). Technical and human support provided by SGIker (UPV/EHU) is gratefully acknowledged.

5.6. References

[1] C. Giannini, J.N. Sarkaria, A. Saito, J.H. Uhm, E. Galanis, B.L. Carlson, et al., Patient tumor EGFR and PDGFRA gene amplifications retained in an invasive intracranial xenograft model of glioblastoma multiforme, Neuro Oncol. 7.2 (2005) 164–176 https://doi.org/10.1215/S1152851704000821.

[2] A.W. Nana, P.M. Yang, H.Y. Lin, Overview of transforming growth factor β super-family involvement in glioblastoma initiation and progression, Asian Pac. J. Cancer Prev. APJCP 16 (16) (2015) 6813–6823 https://doi.org/10.7314/APJCP.2015.16. 16.6813.

[3] N. Attia, M. Mashal, S. Grijalvo, R. Eritja, J. Zárate, G. Puras, et al., Stem cell-based gene delivery mediated by cationic niosomes for bone regeneration, Nanomedicine 14 (2) (2018) 521–531 https://doi.org/10.1016/j.nano.2017.11.005.

[4] C. Tate, R. Pallini, L. Ricci-Vitiani, M. Dowless, T. Shiyanova, G. D'alessandris, et al., BMP7 variant inhibits the tumorigenic potential of glioblastoma stem-like cells, Cell Death Differ. 19 (10) (2012) 1644 https://doi.org/10.1038/cdd.2012.44.

[5] D.W. Chitty, R.G. Tremblay, M. Ribecco-Lutkiewicz, J. Haukenfrers, B. Zurakowski, B. Massie, et al., Development of BMP7-producing human cells, using a third-generation lentiviral gene delivery system, J. Neurosci. Methods 205 (1) (2012) 17–27 https://doi.org/10.1016/j.jneumeth.2011.12.007.

[6] A.U. Ahmed, N.G. Alexiades, M.S. Lesniak, The use of neural stem cells in cancer gene therapy: predicting the path to the clinic, Curr. Opin. Mol. Ther. 12 (5) (2010) 546–552 PMID:20886386 PMCID:PMC2958255.

[7] S. Grijalvo, G. Puras, J. Zárate, M. Sainz-Ramos, N.A. Qtaish, T. López, M. Mashal, N Attia, D. Díaz, R. Pons, E. Fernández, Cationic niosomes as non-viral vehicles for nucleic acids: challenges and opportunities in gene delivery, Pharmaceutics 11.2 (2019) 50 https://doi.org/10.3390/pharmaceutics11020050.

[8] M. Mashal, N. Attia, G. Martínez-Navarrete, C. Soto-Sánchez, E. Fernández, S. Grijalvo, R. Eritja, G. Puras G, J.L. Pedraz, Gene delivery to the rat retina by non-viral vectors based on chloroquine-containing cationic niosomes, J. Control. Release 304 (2019) 181–190 https://doi.org/10.1016/j.jconrel.2019.05.010.

[9] M. Mashal, N. Attia, G. Puras, G. Martinez-Navarrete, E. Fernandez, J.L. Pedraz, Retinal gene delivery enhancement by lycopene incorporation into cationic niosomes based on DOTMA and polysorbate 60, J. Control. Release 254 (2017) 55–64 https://doi.org/10.1016/j.jconrel.2017.03.386.

[10] M. Mashal, N. Attia, C. Soto-Sánchez, G. Martínez-Navarrete, E. Fernández, G. Puras, J.L. Pedraz, Non-viral vectors based on cationic niosomes as efficient gene delivery vehicles to central nervous system cells into the brain, Int. J. Pharm. 552 (1–2) (2018) 48–55 https://doi.org/10.1016/j.ijpharm.2018.09.038.

[11] N. Attia, M. Mashal, C. Soto-Sánchez, G. Martínez-Navarrete, E. Fernández, S. Grijalvo, R. Eritja, G. Puras, J.L. Pedraz, Gene transfer to rat cerebral cortex mediated by polysorbate 80 and poloxamer 188 nonionic surfactant vesicles, Drug Des. Dev. Ther. 12 (2018) 3937 https://doi.org/10.2147/DDDT.S178532.

[12] S.L. Law, T.C. Chuang, M.C. Kao, Y.S. Lin, K.J. Huang, Gene transfer mediated by sphingosine/dioleoylphosphatidylethanolamine liposomes in the presence of poloxamer 188, Drug Deliv. 13 (2006) 61–67 https://doi.org/10.1080/ 10717540500309024.

[13] G. Kokotos, R. VergeR, A. Chiou, Synthesis of 2-oxo amide triacylglycerol analogues and study of their inhibition effect on pancreatic and gastric lipases, Chem. Eur. J. 6 (22) (2000) 4211–4217.

[14] E. Ojeda, M. Agirre, I. Villate-Beitia, M. Mashal, G. Puras, J. Zarate, et al., Elaboration and physicochemical characterization of niosome-based nioplexes for gene delivery purposes, Non-Viral Gene Delivery Vectors, Humana Press, New York, NY, 2016, pp. 63–75.

[15] E. Ojeda, G. Puras, M. Agirre, J. Zárate, S. Grijalvo, R. Pons, et al., Niosomes based on synthetic cationic lipids for gene delivery: the influence of polar head-groups on the transfection efficiency in

HEK-293, ARPE-19 and MSC-D1 cells, Org. Biomol. Chem. 13 (4) (2015) 1068–1081 https://doi.org/10.1039/c4ob02087a.

[16] N. Attia, E. Santos, H. Abdelmouty, S. Arafa, N. Zohdy, R.M. Hernández, et al., Behaviour and ultrastructure of human bone marrow-derived mesenchymal stem cells immobilised in alginate-poly-l-lysine-alginate microcapsules, J. Microencapsul. 31 (6) (2014) 579–589 https://doi.org/10.3109/02652048.2014. 898706.

[17] G. Puras, M. Mashal, J. Zarate, M. Agirre, E. Ojeda, S. Grijalvo, et al., A novel cationic niosome formulation for gene delivery to the retina, J. Control. Release 174 (2014) 27–36 https://doi.org/10.1016/j.jconrel.2013.11.004.

[18] S. Eastman, C. Siegel, J. Tousignant, A. Smith, S. Cheng, R. Scheule, Biophysical characterization of cationic lipid: DNA complexes, Biochim. Biophys. Acta 1325 (1) (1997) 41–62 https://doi.org/10.1016/S0005-2736(96)00242-8.

[19] I. Cacciotti, C. Ceci, A. Bianco, G. Pistritto, Neuro-differentiated Ntera2 cancer stem cells encapsulated in alginate beads: first evidence of biological functionality, Mater Sci Eng C Mater Biol Appl 81 (2017) 32–38 https://doi.org/10.1016/j.msec.2017. 07.033.

[20] N.C. Manley, R.L. Azevedo-Pereira, T.M. Bliss, G.K. Steinberg, Neural stem cells in stroke: intracerebral approaches, Cell Therapy for Brain Injury, Springer, Cham, 2015, pp. 91–109 https://doi.org/10.1007/978-3-319-15063-5_7.

[21] E. Binello, I.M. Germano, Stem cells as therapeutic vehicles for the treatment of high-grade gliomas, Neuro Oncol. 14 (3) (2011) 256–265.

[22] M.J. Tsai, C.F. Weng, S.K. Shyue, D.Y. Liou, C.H. Chen, C.W. Chiu, et al., Dual effect of adenovirus-mediated transfer of BMP7 in mixed neuron-glial cultures: neuro-protection and cellular differentiation, J. Neurosci. Res. 85 (13) (2007) 2950–2959 https://doi.org/10.1002/jnr.21395.

[23] P. Benda, J. Lightbody, G. Sato, L. Levine, W. Sweet, Differentiated rat glial cell strain in tissue culture, Science 161 (3839) (1968) 370–371 https://doi.org/10. 1126/science.161.3839.370.

[24] Y. Guan, J. Chen, Y. Zhan, H. Lu, Effects of dexamethasone on C6 cell proliferation, migration and invasion through the upregulation of AQP1, Oncol Lett 15 (5) (2018) 7595–7602 https://doi.org/10.3892/ol.2018.8269.

[25] A. Caricasole, D. Ward-van Oostwaard, L. Zeinstra, A. Van Den Eijnden-Van Raaij, Mummery, Bone morphogenetic proteins (BMPs) induce epithelial differentiation of NT2D1 human embryonal carcinoma cells, Int. J. Dev. Biol. 44 (5) (2003) 443–450 PMID:11032177.

[26] J.L. Tso, S. Yang, J.C. Menjivar, K. Yamada, Y. Zhang, I. Hong, Y. Bui, A. Stream, W.H. McBride, L.M. Liau, S.F. Nelson, Bone morphogenetic protein 7 sensitizes O6-methylguanine methyltransferase expressing-glioblastoma stem cells to clinically relevant dose of temozolomide, Mol. Cancer 14 (1) (2015) 189 https://doi.org/10. 1186/s12943-015-0459-1.

[27] Z. Li, Q. Zhong, H. Liu, P. Liu, J. Wu, D. Ma, et al., Conditioned medium from neural stem cells inhibits glioma cell growth, Cell. Mol. Biol. 62 (12) (2016) 68–73 https:// doi.org/10.14715/cmb/2016.62.12.12.

[28] S.R. Chirasani, A. Sternjak, P. Wend, S. Momma, B. Campos, I.M. Herrmann, et al., Bone morphogenetic protein-7 release from endogenous neural precursor cells suppresses the tumourigenicity of stem-like glioblastoma cells, Brain 133 (7) (2010) 1961–1972 https://doi.org/10.1093/brain/awq128.

[29] L. Caja, C. Bellomo, A. Moustakas, Transforming growth factor β and bone mor-phogenetic protein actions in brain tumors, FEBS Lett. 589 (14) (2015) 1588–1597 https://doi.org/10.1016/j.febslet.2015.04.058.

[30] K.S. Lau, The Role of Bone Morphogenetic Protein 2 in Ovarian Cancer Migration, Doctoral dissertation, University of British Columbia, 2016, https://dx.doi.org/10. 14288/1.0307514.

[31] K. Savary, D. Caglayan, L. Caja, K. Tzavlaki, S.B. Nayeem, T. Bergström, et al., Snail depletes the tumorigenic potential of glioblastoma, Oncogene 232 (47) (2013) 5409–5420 https://doi.org/10.1038/onc.2013.67.

Chapter 6

General discussion

The use of stem cells as a biological therapeutic tool, including being a vehicle for gene delivery, has created a wide range of possible clinical applications. Various types of stem cells would typically express therapeutic genes to be delivered at targeted sites. With this in mind, mesenchymal stem cells (MSCs) and human neuronal precursor NT2 cells exhibit ideal features for vast gene therapeutic applications. To mention a few, both cell types depict marvelous selective migratory capacity, poor tumorigenicity, and a differentiation potential. Moreover, can be genetically manipulated to express selected therapeutic genes implicated in regenerative and cancer mechanisms. Non-viral carrier-based gene therapy is receiving the most attention recently, as relatively safe vehicles for gene transfer. One of the most promising non-viral gene carriers are the niosomes. Nevertheless, their use is hampered by their limited efficacy to deliver genes to the target cells. The main objective of this thesis is the use of novel cationic niosome vehicles to transfect stem cells (MSCs and NT2 cells) to induce hBMP7 overexpression. Therefore, in the present study, we have prepared and characterized cationic niosomes, based on the cationic lipid 2,3-ditetradecyloxypropan-1 amine (DTPA), to be further used to transfect MSCs and NT2 cells for various applications.

6.1. Stem cell-based gene delivery mediated by cationic niosomes for bone regeneration

Our novel DP80 niosomes were formulated of the cationic lipid salt (DTPA-HCl) and the non-ionic surfactant polysorbate 80 (Fig 1). Although the DTPA cationic lipid has been used for gene delivery applications,[1] this study was the first time to use it in a niosome formulation.

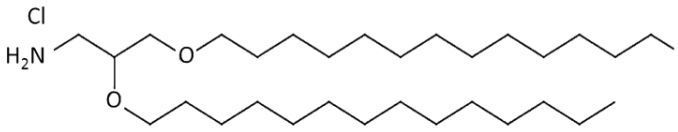

A- 2,3-Di (tetradecyloxy) propan-1-amine (DTPA Chloride salt)

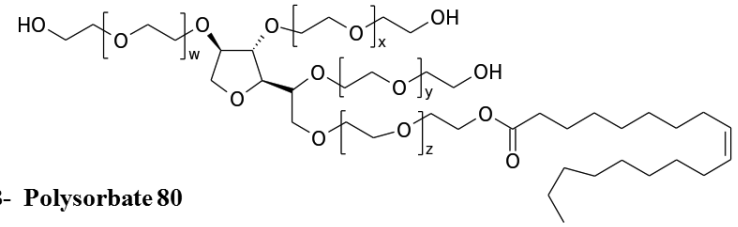

B- Polysorbate 80

Figure 1: Chemical structure of the components of DP80 niosomes (A. Cationic lipid DTPA-Cl, B. Polysorbate 80)

Structurally, DTPA-HCl is composed of the four crucial elements that govern gene transfection, namely, the polar head, backbone, linker and two non-polar tails.[2] During the elaboration of

niosomes, we endeavored to circumvent the potential cytotoxicity of the ether linker of DTPA-HCl by decreasing its molar ratio in proportion to P80 (DTPA-Cl to P80 as 1:2, respectively).

Once synthesized, DP80 niosomes depicted appropriate nano-scaled size for gene delivery purposes (54.0±0.9 nm). The high positive zeta values (41.9±7.1 mV) is believed sufficient to ensure long-term stability[3] and spontaneous electrostatic interaction with plasmid DNA. Additionally, it could enhance proper binding of the resulting nioplexes to the negatively charged cell coat prior to nioplexes internalization.[2] Yet, the previously mentioned parameters "per se" could not ensure optimal behavior of the DP80 niosomes.

To probe the actual behavior of our niosomes, as a proof of concept, DP80-EGFP-nioplexes were obtained by adding pCMS-EGFP reporter plasmid to DP80 niosomes at different cationic lipid/DNA mass ratios. A gradual decrease in the size of nioplexes was observed (168 - 84 nm, Fig.2-A, bars), at mass ratios increased up to 16/1. Such decline in size is governed by balanced events in a delicate multistep self-assembly process of complex formation, such as: electrostatic interaction, further membrane merging, lipid mixing and aggregate growth.[4]

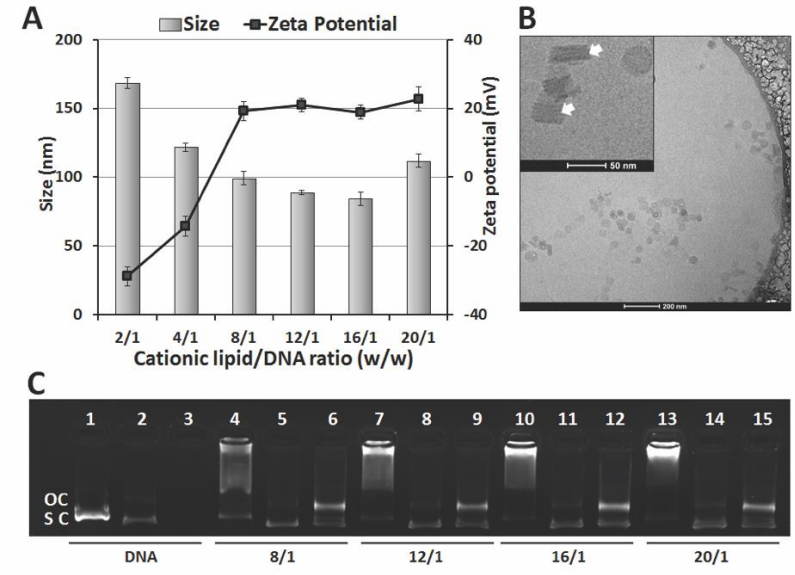

Figure 2: (A) Effect of cationic lipid/DNA ratio (w/w) on both particle size (bars) and ZP (line), n = 3. (B) Cryo-TEM micrographs of nioplexes at 16/1 cationic lipid/DNA ratio (w/w). Arrows indicate lamellar pattern. Scale bar =200 nm (inset scale bar =50 nm). (C) Binding, SDS-induced release and protection of DNA at different cationic lipid/DNA ratios (w/w) of DP80-EGFP-nioplexes visualized by agarose electrophoresis. Nioplexes were treated with SDS (lanes 2, 5, 8, 11 and 14) and DNase I + SDS (lanes 3, 6, 9, 12 and 15). OC: open circular form, SC: supercoiled form.

The size of nioplexes is important for proper interactions with cell components (organelle membranes and cytoskeletal filaments). The small size of nioplexes might be advantageous to improve the rate of cellular uptake.[5] In addition, nioplexes would be able to navigate the mammalian cytoskeleton with mesh size about 200 nm.[6] Regarding the ZP values (Fig.2-A, line), the gradual initial increase of superficial charge along with cationic lipid/DNA ratios (w/w), followed by a plateau phase, demonstrated the ability of cationic niosomes to bind to and neutralize

the negatively charged phosphate groups in plasmid DNA.[7] At small cationic lipid/DNA mass ratios (2/1 and 4/1), the ZP readings were negative and shifted to the positive territory (around +20 mV) at 8/1, 12/1, 16/1, and 20/1 mass ratios. At higher ratios, nioplexes were figured to function as gene delivery carriers taking advantage of their positive surface charge that facilitates proper electrostatic interaction with the anionic glycocalyx during the early steps of the endocytosis.[8] Nevertheless, other studies have reported a similar uptake of negatively and positively charged complexes. Therefore, the limiting step in transfection efficiency lies not in the process of internalization, but in the intracellular trafficking later on.[9]

The shape of complexes has a marked effect on their performance as a gene delivery candidate,[10] Yet, the effect of particle shape on biological interactions is not fully understood. As reviewed by Champion et al,[10] vast studies proved the complexity of cell interactions with particles and revealed the ability of cells to respond differently to different particle shapes.

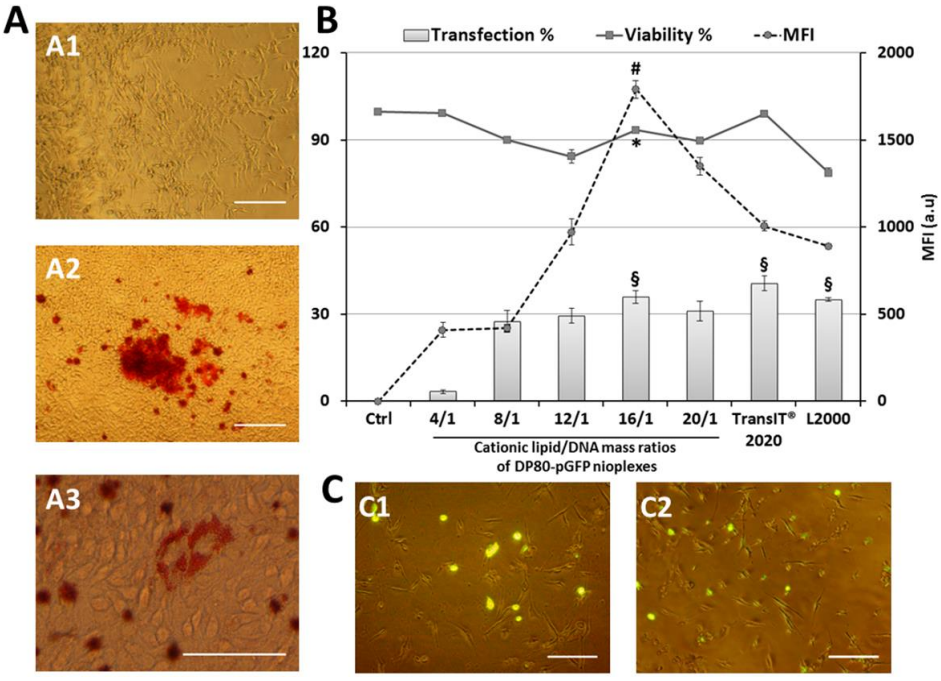

Figure 3: D1-MSCs culture (A1), osteogenic (A2) and adipogenic differentiation (A3). (B) Cell transfection efficiency and viability at different cationic lipid/DNA ratios (w/w). Percentage of EGFP-positive cells (bars), percentage of viable cells (line) and MFI (dashed line), (n = 3). Similar symbol (§) indicate insignificant differences among three bars ($P>0.05$). $^{*}P < 0.05$ vs. TransIT® 2020 and L2000 viability. $^{\#}P < 0.05$ vs. TransIT® 2020 and L200 MFI. (C) Representative overlay micrographs of D1-MSCs 48 h post-transfection via (C1) DP80-EGFP nioplexes (16/1 cationic lipid/DNA mass ratio) and (C2) TransIT® 2020. Scale bars: A1, A2, B1 and B2 = 50 µm and A3= 25 µm.

For instance, non-spherical particles were reported to be internalized faster than the perfectly spherical ones.[5, 11] In our study, the cryo-TEM micrographs (Fig 2-B) illustrated that most of the DP80-EGFP complexes were not perfectly spherical. Additionally, the discrete morphology of nioplexes with no aggregates could be attributed to the moderately positive surface charge of nioplexes. Interestingly, the lamellar pattern observed in several nioplexes is believed to take place

during the process of complex formation due to the topological transformation of both DNA and lipid into compact quasi-spherical complex particles, with diameter of ~ 200 nm, depicting an ordered multi-lamellar planar structure (Fig 2-B, arrows).[12] The regular lamellar spacing of almost 5.5-6 nm (Fig 2-B inset) was similar to that reported by Le Bihan and colleagues, denoting the repetitive motif that corresponded to DNA strands being complexed with the lipid bilayers.[13]

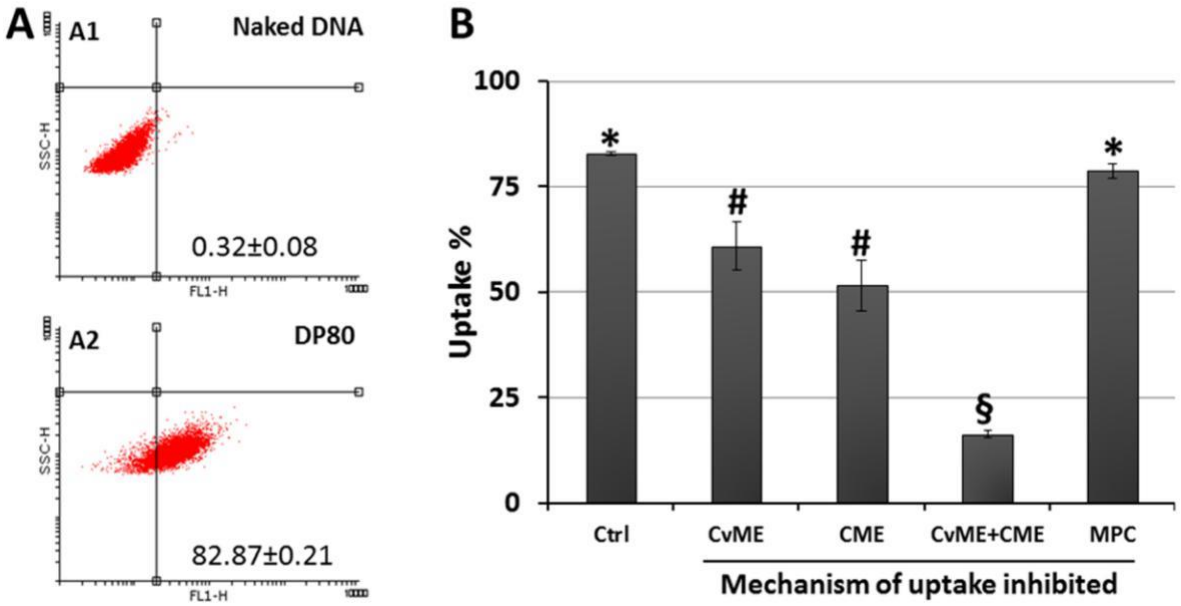

Figure 4: Uptake study of D1-MSCs 4 h post-incubation with FITC-labeled nioplexes. (A) Representative dot plots for cellular uptake, (A1) naked DNA (no carrier), (A2) DP80 nioplexes. (B) Uptake % (FITC-positive cells) in the presence/absence of endocytosis inhibitors. (Ctrl) represents the uptake with no inhibitors. Mean ± SD; n = 3. ($^{*}p<0.05$, $^{***}p< 0.0001$)

Among the factors that can influence the transfection process is the electrostatic interaction between the phosphate groups of DNA (negatively charged) with the amine groups of cationic lipid (positively charged).[7, 14-16] With the help of gel retardation assay, we observed that at all cationic lipid/DNA ratios evaluated, niosomes were able to capture, release and shield DNA from

enzymatic degradation (Fig 2-C). Once we evaluated that DP80-EGFP nioplexes might be a suitable gene delivery vehicle, we proceeded to evaluate their biological performance *in vitro*. BM-MSCs are of utmost importance in bone repair as they home to the fracture site, proliferate, and differentiate into bone-forming cells. Therefore, BM-derived D1-MSCs were selected for the current study. They were known to represent a multipotent platform holding potential for osteogenic fate determination *in vitro*.[17, 18] Moreover, their phenotypic characteristics and osteogenic differentiation potential (Fig 2-A) were reported to be consistent with human primary MSCs.[17, 19] Nevertheless, primary MSCs should be further studied to ensure the ability of our

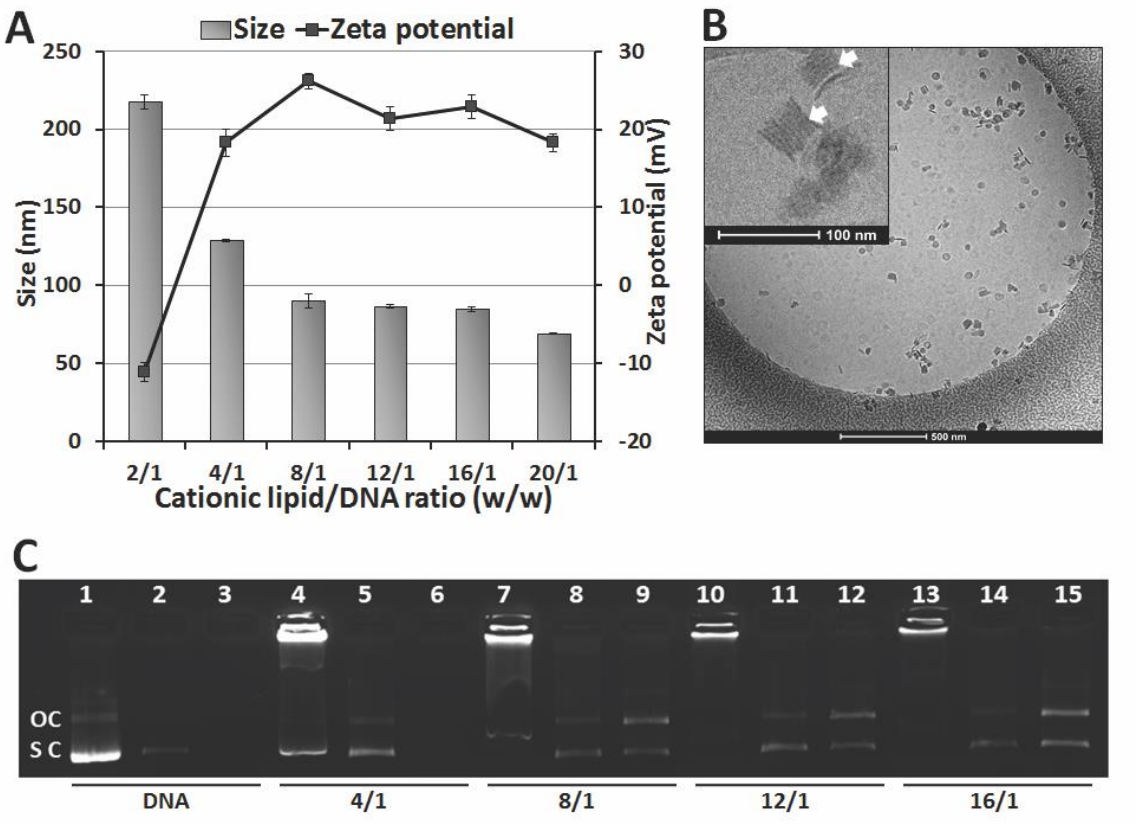

gene carriers to transfect them.

Figure 5: Physicochemical characterization of DP80-hBMP7 nioplexes. (A) Effect of cationic lipid/DNA ratio (w/w) on particle size (bars) and zeta potential (line), n = 3. (B) Cryo-TEM micrographs of nioplexes at ratio of 8/1 cationic lipid/DNA ratio (w/w). Arrows indicate lamellar pattern. Scale bar = 500 nm (inset scale bar =100 nm). (C) Binding, SDS-induced release and protection of DNA at different cationic lipid/DNA ratios (w/w) of DP80-hBMP7 nioplexes visualized by agarose electrophoresis. Nioplexes were treated with SDS (lanes 2, 5, 8, 11 and 14) and DNase I + SDS (lanes 3, 6, 9, 12 and 15). OC: open circular form, SC: supercoiled form.

There is a general belief that niosomes are well tolerated both *in vitro* and *in vivo* conditions.[9] Our results (Fig 3-B) illustrated that DP80 (16/1) induced transfection efficiency similar to that obtained by TransIT® 2020 and L2000 commercial reagents (35.8 %, 40.6% and 35.1%, respectively). However, the MFI of the transfected cells (Figs 3-B and 3-C) were significantly higher with DP80 (1791 a.u.) compared to TransIT® 2020 (1006 a.u). However, cell viability reported with DP80-EGFP nioplexes was significantly higher than that with L2000, while inferior to that reported by TransIT® 2020 commercial reagents. Such cytotoxicity might be induced, even in part, by GFP-induced apoptosis that might result from GFP aggregations or free radicals.[20] In general, the main aim of gene delivery is to attain overexpression of the transfected gene to express the protein in super physiological doses. Thereafter, transfection efficiency is not only a matter of how many cells were transfected, but also the amount of gene expression by the transfected cells.

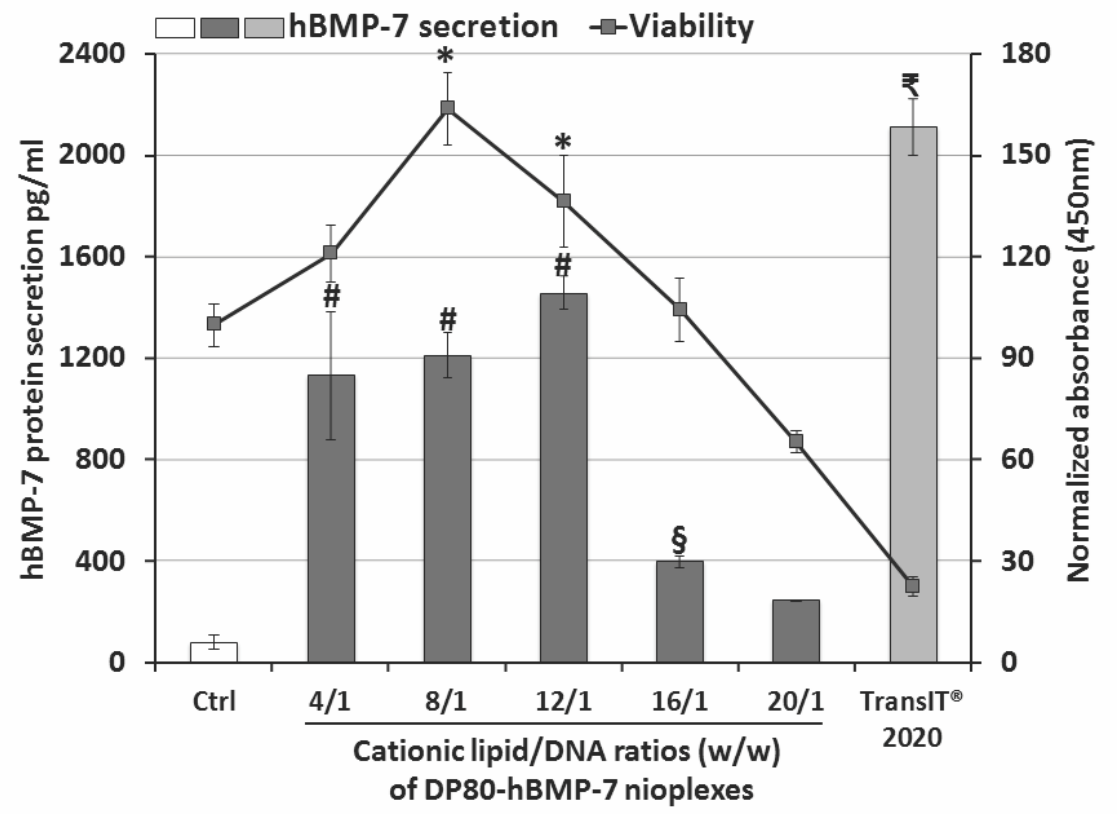

Figure 6: hBMP7 secretion (pg⁄mL) compared to untransfected cells (Ctrl) and TransIT® 2020-transfected cells (Bars). CCK-8 viability assay (line). Values represent mean ± SD (n = 3). Different symbols above bars indicate statistically significant differences. *P < 0.05 compared to all data points of line graph.

The high transfection efficiency values observed were preceded by a great percentage of nioplexes uptake as shown for best transfection efficiency (16/1) (Fig 4-A). However, despite the reported high uptake percentage (~ 83%), the performance of non-viral vectors is known to be clearly affected by their distinct cellular internalization pathway, taking into account the variable effectiveness of every pathway in the release of DNA into the cytoplasm, which is one of the critical steps in the eventual transgene expression.[9]Therefore, we further analyzed intracellular trafficking of our nioplexes by blocking the caveolae-mediated endocytosis (CvME), clathrin-mediated endocytosis (CME) and macropinocytosis (MPC). The selected endocytosis mechanisms are reported as the most important endocytosis pathways in mammalian cells.[5, 21] Nonetheless, more pathways (as caveolae/clathrin independent and lipid raft-mediated endocytosis) should be investigated before a sound inference is made. The results observed in figure 4-B suggested that the main internalization of DP80-EGFP was through CvME and CME with no significant difference in between. Although a robust consensus does not exist, it is widely accepted that the endolysosomal fate is the hallmark feature of CME.[22, 23] Oppositely, CvME and/or MPC routes could be advantageous to avoid lysosomal degradation, which could ensure a better plasmid delivery and integrity.[21, 24]

Consequently, the relevant contribution of the CME pathway, that routes nioplexes to lysosomes, could explain the relatively low transfection efficiency values observed (~36%, Fig 3-B), despite the fact that high number of cells (83%, Fig 4-A) captured the complexes.

The promising results obtained with the reporter EGFP plasmid encouraged us to explore hBMP7 gene transfection. As done before with DP80-EGFP nioplexes, we characterized DP80-hBMP7 nioplexes regarding their physicochemical features. A gradual decline in size paralleled the increased cationic lipid/DNA mass ratio (Fig 5-A, bars). Starting from mass ratio of 4/1, ZP values were found in the positive range fluctuating between 18.3 and 26.2 mV. Particles were of no perfect shape and mostly acquired the planar lamellar pattern (Fig 5-B). Similar to what has been reported in figure 2-C, DP80-hBMP7 nioplexes were able to bind, release and protect plasmid DNA against DNase I enzymatic digestion (Fig 5-C). These findings suggested that DP80-hBMP7 nioplexes could probably transfect D1-MSCs. The hBMP7 secreted after 48 h of transfection (Fig 6) reached its highest value at the ratios of 4-12/1 (up to 1460 pg/ml). These results showed that the mass ratios of best transfection efficiency changed with different plasmids used (EGFP at 16/1).

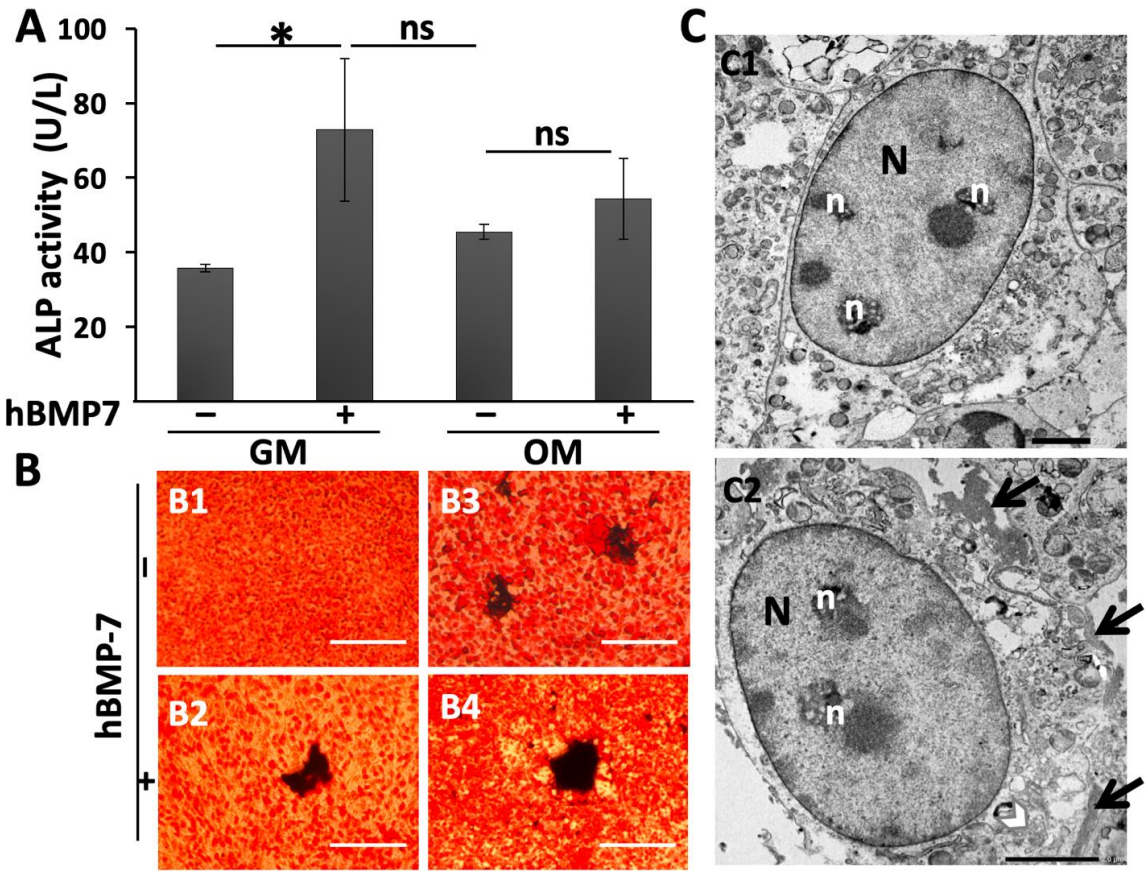

Figure 7: Osteogenic differentiation *in vitro* (A) Validation of ALP activity of the conditioned media of D1-MSCs, n=5. * indicated statistically significant differences ($P < 0.05$). ns indicated no statistically significant differences ($P \geq 0.05$). (B) Representative light micrographs of D1-MSCs culture after Von Kossa staining for calcium deposition. Scale bars = 40µm. GM= Growth Medium, OM = Osteogenic Medium. (C) TEM micrographs for cell ultrastructure in both untransfected (C1) and transfected (C2) cultures. Arrowhead points at Golgi complex, arrows point at extracellular matrix deposits. N = nucleus, n= nucleolus. Scale bars = 2 µm.

The cytotoxicity (CCK-8) assay revealed that transfected cells seemed to proliferate more at transfection mass ratios of 8/1 and 12/1. We believed that this observation might be due to two main factors; first, the negligible cytotoxicity effect of our nioplexes on D1-MSCs at such ratios compared to the higher ratios (16/1 and 20/1); second, the mitotic activity of such cells could be enhanced by the over expressed hBMP7.[25]

Although TransIT® 2020 has significantly induced efficient transfection (with hBMP7 expression of 2111.5 pg/ml, Fig. 6), it has extremely decreased cell viability to ~23%. This might be referred to the cytotoxic impact of the hBMP7-TransIT® 2020 lipopolyplexes that seemed to attenuate the initial population of hBMP7-expressing cells.[26] Since ELISA assay was performed as early as

48 h post-transfection, the number of TransIT® 2020-transfected cells was not obviously enhanced by the putative mitogenic effect of hBMP7 protein.

Noteworthy, the results shown in figures 3-B and 6 elucidated that different plasmids could behave differently in regard to their transfection efficiency and cytotoxicity. In the current study, each of the plasmids EGFP and hBMP7 had a different length (5541bp and 4497bp, respectively) and different promotors. Therefore, the obtained nioplexes rendered different physicochemical characteristics, thus demonstrated discrepant behavior regarding transfection efficiency or cell viability.[27, 28].

We further assessed the effectiveness of hBMP7 overexpression to induce osteogenesis *in vitro* using the alkaline phosphatase activity ALP (Fig 7-A).The ALP, an important parameter of the osteoblastic phenotype, is required for mineralization, thus expressed early during osteoblast differentiation.[29] Both ALP assay and Von Kossa staining (Fig 7-B) of the mineralized bone nodules denoted that hBMP7 expression induced spontaneous osteoblastic differentiation and calcified matrix deposition under standard culture (with GM). The deposition of amorphous extracellular matrix was further shown at the ultrastructural level in figure 7-C2. During this process, the secreted hBMP7 was anticipated to interact with cell membrane receptors, which could induce a signaling cascade that lead to osteoblastic differentiation in autocrine and/or paracrine mode.[30] Nevertheless, BMP7 transfection did not manifest significant difference when cells were cultured in OM for two weeks (Fig 7-B3 vs. 7-B4). Therefore, further investigation is still needed to explain why the hBMP7 expression did not boost the osteogenic differentiation of cells when cultured in osteogenic media. Furthermore, *in vivo*/*ex vivo* experiments are highly encouraged to validate the efficient osteogenic potential of the transfected cells.

6.2. DPP80 cationic niosome-based EGFP gene transfection of neuronal precursor NT2 cells and rat cortical cells

Flattering properties of niosome-based stem cell transfection [31] and neurons in cerebral cortex and retina were recently reported. [32, 33] As well, reports on literature highlighted the benefits of combining two surfactants within the same formulation. [34, 35] Therefore, we decided to explore the impact of combining the non-ionic surfactants poloxamer 188 (P) to polysorbate 80 (P80) (shown in figure 8) in the same niosome gene delivery system based on the cationic lipid DTPA-HCl. We aimed to compare DP80 to DPP80 as gene delivery carriers.

Our data illustrated that particle features were affected according to the type of surfactant implemented (Table 1). The difference in size was assumed due to the different hydrophilic-lipophilic balance value (HLB) of the incorporated surfactant. For example, incorporating P80 (with lower HLB value) resulted in nanovesicles with smaller size.[36] Nevertheless, the interaction between surfactant(s) and cationic lipid in niosomes, on the molecular level, should not be excluded as an additional factor that could influence the size of nanovesicles.[37]

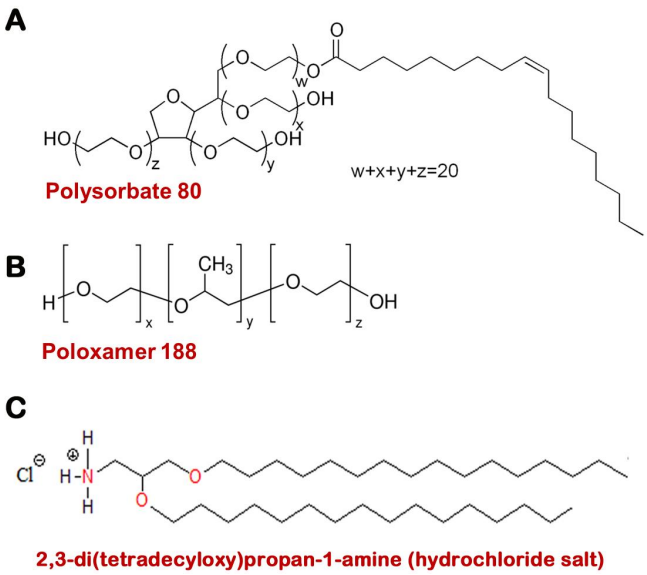

Figure 8: Chemical structure of: (A) polysorbate 80, (B) poloxamer 188, and (C) cationic lipid DTPA. **Abbreviation: DTPA,** 2,3-di(tetradecyloxy)propan-1-amine.

Table 1 Components (in mg) and physical characterization of niosome formulations regarding particle size (nm), PDI, and zeta potential (mV). **Note:** Data represent mean±SD (n=3). **Abbreviations:** DTPA, 2,3-di(tetradecyloxy)propan-1-amine; PDI, polydispersity index.

Niosomes	Components (mg)			Characterization		
	DTPA (D)	Poloxamer 188 (P)	Polysorbate 80 (P80)	Size (nm)	PDI	Zeta potential (mV)
DP80	5	–	25	54.02±0.94	0.52±0.10	41.9±7.10
DPP80	5	12.5	12.5	90.41±0.65	0.42±0.01	44.1±4.39

Before the attempt to transfect cells, we opted to characterize the nioplexes at different cationic lipid /DNA ratios (Fig.9). Although there is no general consensus on the optimal particle size of formulations, it is now widely accepted that this parameter clearly influences their performance.[38] In addition, nioplexes' size varies according to the cationic lipid/DNA mass ratio. Interestingly, when DNA was incorporated to obtain complexes at a mass ratio of 2/1, size

of DP80 and DPP80 exceeded 168 and 200 nm, respectively. However, at higher ratios, size decreased probably due to the electrostatic interactions that condense DNA plasmids more efficiently in multi-lamellar forms as discerned by cryo-TEM examination (Fig 9-B2 and 4, arrows). The morphology of complexes appears to affect their final performance as gene delivery carriers.[39] Interestingly, the discerned lamellar pattern of several nioplexes is believed to happen during the process of complex formation. The topological transformation of both DNA and lipids to form nioplexes would form string-like aggregates, depicting multi lamellar configuration. [13]

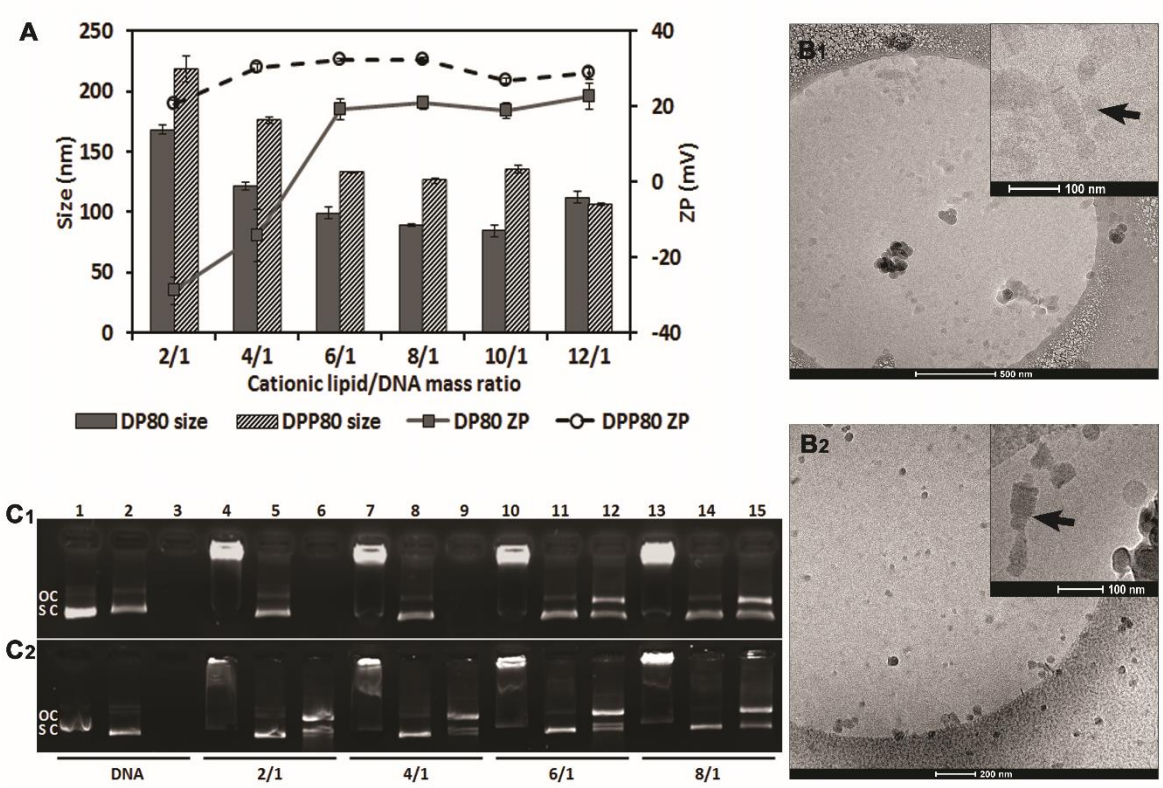

Figure 9: Characterization of DP80 and DPP80 complexes. Notes: (A) Particle size (nm) and ZP (mV). The data represent mean±SD (n=3). (B1–B4) Cryo-TEM pictures of nioplexes. arrows in B2 and B4 point to the multi-lamellar pattern. (C) agarose gel electrophoresis assay at different cationic lipid/DNA ratios of DP80 and DPP80 complexes (upper and lower panels, respectively), based on both formulations. lanes are shown as: 1–3, uncomplexed DNA; 4–6, mass ratio 2/1; 7–9, mass ratio 4/1; 10–12, mass ratio 6/1; and 13–15, mass ratio 8/1. lanes 2, 5, 8, 11, and 14 depict niocomplexes treated with SDS, while lanes 3, 6, 9, 12, and 15 were treated with DNase I+ SDS. OC and SC (open circular and supercoiled forms, respectively). **Abbreviations**: SDS, sodium dodecyl sulphate; ZP, zeta potential.

The discrete arrangement of nioplexes at (cationic lipid/DNA) mass ratio of 6/1 (Fig 9-B) could be attributed to their moderate positive surface charge (> 20 mV).[7] DPP80 nioplexes depicted higher ZP values (> 30 mV), thus had less aggregates as they tend to repel each other.[39] Another

paramount factor that influences the transfection process is the Van der Waals interactions between the phosphate groups of DNA (negatively charged)and the amine groups of the cationic niosomes (positively charged).[40] To analyze such feature, we performed a gel retardation assay (Fig. 9-C). For DPP80 niosomes, all cationic lipid/DNA ratios analyzed were able to release and protect plasmid DNA against the enzymatic digestion. Though, complexes based on DP80 niosomes (Fig. 9-C) failed clearly to protect DNA. In spite of being able to condense and release DNA properly, the DNA protective capacity thanks to DP80 niosomes against enzymatic digestion is key for efficient gene delivery. We propose that electrostatic interactions between DNA and DP80 niosomes at low N/P ratios (2/1 and 4/1) could strongly condense DNA, albeit not sufficient to protect DNA. [15] That might be attributed to the net negative surface charge of the nioplexes at the aforementioned low N/P ratios.

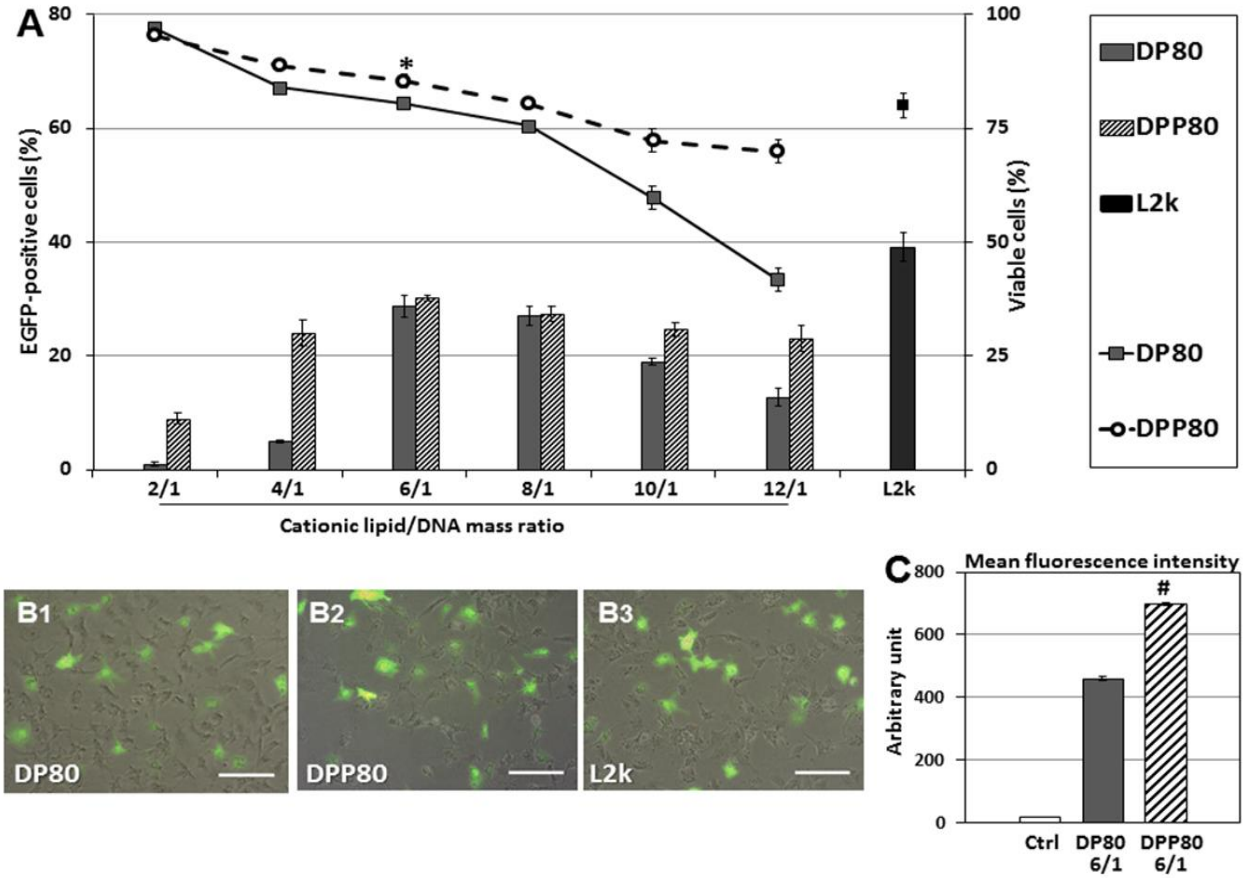

Figure 10: Transfection studies in NT2 culture cells. (A) Flow cytometry analysis of percentage of cells that express EGFP (bars) and percentage of live cells (lines) at different cationic lipid/DNA ratios (w/w). Values represent mean±SD (n=3). *P,0.05 compared with DP80 at 6/1 and L2K at 2/1. Overlay of fluorescence and DIC pictures of control cells (B1), DP80 at 6/1 (B2), DPP80 at 6/1 (B3), and L2K at 2/1 mass ratios (B4). scale bars=100 µm. (C) Mean fluorescence intensity (a.u.). **Abbreviations**: a.u., arbitrary unit; ctrl, control; DIC, digital image correlation; L2K, Lipofectamine® 2000.

Afterwards, both types of nioplexes were analyzed to evaluate *in vitro* NT2 transfection efficiency and cell viability. NT2 cells have been utilized *in vivo* as a promising human cell source for therapeutic application in several neurological disorders.[41, 42] Their therapeutic potential lies, mainly, in their ability to terminally differentiate into stable post-mitotic neurons, upon retinoic acid treatment, even long time after transplantation in animals' brain tissue.[43] In addition,, NT2-mediated recovery of preclinical models of stroke has justified their application in clinical trials.[44] Thanks to their stability and easy culture, NT2 cells are amenable to scale-up for cell production and represent a CNS-like gene/drug delivery vehicle for treatment of glioblastoma.[44-46] In the current study, NT2 cells represent an interesting model to study the efficiency of gene delivery carriers into CNS due to their differentiation potential to neuronal as well as glial cell types.[47]

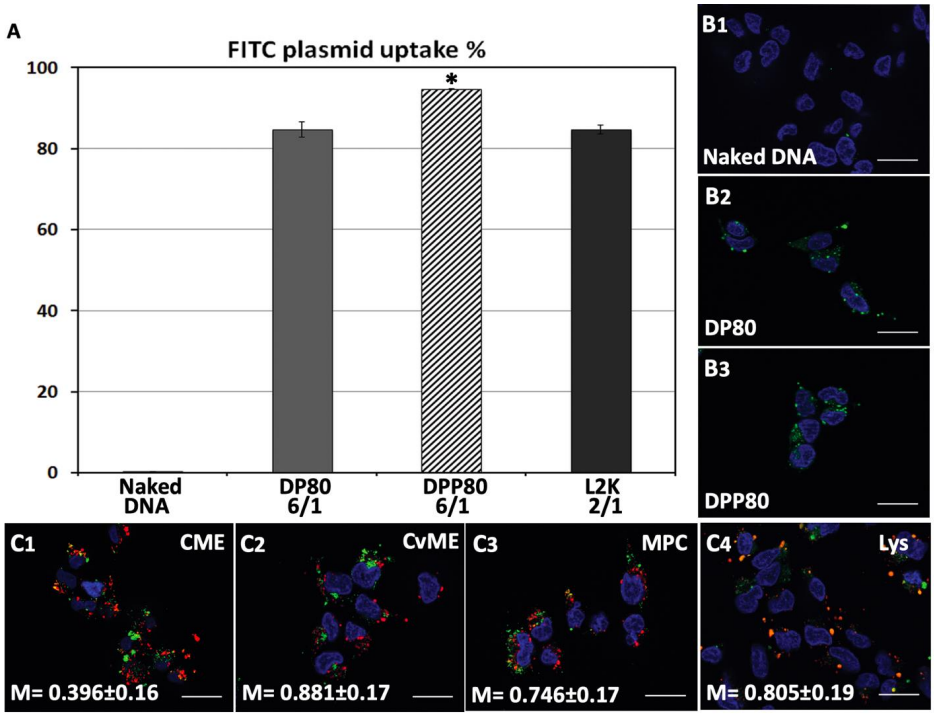

Figure 11: Trafficking studies in NT2 culture cells. (A) Flow cytometry measurement of the percentage of cells that captured plasmid labeled with FITC. error bars represent SD (n=3). *P,0.05 compared with other groups. (B1–B3) Fluorescence micrographs with FITC-labeled naked plasmids, and DP80 and DPP80 niocomplexes (at 6/1 mass ratios), respectively (scale bar=25 µm). (C) confocal micrographs showing intracellular distribution of DPP80 complexes, where plasmid is labeled in green color, and AlexaFluor 546-Transferrin (C1), AlexaFluor 555-Cholera Toxin (C2), AlexaFluor 594-Dextran (C3), and LysoTracker red DND-99 markers (C4), all in red. Nuclei of cells were stained with DAPI-fluoromount G (blue) (scale bar=25 µm). **Abbreviations:** CME, clathrin mediated endocytosis; CvME, caveolae mediated endocytosis; FITC, fluorescein isothiocyanate; M, Mander's co-localization coefficient; MPC, macropinocytosis.

The data of cell transfection (Fig. 10-A) revealed the impact of surfactant (s) composition of the formulation. When P80 was used (in DP80), the values of transfection started to increase at the mass ratio of 6/1. Nioplexes at lower ratios (2/1 and 4/1) had failed to protect DNA from DNase

digestion (Fig. 9-C) which could explain the low transfection efficiencies at those ratios. However, the incorporation of P in the DPP80 niosome formulation had markedly enhanced the transfection at the lower ratios (2/1 and 4/1), compared to that of DP80, and maintained sufficient transfection at the higher ratios. The complexes depicted a positive ZP at low mass ratios (Fig 9-A), compared to the negative charge of DP80, which would enhance cell uptake, thus transfection (Fig 10-A).[48] Yet, the actual mechanism is not fully understood. At the cationic lipid/DNA mass ratio of maximum transfection (6/1), DPP80 depicted an interestingly higher MFI compared to DP80. In practice, one of the serious concerns in gene therapy is to obtain sufficient protein expression to ensure physiological effects. Thus, the amount of protein expression by the transfected cells (as a translation of the transfected gene) needs to be considered in addition to the percentage of transfected cells when designing a new gene carrier.[31]

In regard to cell viability, DPP80 niosomes had cytotoxic effect less than that of DP80 at tested mass ratios. NT2 cell viability at 6/1 mass ratio significantly exceeded that reported by liposome-based transfection reagent (L2K). This represents an appealing feature for further *in vivo* applications where cytotoxicity is of utmost importance. The higher cationic lipid/ DNA mass ratios of DPP80 nioplexes depicted a marked cytotoxic effect which was even higher in case of their DP80 counterparts. Further studies are needed to fully explain the reported increase in cytotoxicity.

The fact that the type and amount of surfactant would influence the biological function of niosomes,[49] might explain the modest transfection and viability results observed when only P (supplementary data, Fig.S1) or P80 (Fig 10-A) surfactants were used in niosome formulations (DP and DP80, respectively). In addition, when the liposomes were manufactured in the absence of surfactants (referred to as D, Fig.S1), both transfection efficiency and cell viability values were way less than their DPP80 counterparts. To understand the transfection process in NT2 cells mediated by DPP80 complexes, we evaluated the cellular uptake and the intracellular distribution of complexes, since those two factors could markedly affect the final performance of gene delivery carriers.[9] Cellular uptake values of DPP80 complexes were compared to that of DP80 and L2K. As observed in Fig.11-A, cell uptake for DPP80 nioplexes exceeded that of DP80. That could be due to their higher net positive ZP value (Fig 9-A), or specific interactions between nioplexes and the lipid components of cell membrane.[12] Moreover, variations in the length of carbon chains and/or the number of unsaturated bonds (inside the carbon chains) of surfactants can affect the

permeability of different membranes towards nioplexes.[37] Anyway, the percentage of transfected cells with DPP80 complexes (30%, Fig.10-A) were clearly lower than the percentage of positive cells for FITC-labeled DPP80 complexes (95%, Fig.11-A), which suggested the potential influence of other biological processes, such as the uptake mechanism or endosome scape, in the eventual expression of EGFP.[50] Those biological processes deserve subsequent experiments to elucidate their effect on gene expression. Despite the lack of consensus on the most efficient endocytosis pathway, we proceeded to analyze three of the most important cellular uptake pathways (CME, CvME and MPC) that are strongly believed to affect the fate of internalized complexes.[51]

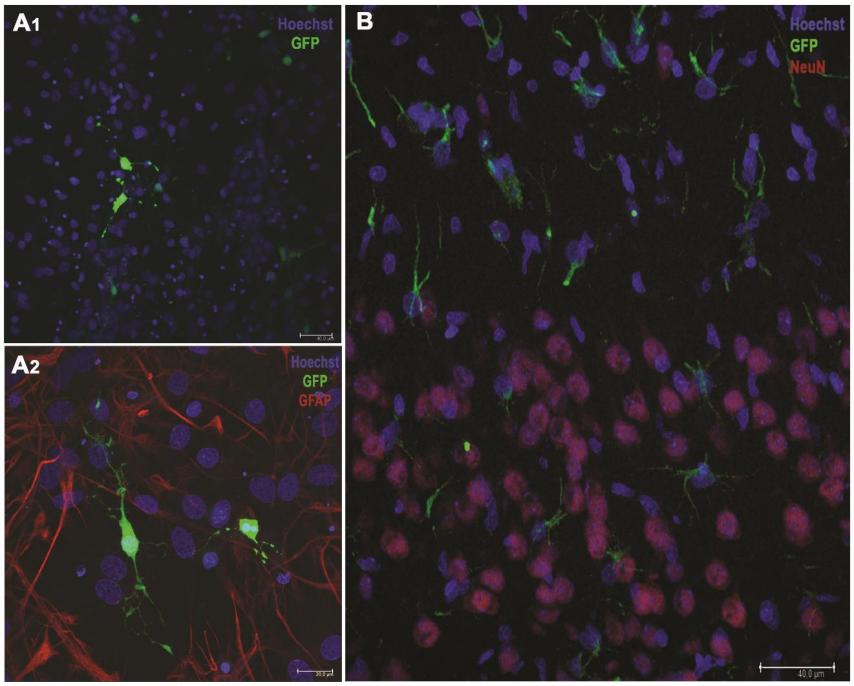

Figure 12: EGFP gene expression in primary neuronal cell cultures (A1 and A2). $GFAP^{+ve}$ neuroglia (red) and nuclei were stained in blue color with Hoechst 33342 (scale bars=40 and 20 µm, respectively). (B) *in vivo* expression green protein (scale bar=40 µm). **Note:** nuclei are shown in blue color (Hoechst), while neurons in red ($neuN^{+ve}$).

The observed results in fig.11-C suggested that DPP80 complexes were mainly internalized by CvME and MPC, while CME had much less participation in their cellular uptake. Both CvME and CME are generally believed to be the endocytosis routes that transfer genetic material to late endosomes/lysosomes, where the acidic environment degrades the DNA, hampering the transfection process.[50] Therefore, co-localization of the complexes with late endosome/lysosome (Fig. 11-C4) could explain the great gap between the 95% of NT2 that captured DPP80 complexes (Fig 11-A), and the ~30% that eventually expressed EGFP (Fig 10).[52]

Subsequently, before proceeding to *in vivo* studies, we evaluated the transfection efficiency of DPP80 nioplexes in primary cortical cultures derived from rat embryos. Primary culture is composed of several

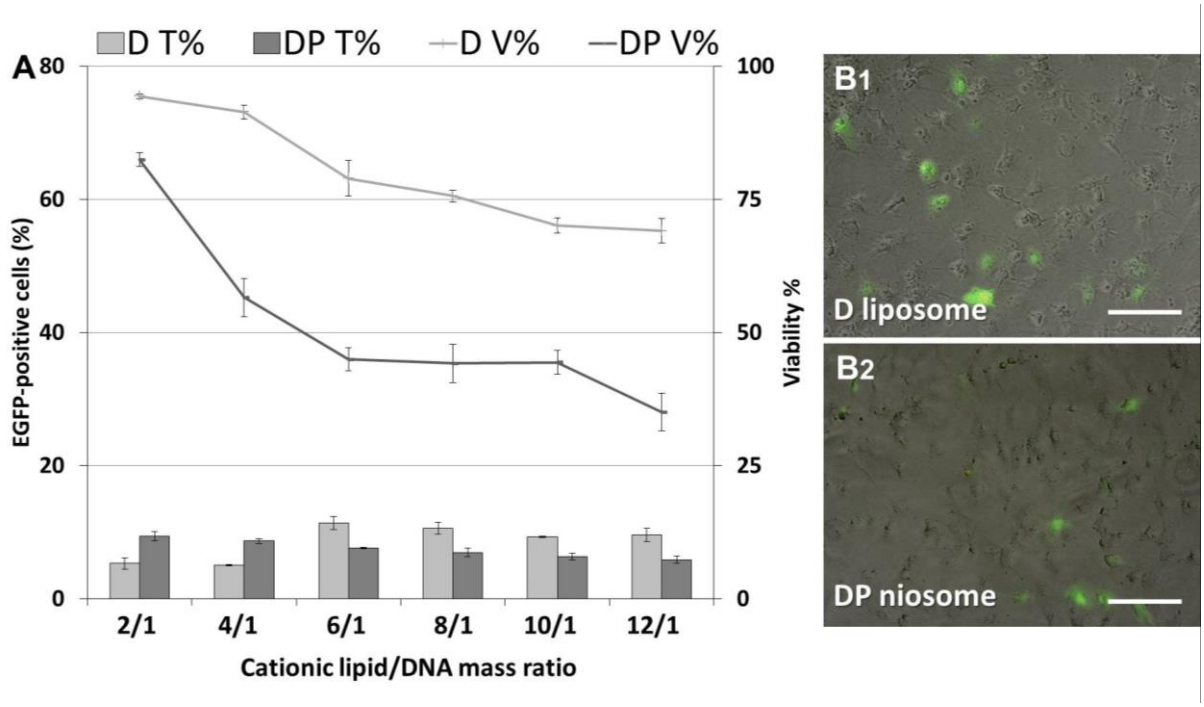

Figure S1 (A) Transfection efficiency of D liposomes and DP niosomes in NT2 cells. Percentages of cells that express green protein (bars) and live cells (lines). Values represent mean±SD (n=3). (B1 and B2) Overlay of fluorescence and DIC pictures of NT2 cells with D liposomes (6/1) and DP niosomes (2/1), respectively (scale bar=100 µm). **Abbreviations:** DIC, digital image correlation; T, transfection; V, viability.

types of neurons and glial cells mixed to form neuronal-glial network set up. Initial data suggested that some neurons expressed EGFP (Fig. 12-A1). This observation was further confirmed by the lack of $GFAP^{+ve}$ immunoreactivity in those EGFP-expressing cells (Fig. 12-A2). Such preferential transfection of neurons encouraged us to proceed to *in vivo* experiments where direct intracranial injection of DPP80 complexes was performed. Despite the lack of toxicity signs in the cortical tissue after injection (data not shown), intravascular injections in larger animal models should be investigated in future studies. Unlike the observations in primary culture, neuroglia ($NeuN^{-ve}$) were the only transfected cells (Fig.12-B). In general, discrepancies between *in vitro* and *in vivo* assays are not uncommon, and most probably due to the major differences in biological context.[53] The reported favorable transfection of glial cells might be attributed to their higher mitotic and/or phagocytic activities.[54] In addition, the number of glial cells constitute over 70% of the total cell

population in the CNS. On the other side, the incapacity of complexes to transfect neurons *in vivo* is probably due to the less uptake and/or the unfavorable intracellular trafficking.[55] Therefore, DPP80 complexes could be of great interest to transfect glial cells in the CNS in glia-related neurological disorders. Glia also play a pivotal role in the normal development and function of nervous tissue.[56] Their perturbation is associated with several neurological disorders such as; stroke, epilepsy, multiple sclerosis, Alzheimer's and Parkinson's diseases.[56, 57]

These novel biocompatible nioplexes were able to induce *in vivo* transfection into glial cells in rat brains after intracortical administration. Interestingly, DPP80 nioplexes do not only represent a promising tool for direct *in vivo* transfection, but also for cell-based gene delivery applications where the transfected NT2 cells or their derived neurons can be used as a cell-based gene delivery carrier to deliver therapeutic genes for CNS disorders including glioblastoma.[58, 59]

6.3. DPP80 cationic niosome-based hBMP7 gene transfection of neuronal precursor NT2 cells to reduce the migration of glioma cell line

The high mortality rate in glioblastoma patients has necessitated the search for novel, safe, and effective therapeutic approaches. Over the past few years, both cell and gene therapies have offered great promise in this realm. In our previous work,[60] DPP80 cationic niosomes were able to transfect NT2 cells with EGFP reporter plasmid. Therefore, we were encouraged to investigate the effectiveness of these niosomes to deliver an expression plasmid (pUNO1-hBMP7) to NT2 cells, then determine their potential to combat glioma cell proliferation and/or migration *in vitro*. First, cationic niosomes were electrostatically complexed with the negatively charged pUNO1-hBMP7 plasmids rendering nioplexes at different cationic lipid/DNA mass ratios. Although the optimal size of non-viral gene carriers is unknown as yet, it is widely accepted that the particle size clearly affects their performance. In the current work, the size of nioplexes was clearly affected by the cationic lipid/DNA mass ratio (Fig. 13-A). At the mass ratio of 2/1, the size was almost 190 nm. Alongside higher mass ratios, the size gradually decreased. Such decrease is most likely due to the electrostatic interactions that condense DNA plasmids more tightly. In addition to the size, the shape of non-viral complexes can also affect their final performance in gene delivery.[31] hBMP7-DPP80 complexes were not perfectly regular in shape (Fig 13-B). As well, the discrete morphology of nioplexes at 6/1 mass ratio (Fig 13-B) may be attributed to the high positive surface charge (> 29 mV) which, in turn, evades the particles' aggregation via the electrostatic repulsion forces.[7]

The electrostatic interaction between DNA (negatively charged phosphate groups) and the cationic niosomes (positively charged amine groups) plays a crucial role during the transfection process, as a precise balance between the capture and release of DNA is necessary.[40] To investigate such parameter, gel retardation assay was carried out (Fig.13-C). We selected nioplexes at cationic lipid/DNA mass ratios higher than 2/1 since the values of ZP were within the positive range (Fig

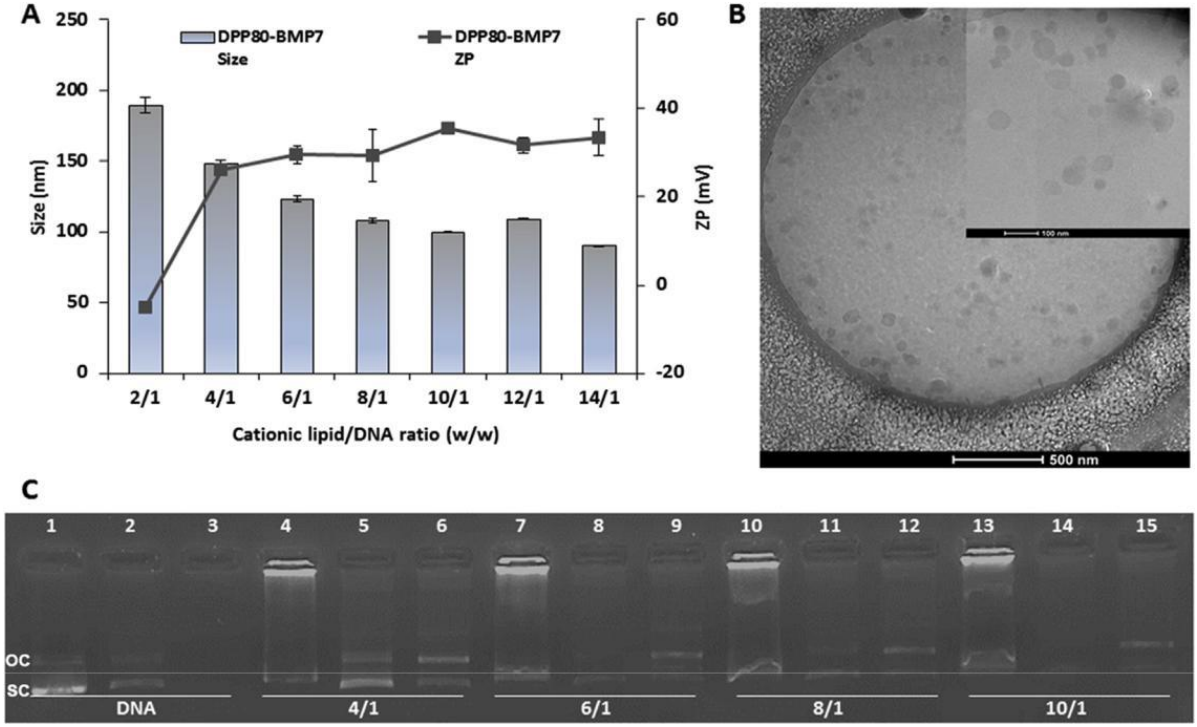

13-A, lines). Interestingly, at all studied cationic lipid/DNA ratios, the niosomes were not only able to partially condense and totally release DNA upon adding SDS, but also to protect DNA against the DNase enzymatic digestion, which is of significance for *in vivo* applications.

Figure 13: (A) Particle size (nm) and Zeta potential (mV). Data represent mean ± SD (n = 3). (B) Cryo-TEM micrographs of nioplexes at 6/1 cationic lipid/DNA mass ratio. Scale bar 500 nm (inset, 100 nm). (C) Gel retardation assay of nioplexes. Lanes 2, 5, 8, 11 and 14 depict nioplexes treated with SDS, while lanes 3, 6, 9, 12 and 15 correspond to DNase I- and SDS-treated nioplexes. OC and SC: open circular and supercoiled forms, respectively.

Thanks to the previously mentioned desirable features of DPP80-hBMP7 nioplexes, we proceeded to *in vitro* transfection in order to evaluate the capacity of nioplexes to deliver hBMP7 gene to NT2 cells. Besides being regarded as a stable cell line suitable for transfection studies, NT2 cells have been reported to be a promising source of human stem cells in CNS-targeted cell therapy applications.[42] Interestingly, NT2 cells have successfully induced recovery in pre-clinical stroke models. Therefore, they have been endorsed in clinical trials.[61] In particular, their intrinsic

glioma-tropism has opened new horizons to treat brain malignancies. NT2 cells are advantageously amenable to scale-up cell production, thus might represent a promising off-the-shelf gene delivery vehicle for cancer therapy.[62] The obtained transfection data (Fig. 14) revealed the release of significant amount of hBMP7 (5.7ng/ml) when the mass ratio of 6/1 (cationic lipid/DNA) was used for transfection. On the other side, Cytotoxicity on NT2 cells was less compared to the positive control, L2K ($p < 0.05$). These results suggest that the hBMP7-secreting NT2 cells might be used as an interesting platform for further studies on the nervous tissue, as well as other tissues where the production of BMP7 is desired. Despite the low level of hBMP7 secretion (5.7 ng/ml) by the transfected NT2 cells, a markedly low dose of hBMP7 (1 ng/ml) could increase SMAD phosphorylation 5–6 fold, thus having a significant therapeutic effect.[63]

In their research work, Tsai et al. have reported that low, yet continuous secretion of hBMP7 was both neuroprotective and differentiation-inductive.[64] Similarly, our research team has recently reported a marked impact of hBMP7 production, even at much lower values, to induce spontaneous osteogenic differentiation of mesenchymal stem cells *in vitro*.[31] Interestingly, a dose of 1.3 ng/ml of hBMP7 was enough to enhance the alkaline phosphatase activity and osteogenic matrix deposition, suggesting the effectiveness of such low concentrations of hBMP7 to achieve desired therapeutic activities.[63] We further proceeded to evaluate the impact of NT2-expressed hBMP7 on glioma cells. Glioma C6 cells are known to express glioma-specific markers. In addition, they are stable both *in vitro* and *in vivo*.[65] Thereafter, they are widely used in experimental studies for the treatment of gliomas.[66] To avoid the drawbacks of the direct co-culture system, an indirect co-culture was adopted by culturing tumor C6 cells in the CM of NT2 cells. In particular, the difficulty to evaluate the effect of one type of cells on another type. The overexpression of hBMP7 can alter the NT2 gene expression and suppress their own tumorigenicity, making them a safe candidate for *in vivo* studies.[67] Moreover, activation of BMP7 signaling in glioma cells could render them more vulnerable, and thereby more sensitive to low doses of chemotherapeutic drugs.[68]

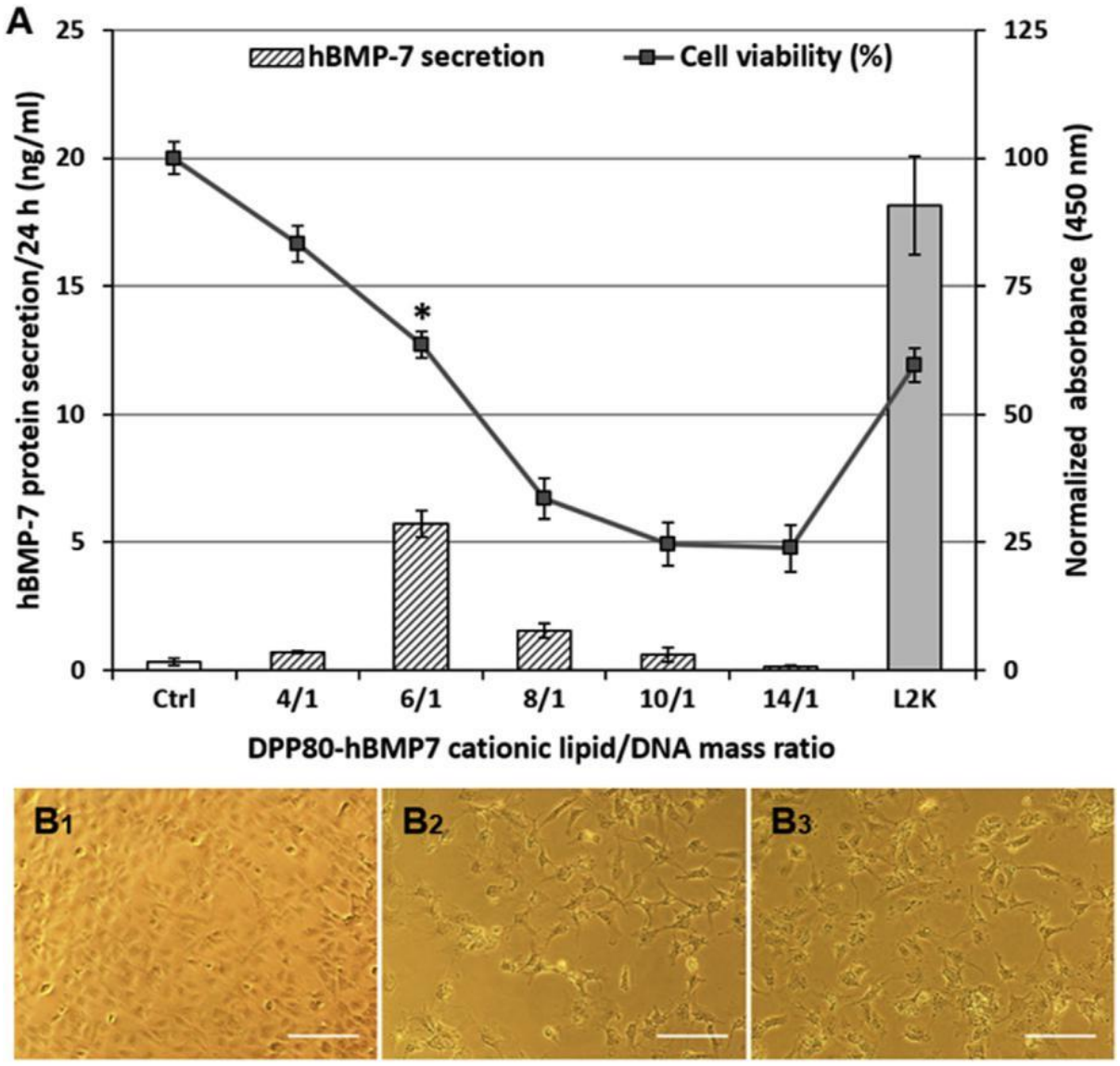

Figure 14: (A) hBMP7 secretion (ng⁄ml) at 24 h (bars). Values represent mean ± SD (n = 3). P < 0.05 versus L2K. (B) Phase contrast micrographs of NT2 cells 24 h post-transfection (B1) control, (B2) hBMP7-DPP80-transfected, (B3) hBMP7-L2K-transfected cells. (Scale bars = 50 μm).

In accordance with Li and colleagues,[69] the anti-glioma effect of NT2-CM could be mediated by the inactivation of mitogen-activated protein kinase (MAPK) pathway. On the other hand, we observed (Fig. 15) that the overexpression of hBMP7 "*per se*" did not add any inhibitory effect on the viability of C6 cells. This effect could most probably be attributed to the presence of anti-BMP signals in the remaining serum content of NT2-CM, such as cytokines, noggin or chordin. The main goal of most antitumor drugs is to reduce cancer cell viability. However, because of the

hyper-mutability of GBM cells, adjuvant anti-migration strategies are also desirable. Among others, Chirasani and co-workers [70] have reported, in agreement with our findings, the ability of BMP7-expressing neural precursor cells to attenuate the tumorigenicity of glioblastoma cells as well as to induce glioma stem cell differentiation.[71]

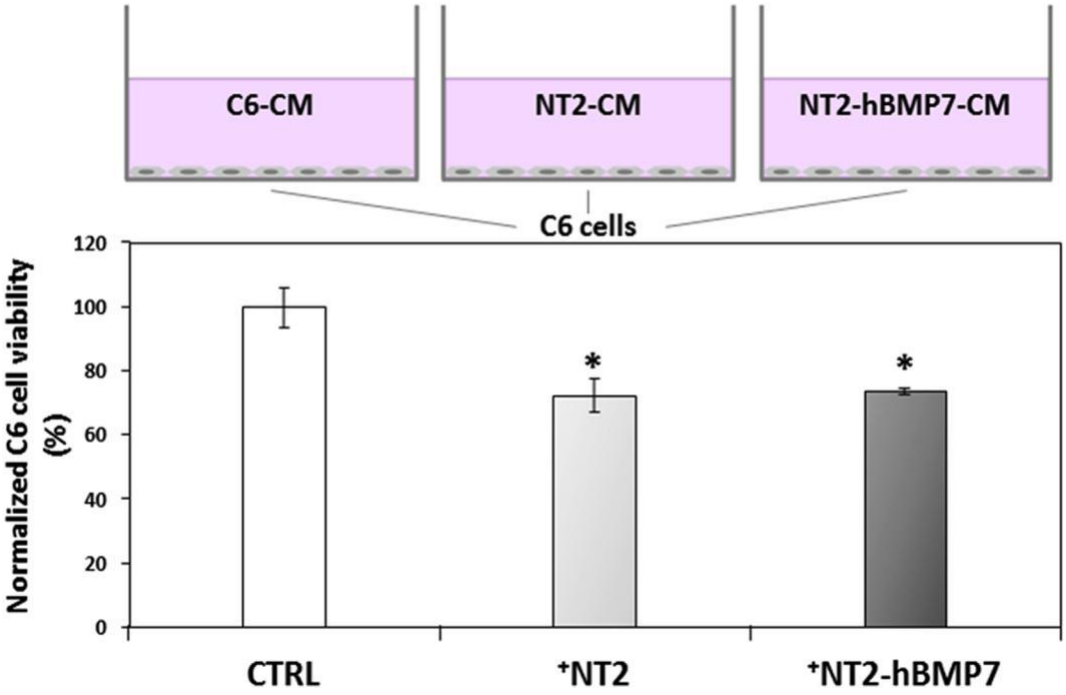

Figure 15: In vitro viability assay of C6 glioma cells after incubation with; C6-CM, untransfected NT2 cells and transfected NT2 cells. (*P < 0.05).

Regarding the observed suppression of migration effect, it should be noted that BMP7 may have contradictory effects depending on the cell line being investigated.[72] The discerned anti-migratory effects of hBMP7-transfected NT2 cells (Fig. 16) could be attributed to the negative effect of hBMP7 on cell motility (across uncoated Transwell filters) [73] or to the induction of tumor stem cell differentiation/senescence.[68] Thus, further studies on the exact mechanism are still required. Adequate understanding of the underlying mechanisms is necessary for the development of effective cellular delivery vehicles for glioma therapy.

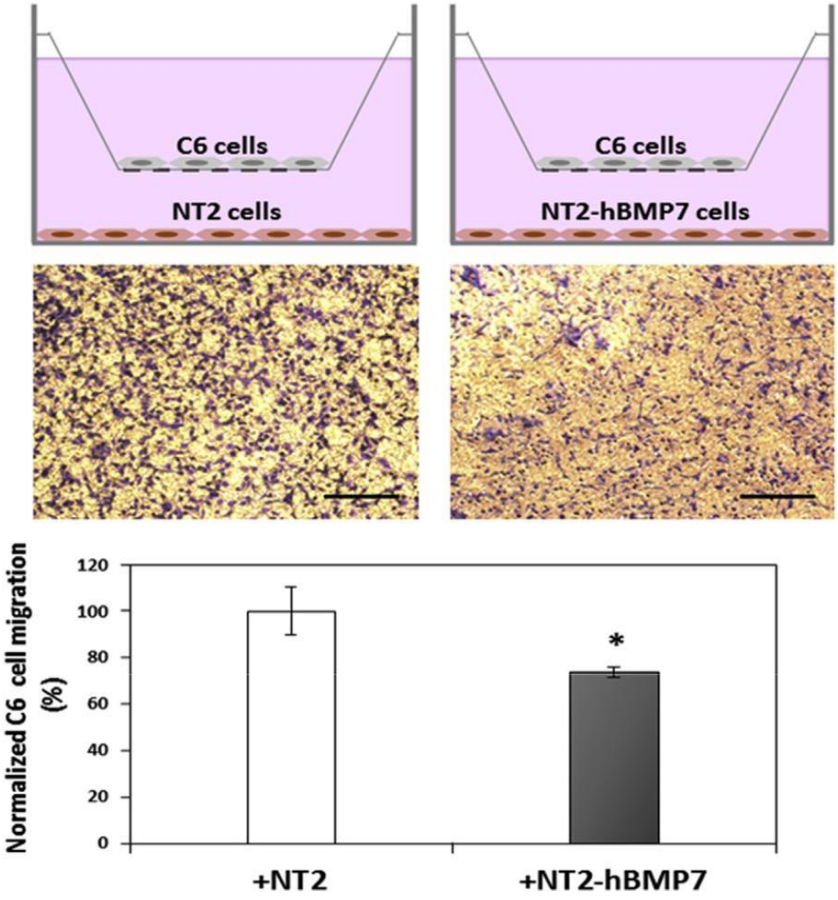

Figure 16: Transwell migration assay of glioma C6 cells co-cultured with transfected NT2 cells (+NT2-hBMP7) compared to the untransfected cells (+NT2) (*P < 0.05). C6 glioma cells on the lower surface of Transwell inserts were stained with

6.4. References

1. Song, Y.K. and D. Liu, *Free liposomes enhance the transfection activity of DNA/lipid complexes in vivo by intravenous administration.* Biochim Biophys Acta, 1998. **1372**(1): p. 141-50.
2. Balazs, D.A. and W. Godbey, *Liposomes for use in gene delivery.* Journal of drug delivery, 2010. **2011**.
3. Szunerits, S. and R. Boukherroub, *Introduction to Plasmonics: Advances and Applications*. 2015: CRC Press.
4. Wasungu, L. and D. Hoekstra, *Cationic lipids, lipoplexes and intracellular delivery of genes.* J Control Release, 2006. **116**(2): p. 255-64.
5. Singh, J., et al., *Evaluation of cellular uptake and intracellular trafficking as determining factors of gene expression for amino acid-substituted gemini surfactant-based DNA nanoparticles.* Journal of nanobiotechnology, 2012. **10**(1): p. 7.
6. Majzoub, R.N., K.K. Ewert, and C.R. Safinya, *Cationic liposome–nucleic acid nanoparticle assemblies with applications in gene delivery and gene silencing.* Phil. Trans. R. Soc. A, 2016. **374**(2072): p. 20150129.
7. Puras, G., et al., *A novel cationic niosome formulation for gene delivery to the retina.* J Control Release, 2014. **174**: p. 27-36.
8. Sakurai, F., et al., *Effect of DNA/liposome mixing ratio on the physicochemical characteristics, cellular uptake and intracellular trafficking of plasmid DNA/cationic liposome complexes and subsequent gene expression.* J Control Release, 2000. **66**(2-3): p. 255-69.

9. Mashal, M., et al., *Retinal gene delivery enhancement by lycopene incorporation into cationic niosomes based on DOTMA and polysorbate 60.* Journal of Controlled Release, 2017.
10. Champion, J.A., Y.K. Katare, and S. Mitragotri, *Particle shape: a new design parameter for micro- and nanoscale drug delivery carriers.* Journal of Controlled Release, 2007. **121**(1): p. 3-9.
11. Gratton, S.E., et al., *The effect of particle design on cellular internalization pathways.* Proceedings of the National Academy of Sciences, 2008. **105**(33): p. 11613-11618.
12. Ma, B., et al., *Lipoplex morphologies and their influences on transfection efficiency in gene delivery.* Journal of Controlled Release, 2007. **123**(3): p. 184-194.
13. Le Bihan, O., et al., *Probing the in vitro mechanism of action of cationic lipid/DNA lipoplexes at a nanometric scale.* Nucleic acids research, 2011. **39**(4): p. 1595-1609.
14. Ojeda, E., et al., *The role of helper lipids in the intracellular disposition and transfection efficiency of niosome formulations for gene delivery to retinal pigment epithelial cells.* International journal of pharmaceutics, 2016. **503**(1): p. 115-126.
15. Ojeda, E., et al., *Niosomes based on synthetic cationic lipids for gene delivery: the influence of polar head-groups on the transfection efficiency in HEK-293, ARPE-19 and MSC-D1 cells.* Organic & biomolecular chemistry, 2015. **13**(4): p. 1068-1081.
16. Puras, G., et al., *Protamine/DNA/Niosome Ternary Nonviral Vectors for Gene Delivery to the Retina: The Role of Protamine.* Mol Pharm, 2015. **12**(10): p. 3658-71.
17. Honda, Y., et al., *Guiding the osteogenic fate of mouse and human mesenchymal stem cells through feedback system control.* Scientific reports, 2013. **3**: p. 3420.
18. Hsiong, S.X., et al., *Cyclic arginine-glycine-aspartate peptides enhance three-dimensional stem cell osteogenic differentiation.* Tissue Engineering Part A, 2008. **15**(2): p. 263-272.
19. Garate, A., et al., *Assessment of the behavior of mesenchymal stem cells immobilized in biomimetic alginate microcapsules.* Molecular pharmaceutics, 2015. **12**(11): p. 3953-3962.
20. Jensen, E.C., *Use of fluorescent probes: their effect on cell biology and limitations.* The Anatomical Record, 2012. **295**(12): p. 2031-2036.
21. Xiang, S., et al., *Uptake mechanisms of non-viral gene delivery.* J Control Release, 2012. **158**(3): p. 371-8.
22. El-Sayed, A. and H. Harashima, *Endocytosis of gene delivery vectors: from clathrin-dependent to lipid raft-mediated endocytosis.* Molecular Therapy, 2013. **21**(6): p. 1118-1130.
23. Bareford, L.M. and P.W. Swaan, *Endocytic mechanisms for targeted drug delivery.* Adv Drug Deliv Rev, 2007. **59**(8): p. 748-58.
24. Kou, L., et al., *The endocytosis and intracellular fate of nanomedicines: Implication for rational design.* Asian Journal of Pharmaceutical Sciences, 2013. **8**(1): p. 1-10.
25. Xu, J., et al., *BMP7 enhances the effect of BMSCs on extracellular matrix remodeling in a rabbit model of intervertebral disc degeneration.* The FEBS journal, 2016. **283**(9): p. 1689-1700.
26. Bahrambeigi, V., et al., *Non-viral gene transfer into murine adipose derived mesenchymal stem cells: A comparative study of different non-viral methods.* Gene Therapy and Molecular Biology, 2013. **15**: p. 164-175.
27. Hornstein, B.D., et al., *Effects of Circular DNA Length on Transfection Efficiency by Electroporation into HeLa Cells.* PloS one, 2016. **11**(12): p. e0167537.
28. Yin, W., P. Xiang, and Q. Li, *Investigations of the effect of DNA size in transient transfection assay using dual luciferase system.* Analytical biochemistry, 2005. **346**(2): p. 289-294.
29. Scarfì, S., *Use of bone morphogenetic proteins in mesenchymal stem cell stimulation of cartilage and bone repair.* World journal of stem cells, 2016. **8**(1): p. 1.
30. Dorman, L., M. Tucci, and H. Benghuzzi, *In vitro effects of bmp-2, bmp-7, and bmp-13 on proliferation and differentation of mouse mesenchymal stem cells.* Biomedical sciences instrumentation, 2011. **48**: p. 81-87.
31. Attia, N., et al., *Stem cell-based gene delivery mediated by cationic niosomes for bone regeneration.* Nanomedicine, 2018. **14**(2): p. 521-531.

32. Ojeda, E., et al., *The influence of the polar head-group of synthetic cationic lipids on the transfection efficiency mediated by niosomes in rat retina and brain.* Biomaterials, 2016. **77**: p. 267-79.
33. Ochoa, G.P., et al., *A novel formulation based on 2,3-di(tetradecyloxy)propan-1-amine cationic lipid combined with polysorbate 80 for efficient gene delivery to the retina.* Pharm Res, 2014. **31**(7): p. 1665-75.
34. Muzzalupo, R., et al., *Niosomes containing hydroxyl additives as percutaneous penetration enhancers: effect on the transdermal delivery of sulfadiazine sodium salt.* Colloids and Surfaces B: Biointerfaces, 2014. **123**: p. 207-212.
35. Wang, Y., et al., *Formulation and pharmacokinetic evaluation of a paclitaxel nanosuspension for intravenous delivery.* Int J Nanomedicine, 2011. **6**: p. 1497-507.
36. Basha, M., et al., *Design and optimization of surfactant-based nanovesicles for ocular delivery of Clotrimazole.* Journal of liposome research, 2013. **23**(3): p. 203-210.
37. Bnyan, R., et al., *Surfactant effects on lipid-based vesicles properties.* Journal of pharmaceutical sciences, 2018. **107**(5): p. 1237-1246.
38. Pezzoli, D., et al., *Size matters for in vitro gene delivery: investigating the relationships among complexation protocol, transfection medium, size and sedimentation.* Scientific reports, 2017. **7**: p. 44134.
39. Mady, M.M., et al., *Biophysical studies on chitosan-coated liposomes.* European Biophysics Journal, 2009. **38**(8): p. 1127-1133.
40. Eastman, S., et al., *Biophysical characterization of cationic lipid: DNA complexes.* Biochimica et Biophysica Acta (BBA)-Biomembranes, 1997. **1325**(1): p. 41-62.
41. Jain, K., *Cell therapy for CNS trauma.* Molecular biotechnology, 2009. **42**(3): p. 367.
42. Cacciotti, I., et al., *Neuro-differentiated Ntera2 cancer stem cells encapsulated in alginate beads: First evidence of biological functionality.* Materials Science and Engineering: C, 2017. **81**: p. 32-38.
43. Hara, K., et al., *Neural progenitor NT2N cell lines from teratocarcinoma for transplantation therapy in stroke.* Progress in neurobiology, 2008. **85**(3): p. 318-334.
44. Hao, S. and B. Wang, *Review on Intracerebral Haemorrhage: Multidisciplinary Approaches to the Injury Mechanism Analysis and Therapeutic Strategies.* Current pharmaceutical design, 2017. **23**(15): p. 2159-2160.
45. Frosina, G., *Stem cell-mediated delivery of therapies in the treatment of glioma.* Mini reviews in medicinal chemistry, 2011. **11**(7): p. 591-598.
46. Ahmed, A.U., N.G. Alexiades, and M.S. Lesniak, *The use of neural stem cells in cancer gene therapy: predicting the path to the clinic.* Current opinion in molecular therapeutics, 2010. **12**(5): p. 546.
47. Ferrari, A., et al., *Immature human NT2 cells grafted into mouse brain differentiate into neuronal and glial cell types.* FEBS letters, 2000. **486**(2): p. 121-125.
48. Midoux, P. and M. Monsigny, *Efficient gene transfer by histidylated polylysine/pDNA complexes.* Bioconjugate chemistry, 1999. **10**(3): p. 406-411.
49. Taymouri, S. and J. Varshosaz, *Effect of different types of surfactants on the physical properties and stability of carvedilol nano-niosomes.* Advanced biomedical research, 2016. **5**.
50. Goldshtein, M., et al., *Mechanisms of cellular uptake and endosomal escape of calcium-siRNA nanocomplexes.* International journal of pharmaceutics, 2016. **515**(1-2): p. 46-56.
51. Zhao, F., et al., *Cellular uptake, intracellular trafficking, and cytotoxicity of nanomaterials.* small, 2011. **7**(10): p. 1322-1337.
52. Ruiz de Garibay, A.P., et al., *Role of endocytic uptake in transfection efficiency of solid lipid nanoparticles-based nonviral vectors.* The journal of gene medicine, 2013. **15**(11-12): p. 427-440.
53. Puras, G., et al., *Oligochitosan polyplexes as carriers for retinal gene delivery.* European Journal of Pharmaceutical Sciences, 2013. **48**(1-2): p. 323-331.

54. Schafer, D.P. and B. Stevens, *Phagocytic glial cells: sculpting synaptic circuits in the developing nervous system.* Current opinion in neurobiology, 2013. **23**(6): p. 1034-1040.
55. Bergen, J.M., et al., *Nonviral approaches for neuronal delivery of nucleic acids.* Pharmaceutical research, 2008. **25**(5): p. 983-998.
56. Barres, B.A., *The mystery and magic of glia: a perspective on their roles in health and disease.* Neuron, 2008. **60**(3): p. 430-440.
57. Milligan, E.D. and L.R. Watkins, *Pathological and protective roles of glia in chronic pain.* Nature reviews neuroscience, 2009. **10**(1): p. 23.
58. Watson, D.J., et al., *Genetically modified NT2N human neuronal cells mediate long-term gene expression as CNS grafts in vivo and improve functional cognitive outcome following experimental traumatic brain injury*. Journal of Neuropathology & Experimental Neurology, 2003. **62**(4): p. 368-380.
59. Longhi, L., et al., *Ex vivo gene therapy using targeted engraftment of NGF-expressing human NT2N neurons attenuates cognitive deficits following traumatic brain injury in mice.* Journal of neurotrauma, 2004. **21**(12): p. 1723-1736.
60. Attia, N., et al., *Gene transfer to rat cerebral cortex mediated by polysorbate 80 and poloxamer 188 nonionic surfactant vesicles.* Drug design, development and therapy, 2018. **12**: p. 3937.
61. Manley, N.C., et al., *Neural stem cells in stroke: Intracerebral approaches*, in *Cell therapy for brain injury*. 2015, Springer. p. 91-109.
62. Binello, E. and I.M. Germano, *Stem cells as therapeutic vehicles for the treatment of high-grade gliomas.* Neuro-oncology, 2011. **14**(3): p. 256-265.
63. Chitty, D.W., et al., *Development of BMP7-producing human cells, using a third generation lentiviral gene delivery system.* Journal of neuroscience methods, 2012. **205**(1): p. 17-27.
64. Tsai, M.J., et al., *Dual effect of adenovirus-mediated transfer of BMP7 in mixed neuron-glial cultures: Neuroprotection and cellular differentiation.* Journal of neuroscience research, 2007. **85**(13): p. 2950-2959.
65. Benda, P., et al., *Differentiated rat glial cell strain in tissue culture.* Science, 1968. **161**(3839): p. 370-371.
66. Guan, Y., et al., *Effects of dexamethasone on C6 cell proliferation, migration and invasion through the upregulation of AQP1*. Oncology letters, 2018. **15**(5): p. 7595-7602.
67. Caricasole, A., et al., *Bone morphogenetic proteins (BMPs) induce epithelial differentiation of NT2D1 human embryonal carcinoma cells.* International Journal of Developmental Biology, 2003. **44**(5): p. 443-450.
68. Tso, J.L., et al., *Bone morphogenetic protein 7 sensitizes O6-methylguanine methyltransferase expressing-glioblastoma stem cells to clinically relevant dose of temozolomide.* Molecular cancer, 2015. **14**(1): p. 189.
69. Li, Z., et al., *Conditioned medium from neural stem cells inhibits glioma cell growth.* Cellular and Molecular Biology, 2016. **62**(12): p. 68-73.
70. Chirasani, S.R., et al., *Bone morphogenetic protein-7 release from endogenous neural precursor cells suppresses the tumourigenicity of stem-like glioblastoma cells.* Brain, 2010. **133**(7): p. 1961-1972.
71. Caja, L., C. Bellomo, and A. Moustakas, *Transforming growth factor β and bone morphogenetic protein actions in brain tumors.* FEBS letters, 2015. **589**(14): p. 1588-1597.
72. Lau, K.S.-K., *The role of bone morphogenetic protein 2 in ovarian cancer migration*. 2016, University of British Columbia.
73. Savary, K., et al., *Snail depletes the tumorigenic potential of glioblastoma.* Oncogene, 2013. **32**(47): p. 5409.

Chapter 7

Conclusions

According with the results obtained in this experimental work, the main conclusions include:

1. DP80 nioplexes could transfect D1 MSCs with pCMS-EGFP and pUNO1-hBMP7 plasmids. Yet, optimization of the process of niosome formulation is required to enhance transfection efficiency and cell safety.
2. The hBMP7-transfected D1-MSCs could be considered not only as an effective delivery tool of hBMP7, but also as a proliferating and bone-forming cells for bone regeneration purpose, which offers reasonable hope to use the approach of stem cell-based gene delivery by niosomes approach to target sites where bone regeneration is needed.
3. To validate that hypothesis, additional *in vivo* experiments are still needed, since the consistent correlation of *in vitro* and *in vivo* experiments does always not exit.
4. Our results showed that the DPP80 niosomes, elaborated with a mixture of both P and P80 non-ionic surfactants, were efficiently able to transfect NT2 cells without compromising their viability after cellular uptake mainly mediated by CME and MPC.
5. DPP80-EGFP complexes were able to preferentially transfect neurons in rat embryonic primary cortical cultures.
6. The DPP80 gene carriers were able to induce direct *in vivo* transfection of glial cells in rat cerebral cortex after intracortical injection.
7. Our results depicted the discrepancy between *in vitro* and *in vivo* transfection preference of the DPP80-EGFP complexes. *In vitro*, neurons were preferentially transfected. On the other side, glial cells were preferentially transfected *in vivo*.
8. This study represents a proof of concept that NT2 cells could be transfected with hBMP7 expression plasmids using the DPP80 cationic niosome gene carrier.
9. The co-culture with either untransfected/transfected NT2 cells may reduce the viability of C6 glioma cells. Nonetheless, the hBMP7-overexpressing NT2 cells hamper the migration of C6 glioma cells. These results highlight the potential of NT2 cell-based delivery of hBMP7 for impeding the metastasis of glioma cells.